Università degli Studi di Cagliari

DOTTORATO DI RICERCA

in Ingegneria Elettronica e Informatica

Ciclo XXIII

TITOLO TESI

A GENERALIZED FINITE DIFFERENCE APPROACH TO THE

COMPUTATION OF MODES

Settore scientifico disciplinari di afferenza

ING-INF/02 Campi Elettromagnetici

Presentata da: Alessandro Fanti

Coordinatore Dottorato   Prof.Alessandro Giua

Tutor/Relatore   Prof. Giuseppe Mazzarella

Esame finale anno accademico 2010 - 2011

A GENERALIZED FINITE DIFFERENCE APPROACH TO THE COMPUTATION OF MODES

Alessandro Fanti

Dedicated to my parents

and my grand parents!

Abstract

This thesis deals with numerical techniques for the computation of modes in electromagnetic structures with arbitrary geometry. The approach proposed in this work is based on the Finite Difference (FD) and Vector Finite Difference (VFD), which are applied to rectangular, circular, elliptical geometries, and to combination of them. The FD is applied using a 2D cartesian, polar and elliptical grid in the waveguide section. A suitable Taylor expansion of the mode function allows, either for scalar and for vector FD, to take exactly into account the boundary condition.

To prevent the raising of spurious modes, the VFD approximation results in a constrained eigenvalue problem, that has been solved using a decomposition method.

All approaches presented have been validated comparing the results to the analytical modes of rectangular and circular waveguide, and to known data for the elliptic case.

The standard calculation of the waveguide modes using FD requires the use of two different grids, namely one for TE modes and the other for TM modes, due to the different boundary condition. It has been shown that a single grid can be used for all modes, thus allowing an effective mode-matching solution.

The FD approach has been extended to waveguides (and apertures) with irregular boundaries, and therefore non-regular discretization grids. It has been shown that a suitable FD approximation of the Laplace operator is still possible. A ridged-waveguide, with trapezoidal ridges, and a rounded-ended waveguide have been considered in detail.

CONTENTS

List of Tables

List of Figures

Chapter I

INTRODUCTION

This thesis deals with numerical techniques for the computation of modes in electromagnetic structures with generic geometry. The structures we analyse are waveguides, and to a smaller extent resonant cavities.

There are many strategies to do this, but a comparative evaluation of the techniques proposed in the literature has selected the finite difference approach (FD) as the most suitable because of its flexibility and low computational cost.

The knowledge of eigenvalues and distribution of field modes of waveguides and resonant cavities is important to design and use such devices, both for standard usages and for other applications, like for the analysis of waveguide junction using mode matching [1-5], or solution of waveguide problems with sources [6]. The same type of information is required in the analysis with the method of moments (MoM), of thick-walled waveguide slot [7,8] and apertures [9]. Indeed, these apertures can be considered as stub waveguide, and the modes of these guides are the natural basic functions for MoM [7].

In literature, different approaches have been proposed to compute the modes of electromagnetic structures:

- Analytical
- Semi-analytical
- Numerical (differential)

1.1) ANALYTICAL TECHNIQUES

The method of separation of variables is a convenient method for solving a partial differential equation (PDE). Basically, it entails seeking a solution which breaks up into a product of functions, each of which involves only one of the variables. For an Helmholtz wave equation,

$$1.1.1.) \ \nabla_t^2 \phi + k_t^2 \phi$$

we can apply the method of separation of variables, letting $\phi(x_1, x_2) = \varphi(x_1) \cdot \varphi(x_2)$ as long as the chosen reference frame allows separation of the Laplace equation. In this way we obtain two different problems in x_1 and x_2 variables, whose solution gives the modes of the waveguide.

The PDE to be solved is subject to boundary conditions. The equation is separable when these boundary conditions can be transformed so that they can be applied directly to the separated equations. This is the case for three typical waveguides [10]:

- Rectangular

- Circular

- Elliptic

In the rectangular case, the cartesian reference system is used. Separation is easy because trigonometric functions are used. The circular case is a bit more complex because it requires the use of cylindrical coordinates, and the Bessel functions are used. The cutoff frequencies for the circular waveguide can be written in terms of the zeros associated with Bessel functions and derivatives of Bessel functions.

On the other hand in the case of elliptic waveguide, it is used a reference system with elliptic coordinates. A closed form solution has been found by Chu [11] since the 30's. Unfortunately, the field distribution is described by the

Mathieu functions [12] and so the eigenvalues are the zeros of these function. Numerical evaluation of the Mathieu functions is very cumbersome: the best approach [13] seems to be the expansion of those functions in a series of (more tractable) Bessel functions. As a consequence, the eigenvalues of an elliptic guide must be computed numerically, looking for the zeroes of a suitable series of Bessel functions. It is not a surprise, therefore, that the availability of a closed-form solution in this case have not prevented different numerical techniques to be proposed, aiming at a simpler procedure or, even, at a greater accuracy [14-17]. For resonant cavities, the approach is the same, and the allowed geometries are the cylindrical (with a separable section) and the spherical one .

1.2) SEMI-ANALYTICAL

Although in many practical cases analytical solution cannot be obtained, we must resort to numerical approximate solution. Is often possible to replace the problem of integrating a differential equation by the equivalent problem of seeking a function that gives a minimum value of some integral. Problem of this type are called variational methods [18], and be considered as semi analytical.

The eigenvalues of the equation can be expressed as a suitable (quadratic) functional of the eigenfunctions. Such functional reach its extreme value for the true eigenfunction. If we compute the functional in a different function (an approximation of the true eigenfunction), we obtain an approximate value of the eigenvalue which, due to the variational nature of the functional, is quadratic in the approximation error of the function. For waveguide problem, different functionals can be used. Some of them require the approximate function to fulfil the boundary condition, others don't, and are therefore more effective. A drawback of this approach is that it is taylored to evaluate the eigenvalues only.

The Rayleigh - Ritz method is a generalization of this method, which obtain an approximation of both eigenvalues and eigenfunctions. This method is based on pioneering work by Lord Rayleigh in 1870 and improvements by Ritz in 1909.

3

The test function for the functional is expressed as a linear combination of known functions and the solution consists of determining the parameters in the combination forcing the maximum condition. This determination involves substitution of the linear combination into the functional and then differentation with respect to each parameter.

1.3) NUMERICAL METHOD

The analytical methods are not valid if the integral region of the structure is complex and therefore we are forced to use numerical methods. Since the problem at hand is the solution of partial different equation (PDE), the most popular numerical methods available for solving PDE are finite-elements method, and finite difference method.

1.3.a) FINITE-ELEMENTS METHOD

The basic concept of the finite-element method [19] is that although the behavior of a function may be complex when viewed over a large region, a simple approximation may suffice for a small subregion. The total region is therefore divided into a number of small non overlapping subregions called *finite elements.* In two dimensions we usually use polygons and the simplest polygons are triangles and squares.

(a)   (b)   (c)   (d)
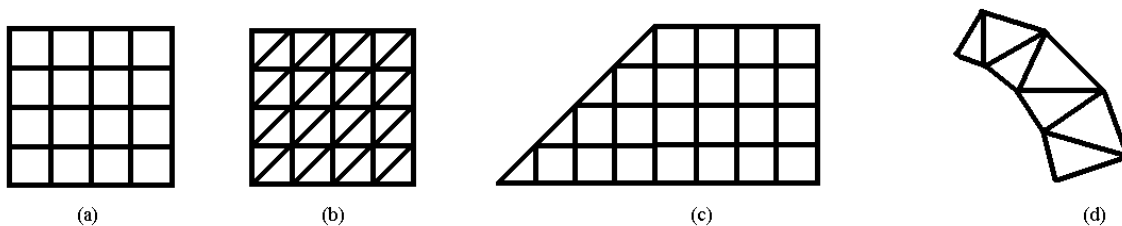
Fig. 1.3.1 a) Division of a region into square elements. b) Division of a region into right Isosceles triangles. c) Division of a region into triangles and squares. d) Division of an irregular region into triangles.

Figure 1.3.1a shows a region divided into squares and Fig. 1.3.1b shows the same region divided into isosceles right triangles. Sometimes as illustrated in Fig. 1.3.1c a combination of triangles and squares is useful. One of the advantages of using triangles is that a fairly arbitrary region can be more easily approximately covered by a set of triangles, as shown in Fig. 1.3.1d. Regardless of the shape of the elements, the field is approximated by a different expression over each element, but where the edges of adjoining elements overlap, the field representations must be chosen as to maintain the continuity of the field. The equations to be solved are usually not stated in terms of the field variables but in terms of an integral-type functional such as energy. The functional is chosen such that the field solution makes the functional stationary. The total functional is the sum of the integral over each element. This technique allow to analyze every type of structure using a suitable "mesh", but needs a big number of points which leads to an increase in the computational load of the matricial problem, and consequentally an increase of the computational burden. In particular, the more curvilinear is the structure's edge the more the mesh will be done in those areas, and the more the computational load increases.

1.3.b)   FINITE-DIFFERENCE METHOD

The finite difference approach (FD) is a method for the solution of numerical partial differential equations. It is based on the replacement of the derivatives with a finite approximation [20]. Therefore, the solution is computed only on a finite sets of points (discretization grid, or mesh)

The most popular FD approach is based on the use of a standard four-point FD approximation [21] of the Laplace operator. But it requires a rectangular discretization grid, and therefore a boundary with all sides parallel to the rectangular axes. As a consequence, many geometries cannot be dealt with exactly with this approach, requiring a staircase approximation of the boundaries (see Fig.1.41). In order to achieve good results comparable with

analytic ones, the discretization step should be significantly reduced, and this operation increases the number of points and consequentally there's an increase of the computational load. This problem makes the FD standard not suitable for curvilinear edge structures analysis. Moreover, the standard FD approach requires different discretization grids for TE and TM modes. On the other hand, FD methods present many advantages:

- Easy implementation
- Flexibility
- Good precision
- Low computational load compared to FEM methods.
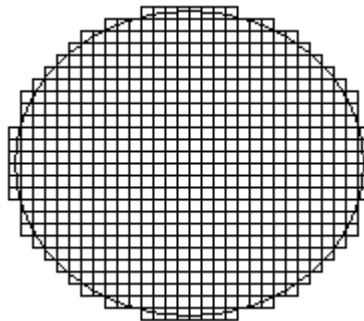
Fig. 1.4.1   Division of a region into square cells

The aim of this thesis is to overcame the drawbacks of FD.

The discretization through a cartesian grid comes from the expression of Laplace operator in (1.1.1) in Cartesian coordinates. It has been tried to use a different grid derived from a form of Laplace operator written in a form suitable to the considered structure.

The first test involved a circular guide, using the Laplace operator and a discretization grid in polar coordinates. We have obtained good results with a low computational load compared to FEM technique and an high precision in the results comparable with analytic results. In particular, as we shall see in chapter

IV, it's been considered the use of circular and elliptic grids for the study of circular [22 - 25] and elliptic [23,25] waveguides.

An other problem, described in chapter 3, is the Laplace operator's redefinition based on boundary conditions in order to use a single grid [26,27]. This is important, e.g. in numerical mode matching analysis of waveguide junctions reducing the computational load (complexity) and the processing time.

The FD is applied to the classical scalar potential, so to compute the waveguide modes numerical derivatives must be used. For regular-shaped guides, the use of numerical derivatives is reasonably accurate and is very easy to implement, but this isn't true for waveguides with irregular section and resonant cavities. In this cases it isn't possible to use the scalar potential, and it is necessary, in order to calculate the modes to introduce a vector FD in this thesis, this problem has been faced introducing the vector finite difference, but in a simplified form respect to the methods present in literature. The computation of the TE and TM modes has been studied by solving the Helmoholtz equation using the vectorial finite differences method, reducing to a constrained eignevalues problems. The vector finite difference approximation of the vector Helmholtz eigenvalues equation on a Cartesian [28,29] an curvilinear grid [23-25] have been considered. In chapter V we present a FD technique for the computation of modes and eigenvalues of a waveguide whose boundary is irregular, such as polygonal, or consisting of segments and circular arcs [22,30], taking exactly into account the boundary of the waveguide and therefore with no loss of accuracy.

Chapter II

WAVEGUIDE MODES

INTRODUCTION

In this chapter we deal with the propagation in guiding structures. First, we use Maxwell equations to describe the field of these structures and then we decompose in TE,TM field using the boundary conditions. Finally, we explain the TE and TM modes..

2.1) MAXWELL EQUATION

Maxwell equations in the Domain Frequency for an homogeneous material, in the absence of sources, take the form

$$2.1.1.) \quad \begin{cases} \nabla x \vec{E} = -j\omega\mu\vec{H} \\ \nabla x \vec{H} = j\omega\varepsilon\vec{E} \end{cases}$$

As we are interested in the study of the propagation in a guiding structure, the direction of propagation, which we assume as "z" direction of a reference system, shall be a preferential direction of the problem. For this reason we decompose all vectors in two components: one transverse and another one alongside "z" : $\vec{E} = \vec{E_t} + E_z \vec{i_z}$, and in a similar way for H. It is also convenient to separate the transverse and longitudinal parts of operator $\nabla : \nabla = \vec{\nabla_t} + \frac{\partial}{\partial z}\vec{i_z}$

To solve the (2.1.1), we can use the scalar potentials of Hertz Debye defined for TE and TM fields. For TM field we have $H_z = 0$, so that, using the $\vec{A}$ potential, we can write:

2.1.2.) $\quad \vec{i}_z \times \vec{H} = \vec{i}_z \cdot \left(\nabla x \vec{A} \right) = \vec{i}_z \cdot \left(\nabla_t x \vec{A}_t \right) = 0$

Since $\nabla_t x \vec{A}_t$ has only the z component , then $\nabla_t x \vec{A}_t = 0$ and from this it follows

that there exists a longitudinal potential $\vec{A}$:

2.1.3.) $\quad \vec{A} = \vec{i}_z \cdot \mu \Psi$

that allows we obtain any field TM (with $\vec{H}_z = 0$). We obtained:

2.1.4.) $\begin{cases} \vec{H}_t = \nabla x \left(\Psi \vec{i}_z \right) = \nabla \Psi x \vec{i}_z \\ j \omega \varepsilon \vec{E} = \nabla x \vec{H}_t = \nabla x \nabla x \left(\Psi \vec{i}_z \right) = \nabla \nabla \cdot \left(\Psi \vec{i}_z \right) - \nabla^2 \Psi \vec{i}_z = \dfrac{\partial}{\partial z} \nabla \Psi - \nabla^2 \Psi \vec{i}_z = \dfrac{\partial}{\partial z} \nabla_t \Psi - \nabla_t^2 \Psi \vec{i}_z \end{cases}$

The equations (2.1.4) allow also to separate the longitudinal and transverse part

of $\vec{E}$. To compute Ψ, we start by Maxwell equation to get:

$\nabla x \nabla x \vec{H} = j \omega \varepsilon \nabla x \vec{E} = j \omega \varepsilon \left(-j \omega \mu \vec{H} \right) = \beta^2 \vec{H}$ and substituting the first to (2.1.4)

2.1.5.) $\nabla x \nabla x \nabla x \left(\Psi \vec{i}_z \right) - \beta^2 \nabla x \left(\Psi \vec{i}_z \right) = \nabla x \left[\nabla x \nabla x \left(\Psi \vec{i}_z \right) - \beta^2 \left(\Psi \vec{i}_z \right) \right] = 0$

the term in the brackets is equal to:

2.1.6.) $\nabla \nabla \cdot \left(\Psi \vec{i}_z \right) - \nabla^2 \Psi \vec{i}_z - \beta^2 \Psi \vec{i}_z = \dfrac{\partial}{\partial z} \nabla \Psi - \nabla^2 \Psi \vec{i}_z - \beta^2 \Psi \vec{i}_z$

9

The rotor of the first term is null and therefore we are left with:

$$2.1.7.) \quad \nabla x \overrightarrow{i_z}\left[\nabla^2\Psi + \beta^2\Psi\right] = 0$$

Then $\overrightarrow{i_z}\left[\nabla^2\Psi + \beta^2\Psi\right] = \nabla\chi'$ where χ' dependes only by z.

Therefore $\nabla^2\Psi + \beta^2\Psi = f(z)$. The solution of this equation is the sum of a particular integral (and there is a function only of z) and the integral of the general homogeneous. The particular integral isn't part of the field and remains:

$$2.1.8.) \quad \nabla^2\Psi + \beta^2\Psi = 0$$

For duality any field TE have a similar expression with a potential ϕ such that $\nabla^2\phi + \beta^2\phi = 0$, as:

$$2.1.9.) \quad \begin{cases} \overrightarrow{E_t} = -\nabla x \left(\phi\,\overrightarrow{i_z}\right) = -\nabla_t\phi \times \overrightarrow{i_z} \\ j\omega\varepsilon\overrightarrow{H} = -\dfrac{\partial}{\partial z}\nabla_t\phi - \nabla_t^2\phi\,\overrightarrow{i_z} \end{cases}$$

2.2) DECOMPOSITION INTO TE AND TM FIELDS

Every electromagnetic field can be expressed as the sum of a TE and a TM field (in absence of sources). Let's consider a field with $E_z \neq 0$, $H_z \neq 0$ and a function $\widetilde{\Psi}$ which satisfies the Poisson equation:

$$2.2.1.) \quad \nabla_t^2\widetilde{\Psi} = -j\omega\varepsilon E_z$$

If $\widetilde{\Psi}$ is considered as Hertz-Debye potential, it allows to determinate a TM-field ($\vec{E}^{TM}$, $\vec{H}^{TM}$) with the same z-component of the assigned field. Therefore ($\vec{E} - \vec{E}^{TM}$, $\vec{H} - \vec{H}^{TM}$) is a TE-field. Finally, the decomposition is:

$$2.2.2.) \quad \begin{cases} \vec{E} = \left(\vec{E} - \vec{E}^{TM}\right) + \vec{E}^{TM} \\ \vec{H} = \left(\vec{H} - \vec{H}^{TM}\right) + \vec{H}^{TM} \end{cases}$$

In general, every field can be determined from the potentials Ψ, ϕ

$$2.2.3.) \quad \begin{cases} \vec{E_t} = \dfrac{1}{j\omega\varepsilon}\dfrac{\delta}{\delta z}\nabla_t\Psi - \nabla_t\phi \, x \, \vec{i_z} \\ \vec{H_t} = \nabla_t\Psi \, x \, \vec{i_z} + \dfrac{1}{j\omega\mu}\dfrac{\partial}{\partial z}\nabla_t\phi \end{cases} \quad \begin{cases} E_z = -\dfrac{1}{j\omega\varepsilon}\nabla_t^2\Psi \\ H_z = -\dfrac{1}{j\omega\mu}\nabla_t^2\phi \end{cases}$$

2.3) TE MODES

The analysis of TEM [31] field is simplified by the possibility of separating the longitudinal variation from the transverse one. In the case of TE or TM [6] fields it's therefore convenient to seek solutions which have an factorized representation

$$2.3.1.) \quad \begin{cases} \vec{E_t} = V(z)\vec{e}(\vec{t}) \\ \vec{H_t} = I(z)\vec{h}(\vec{t}) \end{cases}$$

where V,I have no physical meaning, thus the impedance's choice will be based only on a matter of convenience . In terms of Hertz-Debye potentials

$$2.3.2.) \begin{cases} \vec{E_t} = V(z)\vec{e} = -\nabla_t\phi \times \vec{i_z} \\ \vec{H_t} = I(z)\vec{h} = \dfrac{1}{j\omega\mu}\dfrac{\partial}{\partial z}\nabla_t\phi \\ H_z = -\dfrac{1}{j\omega\mu}\nabla_t^2\phi \end{cases}$$

The field's factorization implies a similar factorization for the potentials

$\phi = \dfrac{1}{k_t}\phi_0(\vec{t})V(z)$, $\dfrac{1}{k_t}[m^{-1}]$ is an arbitrary constant. Thus

$$2.3.3.) \begin{cases} \vec{e} = -\dfrac{1}{k_t}\nabla_t\phi_0 \times \vec{i_z} \\ I(z)\vec{h} = \dfrac{1}{j\omega\mu}\dfrac{\delta}{\delta z}\nabla_t\phi_0 \dfrac{dV}{dz} \Rightarrow \vec{h} = -\dfrac{1}{k_t}\nabla_t\phi_0 \Rightarrow \vec{e} = \vec{h}\times\vec{i_z} \\ -\dfrac{dV}{dz} = j\omega\mu I \end{cases}$$

From the expression for ϕ

$$2.3.4.) \quad V\nabla_t^2\phi_0 + \phi_0 V'' + \beta^2 V\phi_0 = 0$$

$V''(z)$ is proportional to $V(z)$. We can put

$$2.3.5.) \quad V(z) = -\dfrac{1}{k_z^2}V''(z) = j\omega\mu\dfrac{1}{k_z^2}\dfrac{dI}{dz}$$

with k_z^2 constant. We obtain the equations of transmission lines

$$2.3.6.) \begin{cases} -\dfrac{dV}{dz} = j\omega\mu I \\ -\dfrac{dI}{dz} = j\dfrac{k_z^2}{\omega\mu}V \end{cases} \Rightarrow L_{eq} = \mu, \quad C_{eq} = \dfrac{k_z^2}{\omega^2\mu}$$

k_z is the propagation constant, while the impedance is

$$2.3.7.) \; Z = \sqrt{\dfrac{L_{eq}}{C_{eq}}} = \dfrac{\omega\mu}{k_z}$$

This expression for Z is directly linked to the choice $\vec{e} = \vec{h} \times \vec{i_z}$: in general $\vec{e} = A\vec{h} \times \vec{i_z}$, if A varies properly we can obtain any value for Z. Thus V,I,Z are useful in calculations but (for field non-TEM) without any physical meaning.

If we substitute $V^{''} = k_z^2 V$ in the ϕ equation

$$2.3.8.) \; \nabla_t^2 \phi_0 + \left(\beta^2 - k_z^2\right)\phi_0 = 0$$

and, if $k_t = \sqrt{\beta^2 - k_z^2}$

$$2.3.9.) \; \nabla_t^2 \phi_0 + k_t^2 \phi_0 = 0$$

As regards the boundary conditions (fig. 2.3.1), it must be

$\vec{e} \cdot \vec{i_c}\Big|_c = 0$, that is $-\vec{h} \times \vec{i_z} \cdot \vec{i_c}\Big|_c = -\vec{h} \cdot \vec{i_n}\Big|_c = -\dfrac{\delta\phi}{\delta n}\Big|_c = 0$.

13
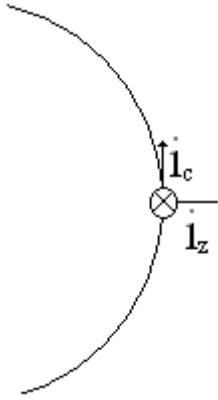
Fig. 2.3.1. Position of versors from the contour of the conductor

So the ϕ potential is obtained by solving the following problem

$$2.3.10.) \quad \begin{cases} \nabla_t^2 \phi + k_t^2 \phi = 0 \\ \dfrac{\delta \phi}{\delta n}\bigg|_c = 0 \end{cases}$$

since ϕ must be not identically zero.

(2.3.10) is an eigenvalues problem, its solutions are couples $\left(k_{tn}^2, \phi_n\right)$ eigenvalue-eigenvector such that if $k_t^2 = k_{tn}^2$ the equation has non-trivial solutions proportional to ϕ_n, while if $k_t^2 \neq k_{tn}^2$, $\forall m$ the only solution is $\phi = 0$.

It can be shown that the eigenvalues of k_t^2 are real and non negative, and that eigenfunctions and eigenvalues are a countable orthogonal (or at least orthogonalizable) and complete set.

Every function ϕ results in a mode, namely a field which can exist alone in the waveguide. The functions V,I and the corresponding vectors $\vec{e}$, $\vec{h}$ are respectively named scalar and vector mode function.

Finally, we note that H_z depends on $V(z)$:

2.3.11.) $\qquad H_z = -\dfrac{1}{j\omega\mu}\dfrac{V(z)}{k_t}\nabla_t^2\phi_0 = \dfrac{k_t V(z)}{j\omega\mu}\phi_0$

2.4) TM MODES

For the TM modes, it's possible to achieve a factorized solution. Starting from $\Psi = \dfrac{1}{k_t} I(z)\Psi_0\left(\vec{t}\right)$, we have:

2.4.1.) $\begin{cases} \vec{H_t} = I(z)\vec{h} = \dfrac{1}{k_t}I(z)\Psi_0\times\vec{i_z} \Rightarrow \vec{h} = \dfrac{1}{k_t}\nabla_t\Psi_0 x\vec{i_z} \\[4mm] \vec{E_t} = V(z)\vec{e} = \dfrac{1}{j\omega\mu}\dfrac{dI}{dz}\dfrac{1}{k_t}\nabla_t\Psi_0 \Rightarrow \vec{e} = -\dfrac{1}{k_t}\nabla_t\Psi_0 \Rightarrow \vec{h} = -\vec{e}\times\vec{i_z} \end{cases}$

Again for the mode scalar function V and I, we have

2.4.2.) $\begin{cases} -\dfrac{dI}{dz} = j\omega\varepsilon V \\[4mm] I''\nabla_t^2\Psi_0 + I\nabla_t^2\Psi_0 + \beta^2 I\Psi_0 = 0 \Rightarrow I'' = k_z^2 I \end{cases}$

And thus they fulfill the line equations:

2.4.3.) $\begin{cases} -\dfrac{dI}{dz} = j\omega\varepsilon V \\[4mm] -\dfrac{dV}{dz} = \dfrac{1}{j\omega\varepsilon}\left(-k_z^2 I\right) = j\dfrac{k_z^2}{\omega\varepsilon}I \end{cases}$

with $L_{eq} = \mu$, $C_{eq} = \dfrac{k_z^2}{\omega^2 \mu}$, $Z = \dfrac{k_z}{\omega \varepsilon} I$. Finally:

$$2.4.4.) \quad \nabla_t^2 \Psi_0 + \left(\beta^2 - k_z^2 \right) \Psi_0 = \nabla_t^2 \Psi_0 + k_t^2 \Psi_0 = 0$$

Since $\vec{i}_n \times \vec{E}$ has two components (transverse and along z), in this case we have two boundary conditions.

From $\vec{e} \cdot \vec{i}_c \big|_c = 0$ we have $\dfrac{\delta \Psi_0}{\delta c} \bigg|_c = 0$, that is $\Psi_0 = 0$ constant on the boundary.

Moreover $\vec{E_z} = -\dfrac{1}{j\omega\varepsilon} \dfrac{I(z)}{k_t} \nabla_t^2 \Psi_0 = -\dfrac{k_t I}{j\omega\varepsilon} \Psi_0$, thus from $E_z \big|_c = 0$ we have

$\Psi_0 \big|_c = 0$, that is the condition to be imposed (with $k_t \neq 0$, otherwise it would be a TEM mode). A similar reasoning can be made for the TE case.

It is noted that the mode with the smallest $k_t \neq 0$ is always a TE mode.

Since the discussion is analog to the TE case, we report directly the eigenvalue problem for the TM case.

$$2.4.5.) \quad \begin{cases} \nabla_t^2 \Psi_0 + k_t^2 \Psi_0 = 0 \\ \Psi_0 \big|_c = 0 \end{cases}$$

Chapter III

COMPUTATION OF WAVEGUIDE MODES USING FINITE DIFFERENCE:
RECTANGULAR WAVEGUIDES

INTRODUCTION

In this chapter we shortly discuss the numerical solution of partial differential equations using finite difference (FD) method.   Then, we focus on the eigenvalue problems in particular, we look at the problem of solving the eigenvalue problems (2.3.10) and (2.4.5) in a rectangular waveguide. Since the laplacian operator determines the spatial behavior of solutions, this operator will be approximated in the form best adapted to the problem at hand. The standard calculation of the waveguide modes using FD requires the use of two different grids, namely one for TE modes and the other for TM modes, due to the different boundary condition. In this way, the FD matrix can include the boundary condition, so that the eigenfunction problem reduces to a matrix eigenvalue problem.

After the discussion of this standard solution, we consider a new approximation of Laplacian operator for use on a single grid for the computation of all waveguide modes. This approximation should include the boundary condition, so that the computational burden is the same.

Eigenvalue problems (2.3.10) and (2.4.5) compute the Hertz-Debye potential of waveguide modes. The mode vectors can be computed only using numerical derivatives, which is an operation strongly sensitive to noise. To avoid such derivatives, we present also the direct computation of mode vector in a waveguide, using a finite difference (FD) approximation of the vector Helmholtz equation on a Cartesian grid. Since we are mainly interested in using those modes in MoM, the entire development will be expressed in term of equivalent magnetic surface currents. At variance of the scalar problem, additional

conditions are required on the mode vector. These conditions will be included as constrains into the eigenvalue problem.

3.1) FINITE DIFFERENCE SCHEME

The finite difference scheme (FD) is a method for partial differential equations numerical solution and is based on a discrete derivation operator introduction, obtained from the derivative's definition via difference quotients [20].

In a single variable function $f(x)$, the first derivate is denoted by:

$$3.1.1.) \quad f'(x) = \frac{df(x)}{dx} \equiv \lim_{h \to 0} \frac{f(x+h) - f(x)}{h}$$

that can then be reasonably approximated with the only difference quotient:

$$3.1.2.) \quad f'(x) \approx \frac{f(x+h) - f(x)}{h}$$

with h sufficiently small but finite. The last expression is commonly referred to as forward finite difference as it is evaluated using only values $\geq x$.

Similarly it is possible to define the backward approximation of the derivative:

$$3.1.3.) \quad f'(x) \approx \frac{f(x) - f(x-h)}{h}$$

Both equations provide a first order of approximation of $f'(x)$, Therefore, the error is proportional to h. Another possibility is to define a central approximation:

$$3.1.4.) \quad f'(x) \approx \frac{f(x+h) - f(x-h)}{2h}$$

It has an accuracy of second order with an error proportional to h^2. Similarly, defining higher order derivatives is possible, but following a different approach based on the Taylor expansion, which will be described in detail below, is more convenient.

The approximation of a partial differential equations system by using the finite difference method for solving a problem with the boundary conditions consists of three steps:

- the domain of definition of the continuous problem Ω, including the border $\partial\Omega$, is replaced by a domain consisting of a discrete finite set of points;

- the derivatives that appear in the expression of the operator are approximated on the discrete domain with finite differences;

- in the discrete approximation of the differential operators the boundary conditions are included.

In this way the continuous problem is approximated with a discrete problem, more specifically with a system of linear equations of finite size, which can be solved with the techniques of classic resolution of linear systems. The finite difference method is particularly effective when the border $\partial\Omega$" has particular symmetries, otherwise it may be difficult to solve.

Here is an example of this procedure, in particular the solution of a one-dimensional Dirichlet problem;

Determine the function:

3.1.5.) $\qquad u = u(x)$

defined in the interval $[0, l]$, that verifies the equation:

19

3.1.6.) $\qquad \dfrac{d^2u}{dx^2} = \lambda x \qquad per \;\; x \in (0,l)$

with boundary conditions:

3.1.7.) $\qquad \begin{cases} u(0) = g_0 \\ u(l) = g_1 \end{cases}$
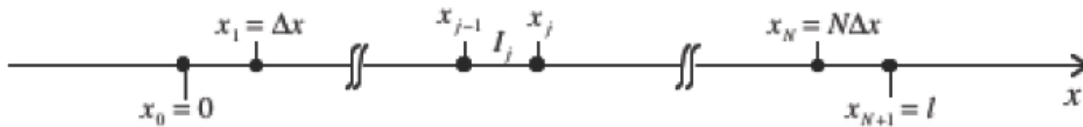
Fig. 3.1.1. Monodimension grid for the Dirichlet problem

We introduce in the range [0, l] a partition $I_j = \left[x_{j-1}, x_j \right]$ con $j = 1,2,.....,N,N+1$, $x_0 = 0$ e $x_{N+1} = l$, (see figures 3.1.1). We assume only for sake of simplicity that the intervals I_j have all the same lenght Δx,

3.1.8.) $\qquad \Delta x = \dfrac{l}{N+1}$

We indicate with $u_i = u(x_i)$ $j = 1,2,.....,N,N+1$ the sample values of the unknown function $u(x)$ on grid points of the domain [0, l] . From the boundary condition (3.1.7) we have:

3.1.9.) $\qquad u_0 = g_0, \;\; u_{n+1} = g_1$

We want to determine $u_1, u_2,.....,u_N$ with a numerical method. It is possible to have N equations for the values $u_1, u_2,.....,u_N$ by imposing that (3.1.6) be true in

the grid $x_1, x_2, \ldots, x_N$ and approximating the second derivate through the finite difference. Imposing that the equation (3.1.1) will be verified in the internal grid point $x_1, x_2, \ldots, x_N$ it comes out that:

3.1.10.) $\qquad \left.\dfrac{d^2u}{dx^2}\right|_{x=x_i} = \lambda x_i \quad per \quad i = 1, 2, \ldots, N$

To translate the (3.1.10) into equations (as we will see approximated) for the values $u_1, u_2, \ldots, u_N$ we should express $\left.\dfrac{d^2u}{dx^2}\right|_{x=x_i}$ as a function of samples. If the function u is sufficiently regular in a neighborhood of the generic point $\overline{x} \in (0, l)$, then the operator:

3.1.11.) $\qquad \partial^2 u(\overline{x}) \equiv \dfrac{u(\overline{x} + \Delta x) - 2u(\overline{x}) + u(\overline{x} - \Delta x)}{\Delta x^2}$

represents a good approximation of the second derivate. Indeed it has:

3.1.12.) $\qquad \dfrac{d^2u}{dx^2} = \partial^2 u(\overline{x}) + O(\Delta x^2)$

The demonstration of (3.1.12) is quite simple. Developing through the Taylor formula $u(\overline{x} + \Delta x)$ e $u(\overline{x} - \Delta x)$ in the neighborhood of $x = \overline{x}$ we obtain:

3.1.13.) $\qquad u(\overline{x} + \Delta x) = u(\overline{x}) + \left.\dfrac{du}{dx}\right|_{x=\overline{x}} \cdot \Delta x + \dfrac{1}{2}\left.\dfrac{d^2u}{dx^2}\right|_{x=\overline{x}} \cdot \Delta x^2 + \dfrac{1}{6}\left.\dfrac{d^3u}{dx^3}\right|_{x=\overline{x}} \cdot \Delta x^3$

21

$$3.1.14.) \qquad u\left(\overline{x}-\Delta x\right)=u\left(\overline{x}\right)-\frac{du}{dx}\bigg|_{x=\overline{x}}\cdot\Delta x+\frac{1}{2}\frac{d^2u}{dx^2}\bigg|_{x=\overline{x}}\cdot\Delta x^2-\frac{1}{6}\frac{d^3u}{dx^3}\bigg|_{x=\overline{x}}\cdot\Delta x^3$$

Where $x_+\in\left[\overline{x},\overline{x}+\Delta x\right]$ and $x_-\in\left[\overline{x}-\Delta x,\overline{x}\right]$. Summing member to member the (3.1.13) and (3.1.14) we have:

$$3.1.15.) \qquad \frac{d^2u}{dx^2}\bigg|_{x=\overline{x}}=\frac{u\left(\overline{x}+\Delta x\right)-2u\left(\overline{x}\right)+u\left(\overline{x}-\Delta x\right)}{\Delta x^2}+O\left(\Delta x^3\right)$$

that is:

$$3.1.16.) \qquad \frac{d^2u}{dx^2}\bigg|_{x=x_i}\cong\frac{u_{i+1}-2u_i+u_{i-1}}{\Delta x^2}$$

3.2) STANDARD FINITE DIFFERENCE SCHEME

Let use consider a rectangular waveguide. As described in chapter II both TE and TM modes can be found from a suitable scalar eigenfunction ϕ, solution of the Helmothz equation:

$$3.2.1.) \qquad \nabla_t^2\phi+k_t^2\phi=\frac{\partial^2\phi}{\partial x^2}+\frac{\partial^2\phi}{\partial y^2}+k_t^2\phi=0$$

 with the boundary condition (BC)

$$3.2.2.) \qquad \frac{\partial\phi}{\partial n}=0 \qquad \text{TE modes}$$

$$3.2.3.) \qquad \phi=0 \qquad \text{TM modes}$$

22

at the boundary of the rectangular waveguide.

Numerical solution of this eigenvalue problem using the FD approach requires that both the equation (3.2.1) and the BC (3.2.2,3.2.3) are replaced by a discretizead version e.g., replacing derivatives with finite approximations. This transforms (3.2.1) into a matrix eigenvalue problem, whose eigenvectors contain the samples of ϕ at the discretization nodes. Assuming a regular Cartesian grid with spacing $\Delta x, \Delta y$, and letting $\phi_{i,j} = \phi(i\Delta x, j\Delta y)$ as sample values of $\phi(x,y)$, we need a discretized version of (3.2.1) on each sampling point. For a point P see (fig 3.2.1) we can use a second-order Taylor expression as :
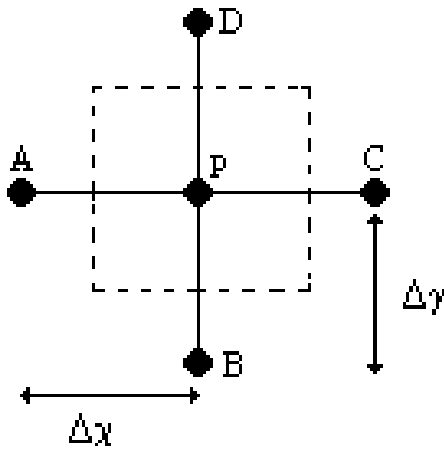
Fig. 3.2.1 Internal point of grid TE and TM

$$3.2.4.) \qquad \phi_B = \phi_P + \frac{\partial \phi}{\partial y}|_P \cdot (-\Delta y) + \frac{1}{2}\frac{\partial^2 \phi}{\partial y^2}|_P \cdot (-\Delta y)^2$$

$$3.2.5.) \qquad \phi_D = \phi_P + \frac{\partial \phi}{\partial y}|_P \cdot (\Delta y) + \frac{1}{2}\frac{\partial^2 \phi}{\partial y^2}|_P \cdot (\Delta y)^2$$

Adding the two last equations we find:

23

3.2.6.) $$\frac{\partial^2 \phi}{\partial y^2}\Big|_P = \frac{1}{\Delta y^2} \cdot (\phi_B + \phi_D - 2\phi_P)$$

Likely in x direction

3.2.7.) $$\frac{\partial^2 \phi}{\partial x^2}\Big|_P = \frac{1}{\Delta x^2} \cdot (\phi_A + \phi_C - 2\phi_P)$$

Therefore to be substituted in (3.2.1)

3.2.8.) $$\nabla_t^2 \phi_p = \frac{\phi_A}{\Delta x^2} + \frac{\phi_C}{\Delta x^2} + \frac{\phi_B}{\Delta y^2} + \frac{\phi_D}{\Delta y^2} + \left(\frac{2}{\Delta x^2} + \frac{2}{\Delta y^2}\right)\phi_P$$

This equation can be used for all internal points to get the discretized form of (3.2.1)

3.2.9.) $$\frac{\phi_{i,j-1}}{\Delta x^2} + \frac{\phi_{i,j+1}}{\Delta x^2} + \frac{\phi_{i-1,j}}{\Delta y^2} + \frac{\phi_{i+1,j}}{\Delta y^2} + \left(\frac{2}{\Delta x^2} + \frac{2}{\Delta y^2}\right)\phi_{i,j} = -k_t^2 \phi_{i,j}$$

Equation (3.2.9) cannot be used for boundary points, where BC (3.2.2) or (3.2.3) must be enforced. The standard solution is to use different grids for TE and TM, as in fig (3.2.3).
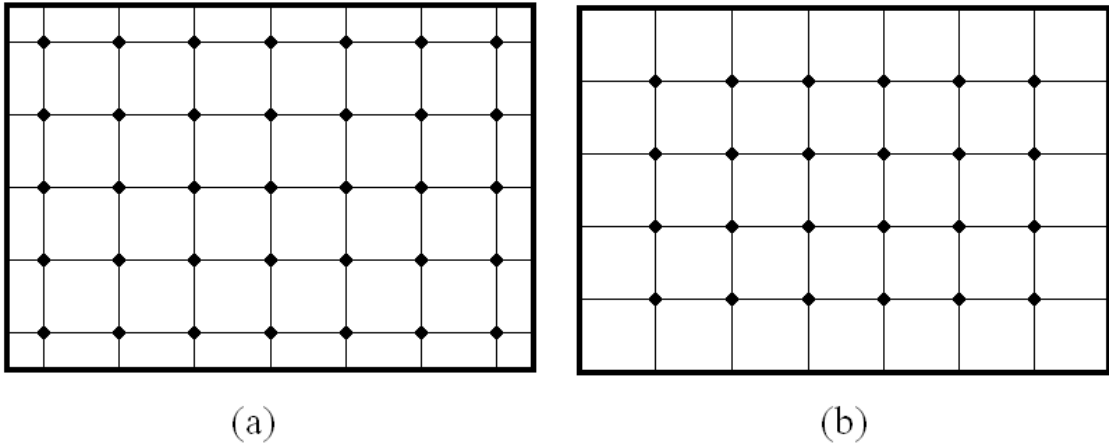
Fig. 3.2.3. Standard TE and TM grid, as suggested from BC

We first discuss for TE case an external point P, we consider the three nearby points A,B and C ad shown in fig (3.2.4).

(a) case (TE)   (b) case (TM)
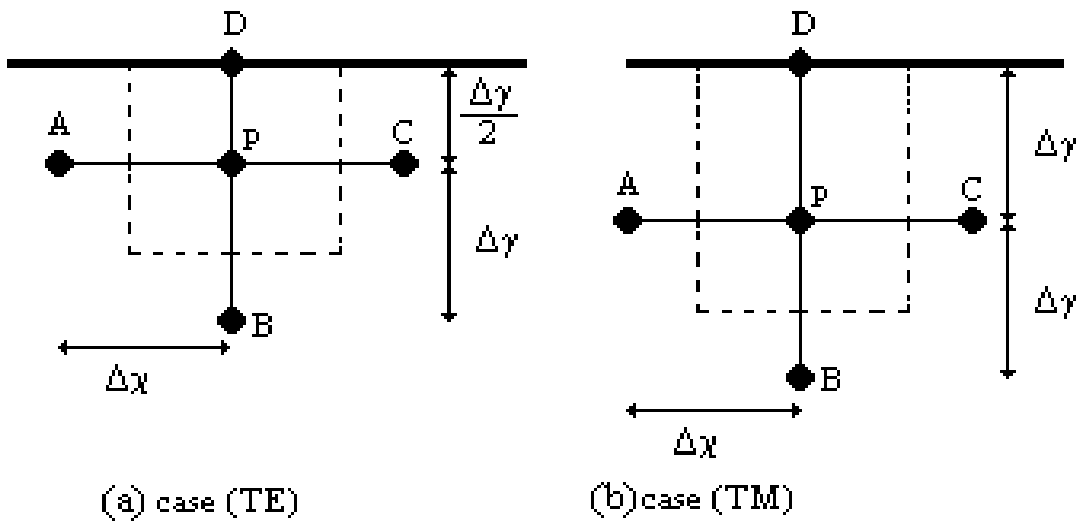
Fig. 3.2.4. Boundary point for TE case and TM case

25

We can replace (3.2.5) by a first-order approximation $\phi_P = \phi_D + \left.\dfrac{\partial \phi}{\partial y}\right|_D \cdot \left(\dfrac{\Delta y}{2}\right) = \phi_D$

since the BC require $\left.\dfrac{\partial \phi}{\partial y}\right|_D = 0$. As a consequence (3.2.6) becomes:

$\left.\dfrac{\partial^2 \phi}{\partial y^2}\right|_P = \dfrac{1}{\Delta y^2} \cdot (\phi_B - \phi_P)$ and (3.2.8) is replaced by:

$$3.2.10.) \qquad \dfrac{\phi_A}{\Delta x^2} + \dfrac{\phi_C}{\Delta x^2} + \dfrac{\phi_B}{\Delta y^2} + \left(\dfrac{2}{\Delta x^2} + \dfrac{1}{\Delta y^2}\right)\phi_P \qquad TE$$

For TM case, on the other hand, $\phi_d = 0$ and since D is a sampling point, we can put directly in to (3.2.8) to get:

$$3.2.11.) \qquad \dfrac{\phi_A}{\Delta x^2} + \dfrac{\phi_C}{\Delta x^2} + \dfrac{\phi_B}{\Delta y^2} + \left(\dfrac{2}{\Delta x^2} + \dfrac{2}{\Delta y^2}\right)\phi_P \qquad TM$$

The discretized eigenvalues problems (2.3.10), (2.4.5) have the form:

$Ax = \lambda x$

where A is a matrix (n,n) , obtained collecting equations (3.2.9),(3.2.10) for TE case, and equations (3.2.9),(3.2.11) for TM case. The discretized eigenvalues problem obtained must be solved by a numerical routine. As a matter of fact, an highly sparse matrix us obtained, so the sparse matrix routines of Matlab has been used.

3.3) FINITE DIFFERENCE SINGLE GRID TE EVALUATION OF TE AND TM MODES IN METALLIC WAVEGUIDES

In order to use a single grid we need to enforce both BC on a single grid. We describe here in detail the use of TE grid [26] (fig 3.2.3a) for TM modes.

Only the inclusion of BC into the eigenvalue matrix problems is modified, so let us consider again the external point P on the TE grid (fig 3.2.4 a). Since the BC (3.2.3) require $\phi_D = 0$, we can express the potential in B and D through a Taylor approximation:

3.3.1.)
$$\phi_B = \phi_P + \left.\frac{\partial \phi}{\partial y}\right|_P \cdot (-\Delta y) + \frac{1}{2}\left.\frac{\partial^2 \phi}{\partial y^2}\right|_P \cdot (-\Delta y)^2$$

$$\phi_D = \phi_P + \left.\frac{\partial \phi}{\partial y}\right|_P \cdot \left(\frac{\Delta y}{2}\right) + \frac{1}{2}\left.\frac{\partial^2 \phi}{\partial y^2}\right|_P \cdot \left(\frac{\Delta y}{2}\right)^2$$

Adding $\phi_B + 2 \cdot \phi_D$ we get: $\left.\dfrac{\partial^2 \phi}{\partial y^2}\right|_P = \dfrac{4}{3 \cdot (\Delta y)^2} \cdot (\phi_B + 2\phi_D - 3\phi_P)$

and recalling that the BC prescribes $\phi_D = 0$, we get:

3.3.2.)
$$\left.\frac{\partial^2 \phi}{\partial y^2}\right|_P = \frac{4}{3 \cdot (\Delta y)^2} \cdot (\phi_B - 3\phi_P)$$

which, together with (3.2.7) gives the discretized form of the laplacian

3.3.3.)
$$\nabla_t^2 \phi_P = \frac{\phi_A}{(\Delta x)^2} + \frac{\phi_C}{(\Delta x)^2} + \frac{4}{3 \cdot (\Delta y)^2} \phi_B + \left(\frac{2}{(\Delta x)^2} + \frac{4}{(\Delta y)^2}\right) \phi_P$$

as a replacement of (3.2.11) for external points in TM modes.

Let us now consider, the dual case use of the TM grid [27] for TE modes. The geometry for an edge point P, is shown in Fig.3.3.1 We express the potential in B, P, D and H through a third order polynomial approximation:

case (TM)
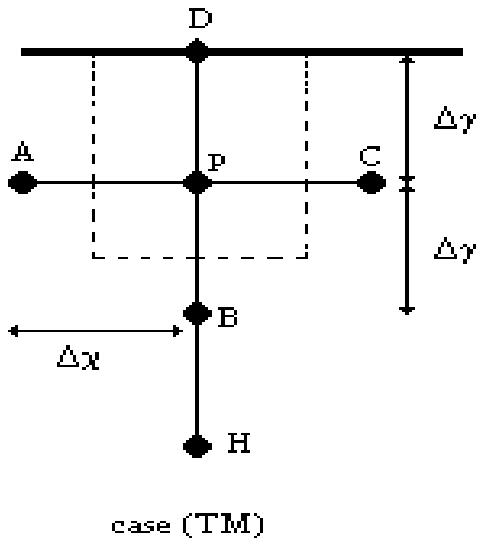
Fig. 3.3.1. Boundary point TM case

$$3.3.4.) \qquad \phi = \frac{1}{3}ay^3 + \frac{1}{2}by^2 + cy + d$$

Forcing both the BC in D and the potential sample values:

$$3.3.5.) \qquad \begin{cases} \left.\dfrac{\partial \phi}{\partial y}\right|_D = a\Delta y^2 + b\Delta y + c = 0 \\[2mm] \phi_P = d \\[2mm] \phi_B = -\dfrac{1}{3}a\Delta y^3 + \dfrac{1}{2}b\Delta y^2 - c\Delta y + \phi_P \\[2mm] \phi_H = -\dfrac{8}{3}a\Delta y^3 + \dfrac{4}{2}b\Delta y^2 - 2c\Delta y + \phi_P \end{cases}$$

The linear system (3.3.5) can be easily solved obtaining:

$$3.3.6.) \quad \left.\frac{\partial^2 \phi}{\partial y^2}\right|_P = 2ay + b \qquad y = 0$$

$$b = \frac{2}{11\Delta y^2} \cdot \left(\phi_H + \phi_B - 2\phi_P\right)$$

(3.3.7), together with (3.2.8) gives the discretized form of the laplacian in P

$$3.3.7.) \quad \nabla_t^2 \phi_p = \frac{\phi_A}{\Delta x^2} + \frac{\phi_C}{\Delta x^2} + \frac{2\phi_B}{11\Delta y^2} + \frac{2\phi_H}{11\Delta y^2} - \left(\frac{2}{\Delta x^2} + \frac{4}{11\Delta y^2}\right)\phi_P$$

which is the replacement of (3.2.10) for external points in TE modes.

3.4) VECTOR FINITE DIFFERENCE APPROACH: TE MODES

Up to now, we have computed the waveguide modes through the Hertz-Debye (scalar) potentials. The mode vectors must therefore be computed using numerical derivatives. An alternative approach is to compute directly the mode vector [28].

Let use consider a waveguide. The TE mode vector $\vec{e}$ is an eigenfunction of Laplace operator, with suitable conditions:

$$3.4.1.) \quad \begin{cases} \nabla_t^2 \vec{e} + k_t^2 \vec{e} = 0 \\ \nabla_t \cdot \vec{e} = 0 \\ \left.\vec{e} \times \vec{i}_n\right|_C = 0 \end{cases}$$

where C is the contour of the waveguide (see Fig.3.4.1).
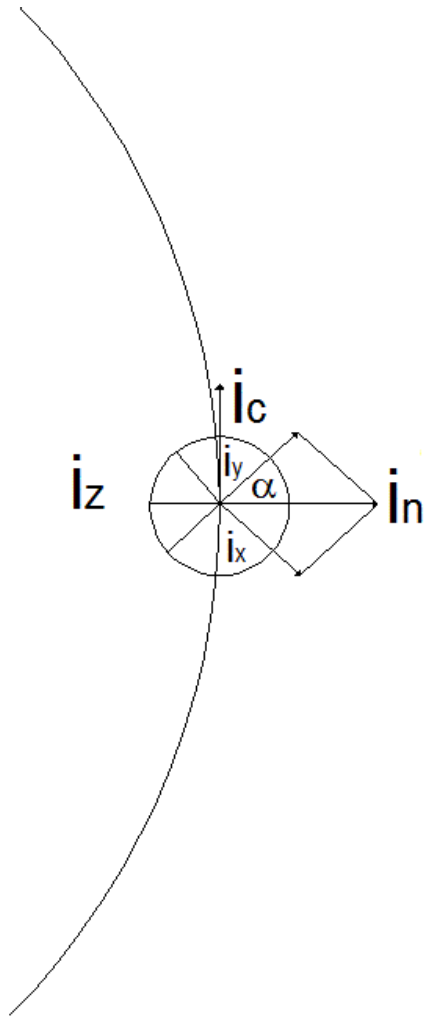
Fig. 3.4.1. Vectors geometry with respect to the contour of the conductor.

If we introduce the (two-dimensional) magnetic current $\overline{M}$ equivalent to the transverse field $\vec{e} = \vec{i}_z \times \overline{M}$ we get from (3.4.1)

3.4.2.) $\qquad \nabla_t^2 \vec{e} = -\nabla_t \times \nabla_t \times \vec{e} = -\nabla_t \times \left[\vec{i}_z \nabla_t \cdot \overline{M} \right] = \left[-\nabla_t \times \nabla_t \times \overline{M} + \nabla_t^2 \overline{M} \right] \times \vec{i}_z$

3.4.3.) $\qquad \nabla_t \cdot \vec{e} = \nabla_t \cdot \left[\vec{i}_z \times \overline{M} \right] = -\vec{i}_z \cdot \left[\nabla_t \times \overline{M} \right] = 0$

By (3.4.3), it follows that $\nabla_t \times \vec{M} = 0$. When substituted in (3.35) , after replacing and collecting terms we get:

3.4.4.)
$$\nabla_t^2 \vec{e} + k_t^2 \vec{e} = \left[-\nabla_t \times \nabla_t \times \vec{M} + \nabla_t^2 \vec{M} \right] \times \vec{i_z} + k_t^2 \left(\vec{i_z} \times \vec{M} \right) =$$
$$= \vec{i_z} \times \left[-\left(\nabla_t^2 \vec{M} + k_t^2 \vec{M} \right) \right]$$

the TE eigenvalue problem can therefore be rewritten in this form:

3.4.5.)
$$\begin{cases} \nabla_t^2 \vec{M} + k_t^2 \vec{M} = 0 \\ \nabla_t \times \vec{M} = 0 \\ \left. \vec{M} \cdot \vec{i_n} \right|_C = 0 \end{cases}$$

and in (x,y) components, as:

3.4.6.)
$$\begin{cases} \nabla_t^2 \vec{M} = -k_t^2 \vec{M} \\ \dfrac{\partial M_y}{\partial x} - \dfrac{\partial M_x}{\partial y} = 0 \\ M_x \cos(\alpha) + M_y \sin(\alpha) = 0 \end{cases}$$

where the third of (3.4.6) is the boundary condition (BC) on the contour C. FD approach to the solution of this problem is based on the replacement of problem (3.4.6) with a discretized version. The main difference with the previous paragraphs is that only the BC are inserted into the approximation of the Laplace operator. The second of (3.4.6) is dealt with as a constrain on the eigenvectors. In this way (3.4.6) becomes a constrained matrix eigenvalue problem.

 For an internal point P as in Fig.3.2.1 we can use a second-order Taylor expression as :

$$\vec{M}_B = \vec{M}_P + \frac{\partial \vec{M}}{\partial y}\bigg|_P \cdot (-\Delta y) + \frac{1}{2}\frac{\partial^2 \vec{M}}{\partial y^2}\bigg|_P \cdot (-\Delta y)^2$$

3.4.7.)

$$\vec{M}_D = \vec{M}_P + \frac{\partial \vec{M}}{\partial y}\bigg|_P \cdot (+\Delta y) + \frac{1}{2}\frac{\partial^2 \vec{M}}{\partial y^2}\bigg|_P \cdot (+\Delta y)^2$$

Adding to these equation and we find:

3.4.8.) $\qquad \dfrac{\partial^2 \vec{M}}{\partial y^2}\bigg|_P = \dfrac{1}{\Delta y^2} \cdot \left(\vec{M}_B + \vec{M}_D - 2\vec{M}_P\right)$

Likely in x direction:

3.4.9.) $\qquad \dfrac{\partial^2 \vec{M}}{\partial x^2}\bigg|_P = \dfrac{1}{\Delta x^2} \cdot \left(\vec{M}_A + \vec{M}_C - 2\vec{M}_P\right)$

Summing (3.4.8) and (3.4.9) we obtain :

3.4.10.) $\qquad \nabla_t^2 \vec{M}_P = \dfrac{\vec{M}_A}{\Delta x^2} + \dfrac{\vec{M}_C}{\Delta x^2} + \dfrac{\vec{M}_B}{\Delta y^2} + \dfrac{\vec{M}_D}{\Delta y^2} - \left(\dfrac{2}{\Delta x^2} + \dfrac{2}{\Delta y^2}\right)\vec{M}_P$

To discretize the second condition of (3.4.6) we can use a first -order Taylor expression. Starting from (3.4.7) without the second-order term we can easily get:

3.4.11.) $\qquad \left(\dfrac{\partial M_y}{\partial x} - \dfrac{\partial M_x}{\partial y}\right) = \dfrac{M_{C,y}}{2\Delta x} - \dfrac{M_{A,y}}{2\Delta x} - \dfrac{M_{D,x}}{2\Delta y} + \dfrac{M_{B,x}}{2\Delta y} = 0$

For a boundary point P, such as P in Fig.3.4.2, we need a different approach, since D is not a sampling point for the current. The BC is now $M_{D,y} = 0$ and this condition can be incorporated into the FD matrix. Adding the Taylor expansion of $M_{D,y}$
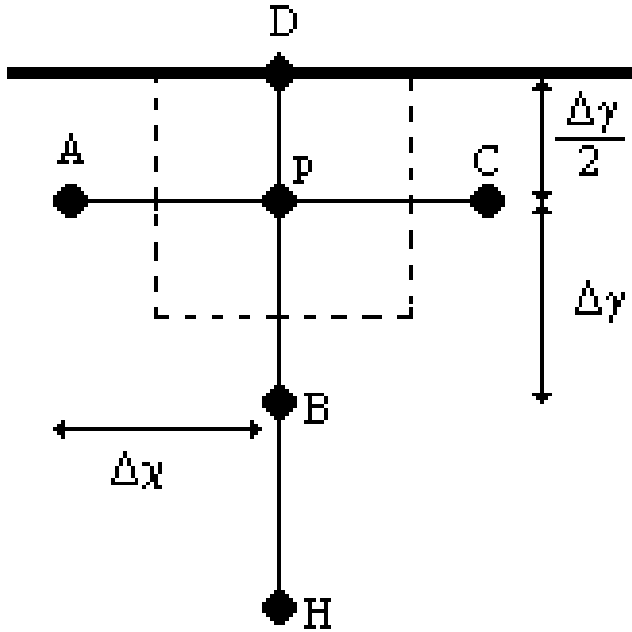
Fig. 3.4.2. Boundary point of TE grids

$$3.4.12.) \qquad M_{D,y} = M_{P,y} + \left.\frac{\partial M_y}{\partial y}\right|_P \cdot \left(+\frac{\Delta y}{2}\right) + \frac{1}{2}\left.\frac{\partial^2 M_y}{\partial y^2}\right|_P \cdot \left(+\frac{\Delta y}{2}\right)^2 = 0$$

with $\frac{1}{2}M_{B,y} = 0$ given by (3.4.7) and using $M_{D,y} = 0$ we get:

$$3.4.13.) \qquad \left.\frac{\partial^2 M_y}{\partial y^2}\right|_P = \frac{4}{3\Delta y^2}\cdot\left(M_{B,y} - 3M_{P,y}\right)$$

so

$$3.4.14.) \qquad \nabla_t^2 M_{P,y} = \frac{M_{A,y}}{\Delta x^2} + \frac{M_{C,y}}{\Delta x^2} + \frac{3M_{B,y}}{4\Delta y^2} - \left(\frac{2}{\Delta x^2} + \frac{4}{\Delta y^2} \right) M_{P,y}$$

Also the x component of (3.4.10) relevant to P needs to be modified, for the same reason. To do this we need another point H (see Fig.3.4.1) . Summing the Taylor expansion :

$$3.4.15.) \qquad M_{H,x} = M_{P,x} + \frac{\partial M_x}{\partial y}\bigg|_P \cdot (2\Delta y) + \frac{1}{2}\frac{\partial^2 M_x}{\partial y^2}\bigg|_P \cdot (2\Delta y)^2$$

with $M_{B,x}$ given by (3.4.7) we get:

$$3.4.16.) \qquad \frac{\partial^2 M_x}{\partial y^2}\bigg|_P = \frac{1}{\Delta y^2} \cdot \left(M_{H,x} - 2M_{B,x} + M_{P,x} \right)$$

and the x-components of (3.4.10) is replaced by:

$$3.4.17.) \qquad \nabla_t^2 M_{P,x} = \frac{M_{A,x}}{\Delta x^2} + \frac{M_{C,x}}{\Delta x^2} + \frac{M_{H,x}}{\Delta y^2} - 2\frac{M_{B,x}}{\Delta y^2} - \left(\frac{2}{\Delta x^2} + \frac{1}{\Delta y^2} \right) M_{P,x}$$

At the same time, the condition (3.4.11) becomes analogously:

$$3.4.18.) \qquad \frac{M_{C,y}}{2\Delta x} - \frac{M_{A,y}}{2\Delta x} - \frac{M_{H,x}}{2\Delta y} + 4\frac{M_{B,x}}{2\Delta y} - 3\frac{M_{P,x}}{2\Delta y} = 0$$

The discretized version of (3.4.6) is obtained collecting (3.4.10) and the constraint (3.4.11) to get the constrained eigenvalue problems:

3.4.19.)
$$\begin{cases} Ax = \lambda x \\ C^T x = 0 \end{cases}$$

where A is a (2n,2n) matrix, and C is (2n,m) with n>m and $\lambda = -k_t^2$. Of course, for all boundary points the equations (3.4.10) (3.4.11) are replaced by the modified ones (such as (3.4.14),(3.4.17) and (3.4.18)).

3.5) VECTOR FINITE DIFFERENCE APPROACH: TM MODES

The TM mode vectors $\vec{h}$ are eigenfunction of the Helmholtz equation:

3.5.1.)
$$\begin{cases} \nabla_t^2 \vec{h} + k_t^2 \vec{h} = 0 \\ \nabla_t \cdot \vec{h} = 0 \\ \left. \vec{e} \times \vec{i_n} \right|_C = \frac{1}{A} \cdot \left(\vec{h} \times \vec{i_z} \right) \times \vec{i_n} \Big|_C = \frac{1}{A} \cdot \left(\vec{h} \times \vec{i_n} \right) \Big|_C \times \vec{i_z} = 0 \end{cases}$$

where C is the contour of the waveguide (see Fig.3.4.1).

If we introduce the (two-dimensional) magnetic current $\vec{M}$ equivalent to the transverse field $\vec{M} = \frac{1}{A} \vec{h}$ and replacing in equation (3.5.1), the TM eigenvalue problem [29] can therefore be rewritten as:

3.5.2.)
$$\begin{cases} \nabla_t^2 \vec{M} + k_t^2 \vec{M} = 0 \\ \nabla_t \cdot \vec{M} = 0 \\ \left. \vec{M} \cdot \vec{i_n} \right|_C = 0 \end{cases}$$

and in (x,y) components, as:

$$3.5.3.) \quad \begin{cases} \nabla_t^2 \overrightarrow{M} = -k_t^2 \overrightarrow{M} \\ \dfrac{\partial M_x}{\partial x} + \dfrac{\partial M_y}{\partial y} = 0 \\ M_x \cos(\alpha) + M_y \sin(\alpha) = 0 \end{cases}$$

The main difference is the constrain given by the second of (3.5.3.) To discretize it we can use a first-order Taylor expression. Starting from equation (3.4.7) without the second-order term we can easily get:

$$3.5.4.) \quad \left(\frac{\partial M_x}{\partial x} + \frac{\partial M_y}{\partial y} \right) = \frac{M_{C,x}}{2\Delta x} - \frac{M_{A,x}}{2\Delta x} + \frac{M_{D,y}}{2\Delta y} - \frac{M_{B,y}}{2\Delta y} = 0$$

For a boundary points (see Fig.3.3.1) the equation (3.4.14) change respect to the TM case, because the boundary condition on the TM grids are different . For the laplacian we have:

$$3.5.5.) \quad \nabla_t^2 M_{P,y} = \frac{M_{A,y}}{\Delta x^2} + \frac{M_{C,y}}{\Delta x^2} + \frac{M_{B,y}}{\Delta y^2} - \left(\frac{2}{\Delta x^2} + \frac{2}{\Delta y^2} \right) M_{P,y}$$

At the same time, the condition (3.5.4) becomes analogously:

$$3.5.6.) \quad \frac{M_{C,x}}{2\Delta x} - \frac{M_{A,x}}{2\Delta x} + \frac{M_{H,y}}{2\Delta y} - 4\frac{M_{B,y}}{2\Delta y} + 3\frac{M_{P,y}}{2\Delta y} = 0$$

In this case the constrained eigenvalue problems (3.4.19) is obtained collecting (3.4.10) and the constraint (3.5.4). For all boundary points the equations (3.4.10) (3.5.4) are replaced by the modified ones (such as (3.5.5),(3.4.17) and (3.5.6)).

3.6) EXTENSION TO 3D PROBLEM

The extension of F approach described in the previous sections can be devised also for the evaluation of modes in cavities to assess the feasibility of such extension in the cavity cases, we describe here the computation of scalar eigenfunction on a single grid, irrespective of the boundary condition (Dirichlet or Newmann). Let use consider a rectangular cavities. The modes can be found from a suitable scalar eigenfunction ϕ, solution of the Helmothz equation:

$$3.6.1.) \quad \nabla_t^2 \phi + k_t^2 \phi = \frac{\partial^2 \phi}{\partial x^2} + \frac{\partial^2 \phi}{\partial y^2} + \frac{\partial^2 \phi}{\partial z^2} + k_t^2 \phi = 0$$

with the boundary condition (BC)

$$3.6.2.) \qquad \phi = 0 \qquad\qquad\qquad \text{Dirichlet}$$

$$3.6.3.) \qquad \frac{\partial \phi}{\partial n} = 0 . \qquad\qquad \text{Newmann}$$

at the boundary of the resonant cavities.

The FD approach follows the one described in 3.2 an 3.3. The chosen sampling grid is shown in Fig.3.6.1 (and is the standard one for Fig.3.6.1   Dirichlet, Newmann boundary condition).
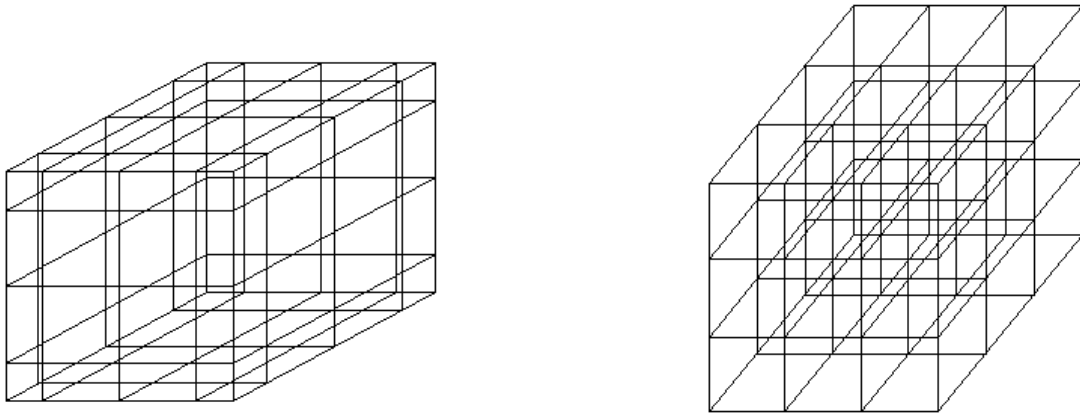
Fig. 3.6.1. Standard Newmann and Dirichlet grid, as suggested from BC

For an internal point P see (Fig 3.6.2) we can use a second-order Taylor expression as in (3.2.4-3.2.8). The final expression of Laplacian is :
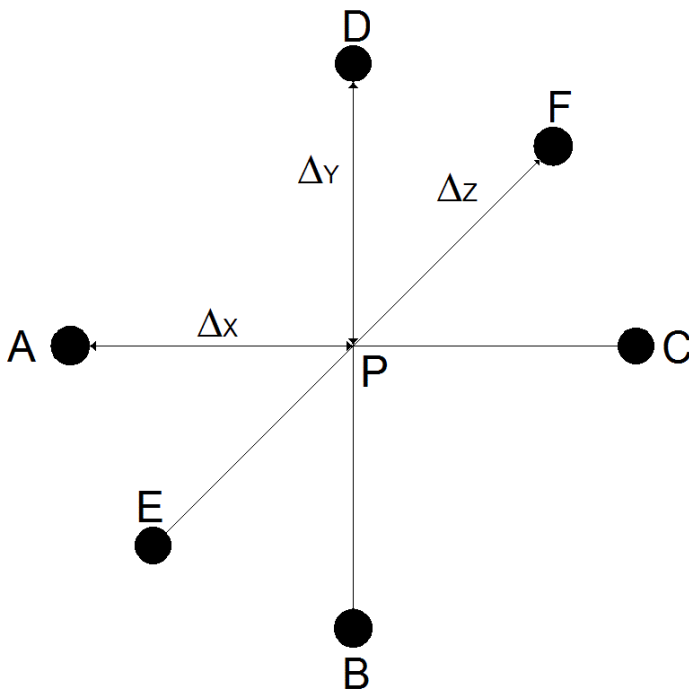
Fig. 3.6.2. Internal point of 3D Newmann grid

$$3.6.4.) \quad \nabla_t^2 \phi_p = \frac{\phi_A}{\Delta x^2} + \frac{\phi_C}{\Delta x^2} + \frac{\phi_B}{\Delta y^2} + \frac{\phi_D}{\Delta y^2} + \frac{\phi_E}{\Delta z^2} + \frac{\phi_F}{\Delta z^2} - \left(\frac{2}{\Delta x^2} + \frac{2}{\Delta y^2} + \frac{2}{\Delta z^2} \right) \phi_P$$
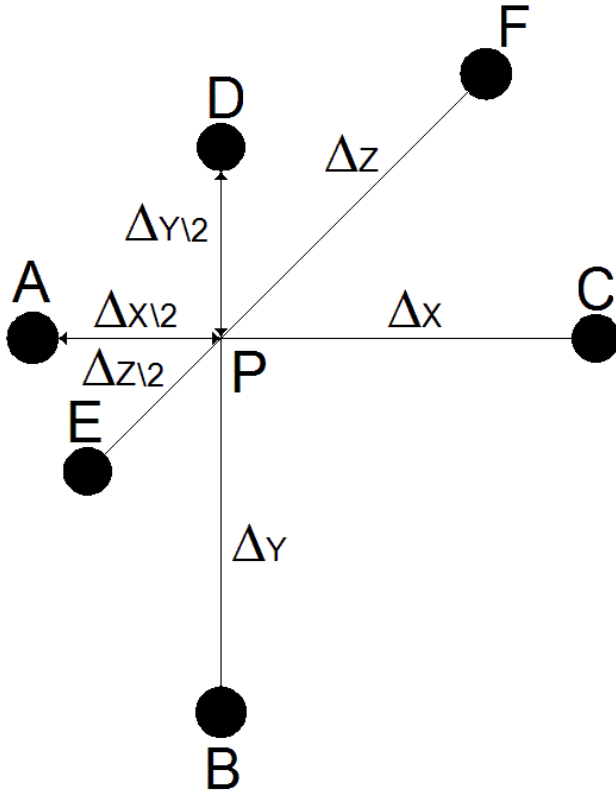
Fig. 3.6.3. Boundary point of 3D Newmann grid

For a boundary point see (fig.3.6.3) the expression (3.6.4) becomes, for the boundary condition (3.6.2):

$$3.6.5.) \quad \nabla_t^2 \phi_p = \frac{\phi_C}{\Delta x^2} + \frac{\phi_B}{\Delta y^2} + \frac{\phi_F}{\Delta z^2} - \left(\frac{1}{\Delta x^2} + \frac{1}{\Delta y^2} + \frac{1}{\Delta z^2} \right) \phi_P$$

since the development is the same as the one leading to 3.2.10. For the Dirichlet BC we can follows:

$$3.6.6.) \; \nabla_t^2 \phi_p = \frac{4\phi_C}{3\Delta x^2} + \frac{4\phi_D}{3\Delta y^2} + \frac{4\phi_F}{3\Delta z^2} - \left(\frac{4}{\Delta x^2} + \frac{4}{\Delta y^2} + \frac{4}{\Delta z^2} \right) \phi_P$$

Chapter IV

FINITE DIFFERENCE IN POLAR AND ELLIPTICAL GRID

INTRODUCTION

In this chapter we discuss the numerical computation of the eigenvalue of the Laplace operator using a curvilinear finite difference method. This allows to analyze the circular and elliptical waveguide modes using a finite difference approach.

4.1) POLAR FINITE DIFFERENCE

In FD approach both the equation (3.2.1) and the BC (3.2.2),(3.2.3) are replaced by a discretized version. If the waveguide boundary consists of straigh lines, parallel to the coordinate axes, the FD method can be applied on a cartesian grid [21]. This grid defines also a partition of the waveguide surface into rectangular cells, which completely fill the waveguide section. For every other waveguide, the section cannot be exactly partitioned using rectangular cells and this leads to numerical errors (since the eigenvalue problem is quite ill – conditioned [32])

In order to obtain high accuracy, the waveguide surface must be discretized maintaining also the correct geometry of the boundary. So a different discretization scheme should be used, which matches exactly the waveguide boundary. Therefore the discretization nodes must be at the intersections of a suitable framework, of which the waveguide boundary is a coordinate curve. In this way the waveguide section is exactly partitioned into   discretization cell.

The discretized equations can be obtained in two ways. The standard approach is to sum the   Taylor expansion of the potentials [20], as in chapter III. Alternatively we can integrate (3.2.1) over a discretization cell [21]

4.1.1.) $$\int \nabla_t^2 \phi \cdot dS = -k_t^2 \int \phi \cdot dS$$

Use of Gauss Theorem then gives:

4.1.2.) $$\int_{\Gamma_F} \nabla_t \phi \cdot i_n dl$$

i.e

4.1.3.) $$\int_{\Gamma_F} \frac{\partial \phi}{\partial n} \cdot dl = -k_t^2 \int_{S_F} \phi \cdot dS$$

where Γ_F is the cell boundary, S_F is the cell surface in the r.h.s. The Integral in the l.h.s can be numerical evaluated, replacing $\frac{\partial \phi}{\partial n}$ with its FD approximation, while the integral in the r.h.s in the spirit of FD approach, is evaluated as:

4.1.4.) $$\int_{S_F} \phi \cdot dS = \phi \cdot S$$

wherein ϕ is evaluated at the discretization point of cell S_F, and S is the cell area. So equation (4.1.3) becomes:

4.1.5.) $$\frac{1}{S} \int_{\Gamma_F} \frac{\partial \phi}{\partial n} \cdot dl = -k_t^2 \phi$$

where the l.h.s is expressed in discretized form.

The l.h.s of (4.1.3) is then divided into four (or more) sides, along the coordinate curves, and the normal derivative is evaluated in finite terms.

The two approaches apply in non-overlapping sets of cases, but, when both can be used, the results is the same, as we will show later.

Since both discretizations (either the standard FD and that based on (4.3)) can easily include the BC (3.2.2),(3.2.3), the resulting FD formulation to equivalent to the complete eigenvalue problem (3.2.1),(3.2.2),(3.2.3).

In order to explain the difference with the standard grid FD, and to assess our approach, we start considering a circular waveguide [22,23] (see Fig. 4.1.1), using as grid lines the coordinate lines of a polar framework.

We assume a regular spacing on the coordinate lines, with step Δr, $\Delta \vartheta$, and let $\phi_{nq} = \phi(n\Delta r, q\Delta \vartheta)$.

(b) Case TE   (a) Case TM
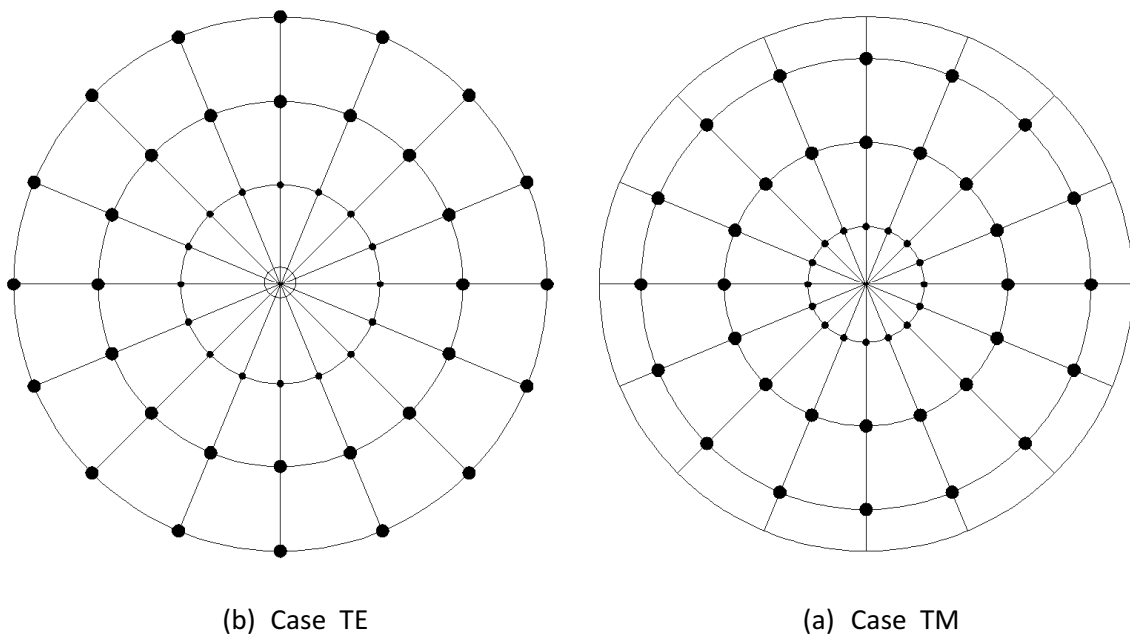
Fig. 4.1.1. Standard TE and TM grid, as suggested from BC
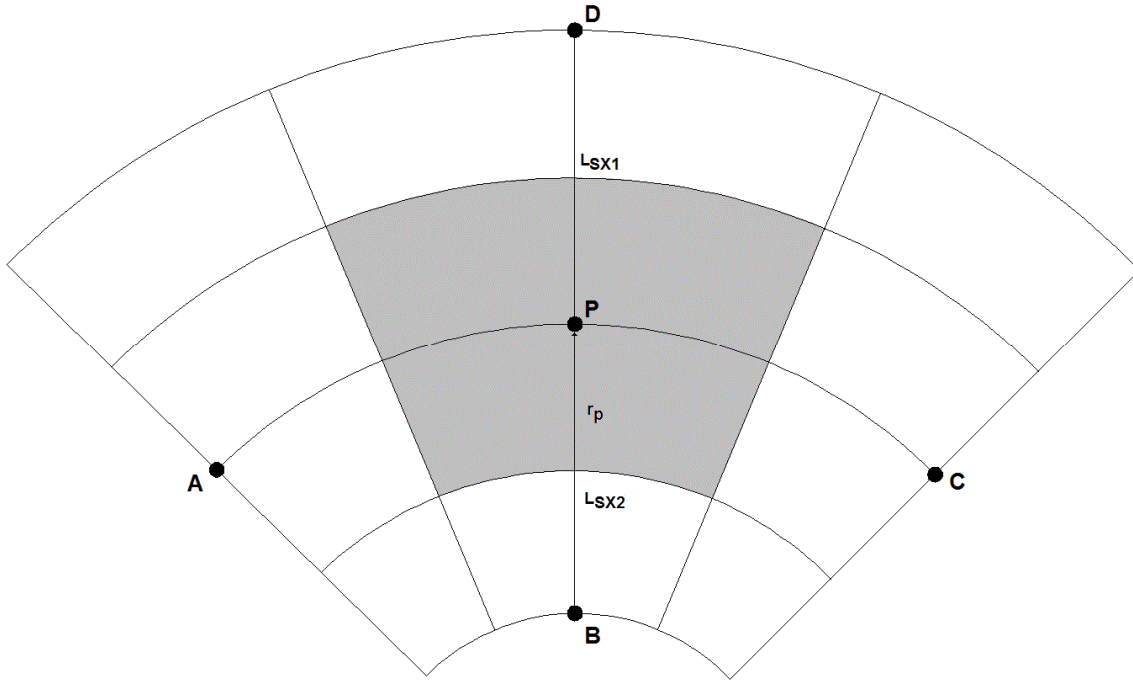
Fig. 4.1.2. Internal point of grid TE and TM

Let P the point of coordinates $(n\Delta r, q\Delta\vartheta)$, and consider the four nearby points A, B, C and D, as shown in Fig. 4.1.2. We get, for the l.h.s of (4.1.3)

$$4.1.6.) \quad \frac{1}{S_F} \cdot \left[\frac{(\phi_D - \phi_P)}{\Delta r} \cdot L_{Sx1} + \frac{(\phi_B - \phi_P)}{\Delta r} \cdot L_{Sx2} + \frac{(\phi_A - \phi_P)}{\Delta\vartheta \cdot r_p} \cdot \Delta r + \frac{(\phi_C - \phi_P)}{\Delta\vartheta \cdot r_p} \cdot \Delta r \right]$$

where $S_F = r_P \cdot \Delta r \cdot \Delta\vartheta$, $L_{SX1} = \left(r_P + \frac{\Delta r}{2} \right) \cdot \Delta\vartheta$ and $L_{SX2} = \left(r_P - \frac{\Delta r}{2} \right) \cdot \Delta\vartheta$

Replacing and collecting term we get the discretized form of (3.2.1) as:

$$4.1.7.) \quad \frac{1}{r_p^2 (\Delta\vartheta)^2} \cdot \phi_A + \left(\frac{1}{2r_p\Delta r} + \frac{1}{(\Delta r)^2} \right) \cdot \phi_D + \frac{1}{r_p^2 (\Delta\vartheta)^2} \cdot \phi_C + \left(\frac{1}{(\Delta r)^2} - \frac{1}{2r_p\Delta r} \right) \cdot \phi_B +$$
$$- \left(\frac{2}{(\Delta r)^2} + \frac{2}{r_p^2 (\Delta\vartheta)^2} \right) \cdot \phi_P \cong -k_t^2 \phi_P^2$$

This expression can be used for all internal point, except the circle center. It is worth noting that (4.1.8) can be obtained also starting from the laplacian operator in polar coordinates:

$$4.1.8.) \quad \left[\frac{1}{r_p^2} \cdot \frac{\partial^2 \phi}{\partial\vartheta^2} + \frac{1}{r_p} \cdot \frac{\partial \phi}{\partial r} + \frac{\partial^2 \phi}{\partial r^2} \right] = -k_t^2 \phi$$

and using a Taylor approximation

$$4.1.9.) \quad \phi_B = \phi_P + \left. \frac{\partial \phi}{\partial r} \right|_P \cdot (-\Delta r) + \frac{1}{2} \left. \frac{\partial^2 \phi}{\partial r^2} \right|_P \cdot (-\Delta r)^2$$

$$4.1.10.) \quad \phi_D = \phi_P + \left. \frac{\partial \phi}{\partial r} \right|_P \cdot (+\Delta r) + \frac{1}{2} \left. \frac{\partial^2 \phi}{\partial r^2} \right|_P \cdot (+\Delta r)^2$$

Adding and subtracting the last two equations we find:

$$4.1.11.) \quad \left. \frac{\partial^2 \phi}{\partial r^2} \right|_P = \frac{1}{(\Delta r)^2} \cdot (\phi_B + \phi_D - 2\phi_P)$$

and:

4.1.12.) $\qquad \dfrac{\partial \phi}{\partial r}\bigg|_P = \dfrac{\phi_D - \varphi_B}{2 \cdot \Delta r}$

Likely in ϑ direction

4.1.13.) $\qquad \dfrac{\partial^2 \phi}{\partial \vartheta^2}\bigg|_P = \dfrac{1}{(\Delta \vartheta)^2} \cdot (\phi_A + \phi_C - 2\phi_P)$

Collecting all those equation in (4.1.8) we get (4.1.7).

Equation (4.1.7) cannot be used for the center of the circle, since it is a point of singularity for the polar frame. As a consequence, Taylor expression cannot be used there. So we use (4.1.5) instead. Its l.h.s is divided into $N = \dfrac{2\pi}{\Delta \vartheta}$ sides, along the coordinate curves, and the normal derivative is evaluated in finite terms using (4.1.11) and (4.1.12).
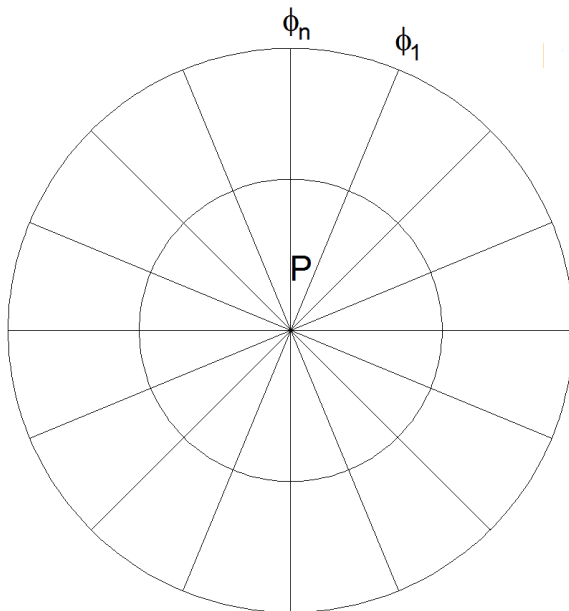
Fig. 4.1.3. Center of circle

46

Therefore the discretized form of the Laplace operator at the circle center is:

$$4.1.14.) \qquad \left(\frac{1}{\pi \cdot \left(\frac{\Delta r}{2} \right)^2} \right) \cdot \sum_{q=1}^{N} \frac{\left(\phi_q - \phi_P \right)}{\Delta r} \cdot \frac{\Delta r}{2} \cdot \Delta \vartheta =$$

$$= \left(\frac{4}{\pi \cdot \Delta r^2} \right) \cdot \left(\sum_{q=1}^{N} \phi_q \frac{\Delta \vartheta}{2} - N \frac{\Delta \vartheta}{2} \phi_P \right) \cong -k_t^2 \phi_P$$

Boundary points, where BC (3.2.1),(3.2.2) must be enforced required a modification of (4.1.7). As a matter of fact, BC (3.2.1),(3.2.2) needs to be included in the algebraic eigenvalue problem. The standard solution, widely used for the rectangular grid case, makes use of different grids for TE and TM, as in Fig.4.1.1. Let us consider an edge point, and consider the three nearby points A,B,C ad shown in Fig.4.1.4.
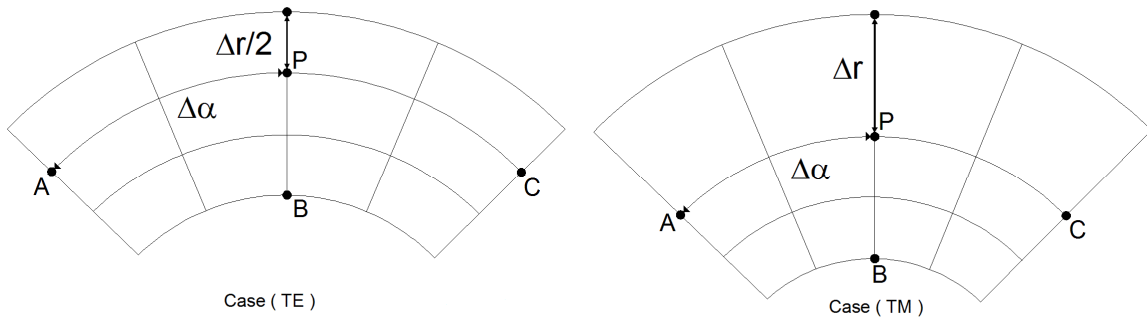
Fig. 4.1.4. Boundary point of circular waveguide

For Te modes, we can evaluate ϕ_X by a first-order approximation (compare (4.1.10))

4.1.15.) $\qquad \phi_P = \phi_X + \dfrac{\partial \phi}{\partial r}\Big|_X \cdot \left(\dfrac{\Delta r}{2}\right)$

since the BC require $\dfrac{\partial \phi}{\partial r}\Big|_D = 0$, we get:

4.1.16.) $\qquad \phi_P = \phi_D$.

As a consequence (4.1.11) and (4.1.12) becomes :

4.1.17.)

$$\dfrac{\partial^2 \phi}{\partial r^2}\Big|_P = \dfrac{1}{\Delta r^2} \cdot (\phi_B - \phi_P)$$

$$\dfrac{\partial \phi}{\partial r}\Big|_P = -\dfrac{1}{2 r_p \Delta r} \cdot (\phi_B - \phi_P)$$

and (4.1.7) by:

4.1.18.)

$$\dfrac{1}{r_p^2 \Delta \vartheta^2} \cdot \phi_A + \dfrac{1}{r_p^2 \Delta \vartheta^2} \cdot \phi_C + \left(\dfrac{1}{\Delta r^2} - \dfrac{1}{2 r_p \Delta r}\right) \cdot \phi_B +$$

$$-\left(\dfrac{1}{\Delta r^2} - \dfrac{1}{2 r_p \Delta r} + \dfrac{2}{r_p^2 \Delta \vartheta^2}\right) \cdot \phi_P \cong -k_t^2 \phi_P$$

For TM case, on the other hand, the standard approach requires each boundary point X to be a sampling point, so that $\phi_x = 0$ (see Fig.4.1.1.b), which can be directly put in to (4.1.11) and (4.1.12) to get, instead of (4.1.7) the equation:

4.1.19.)

$$\dfrac{1}{r_p^2 \Delta \vartheta^2} \cdot \phi_A + \dfrac{1}{r_p^2 \Delta \vartheta^2} \cdot \phi_C + \left(\dfrac{1}{\Delta r^2} - \dfrac{1}{r_p \Delta r}\right) \cdot \phi_B +$$

$$-\left(-\dfrac{1}{r_p \Delta r} + \dfrac{2}{\Delta r^2} + \dfrac{2}{r_p^2 \Delta \vartheta^2}\right) \cdot \phi_P \cong -k_t^2 \phi_P^2$$

Since TE and TM modes need to be considered together in many applications, e.g., mode matching or FDTD (using[5]), use of a single grid for all modes will be considered here. This requires to rephrase the FD of BC (3.2.1),(3.2.2) to match the other grid.

We describe here in detail the use of TE grid [26] (Fig.4.1.1a) for TM modes. Let us consider again the external point P on the TE grid (Fig.4.1.4a). Since the BC (3.2.1),(3.2.2) require $\phi_X = 0$, we can express the potential in B and X through a Taylor approximation:

4.1.20.)
$$\phi_B = \phi_P + \left.\frac{\partial \phi}{\partial r}\right|_P \cdot (-\Delta r) + \frac{1}{2}\left.\frac{\partial^2 \phi}{\partial r^2}\right|_P \cdot (-\Delta r)^2$$

$$\phi_X = 0 = \phi_P + \left.\frac{\partial \phi}{\partial r}\right|_P \cdot \left(\frac{\Delta r}{2}\right) + \frac{1}{2}\left.\frac{\partial^2 \phi}{\partial r^2}\right|_P \cdot \left(\frac{\Delta r}{2}\right)^2$$

recalling the BC for TM $\phi_X = 0$. Adding these equation and solving for the second derivative we get:

4.1.21.)
$$\left.\frac{\partial^2 \phi}{\partial r^2}\right|_P = \frac{4}{3 \cdot (\Delta r)^2} \cdot (\phi_B - 3\phi_P)$$

which, together with (4.1.13) gives the discretized form of eigen function equation for point P:

4.1.22.)
$$\nabla_t^2 \phi_p = \frac{1}{r_p^2 \Delta \alpha^2} \cdot \phi_A + \frac{1}{r_p^2 \Delta \alpha^2} \cdot \phi_C + \left(\frac{4}{3\Delta r^2} - \frac{1}{3r_p \Delta r}\right) \cdot \phi_B +$$

$$-\left(\frac{4}{\Delta r^2} + \frac{1}{r_p \Delta r} + \frac{2}{r_p^2 \Delta \alpha^2}\right) \cdot \phi_P \cong -k_t^2 \phi_P^2$$

as a replacement of (4.1.7) for this point in TM modes. To use the TM grids [27]

for TE modes, we apply the procedure leading to (3.3.4) replacing the y axis with an r axis pointing toward the circle center. The results are:

4.1.23.)

$$\left.\frac{\partial \phi}{\partial r}\right|_P = -\frac{1}{2\Delta r} \cdot \left(\phi_H - 4\phi_B + 3\phi_P\right)$$

$$\left.\frac{\partial^2 \phi}{\partial r^2}\right|_P = \frac{2}{11\Delta r^2} \cdot \left(\phi_H + \phi_B - 2\phi_P\right)$$

and (4.1.22) is replaced by:

4.1.24.)

$$\frac{\phi_A}{r_p^2 \Delta \vartheta^2} + \frac{\phi_C}{r_p^2 \Delta \vartheta^2} + \left(\frac{2}{11\Delta r^2} + \frac{1}{2r_p\Delta r}\right)\phi_H + \left(\frac{2}{11r_p\Delta r} - \frac{2}{r_p\Delta r}\right)\phi_B +$$

$$-\left(-\frac{3}{2r_p\Delta r} + \frac{4}{11\Delta r^2} + \frac{2}{r_p^2\Delta \vartheta^2}\right)\phi_P = -k_t^2\phi$$

4.2) FINITE DIFFERENCE IN ELLIPTICAL WAVEGUIDE

Aim of this paragraph is to develop a FD technique for the calculation of modes and eigenvalues of an elliptical waveguide, taking exactly into account the curved boundary of the waveguide. To do this we build up the discretization grid using the coordinate lines of an elliptic cylindrical framework [22] (Fig. 4.2.1).

$$x = a \cosh u \cos v$$
$$y = a \sinh u \sin v$$
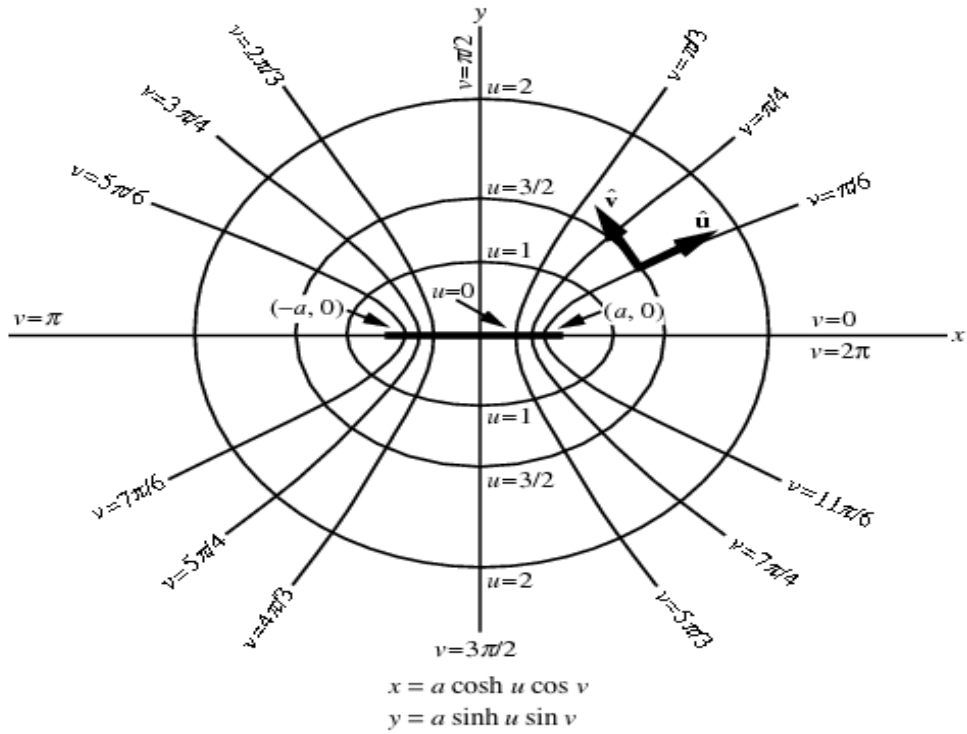
Fig. 4.2.1. Geometry of the elliptic cylindrical coordinates.

Assuming a regular spacing on the coordinate lines, with step $\Delta u, \Delta v,$ and letting the standard set of grid points for TE and TM modes are shown in Fig.4.2.2. Letting $\phi_{pq} = \phi(p\Delta u, q\Delta v)$ the eigenvalues equation (3.2.1) can be expressed us:

4.2.1.)
$$\frac{1}{a^2 \left(\sinh^2 p\Delta u + \sin^2 q\Delta v \right)} \cdot \left[\frac{\partial^2 \phi}{\partial u^2} + \frac{\partial^2 \phi}{\partial v^2} \right]_{pq} = -k_t^2 \phi_{pq}$$

51
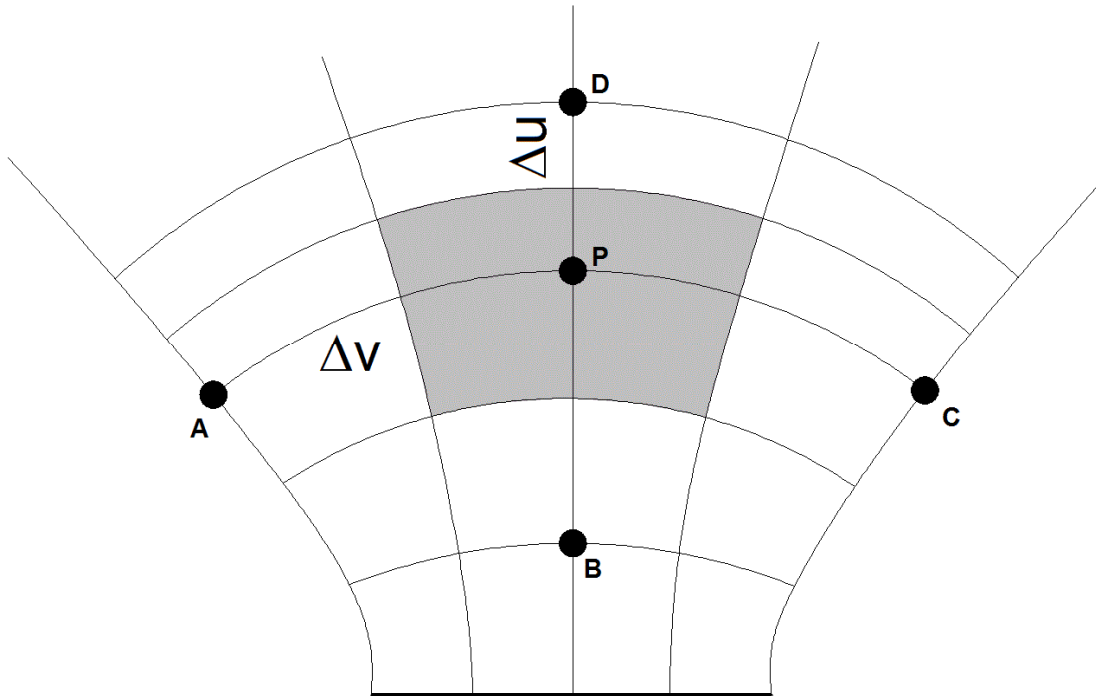
Fig. 4.2.2. Internal point of the elliptic cylindrical coordinates grid TE and TM

In this case it is simpler to discretize (4.2.1) using a Taylor expansion, for each internal point P since the term in brackets expanded exactly as in a rectangular grid:

4.2.2.)
$$\left[\frac{\partial^2\phi}{\partial u^2}+\frac{\partial^2\phi}{\partial v^2}\right]=$$
$$\frac{1}{\Delta v^2}\cdot\phi_A+\frac{1}{\Delta u^2}\cdot\phi_D+\frac{1}{\Delta v^2}\cdot\phi_C+\frac{1}{\Delta u^2}\cdot\phi_B-\left(\frac{2}{(\Delta u)^2}+\frac{2}{(\Delta v)^2}\right)\cdot\phi_P$$

Equation (4.2.2) cannot be used for the two foci, for points between them and for external points. For a point P lying on the segment joining the two foci (see Fig.4.2.3, u=0. Since P is a singular points we use (4.1.5) and we write:

52
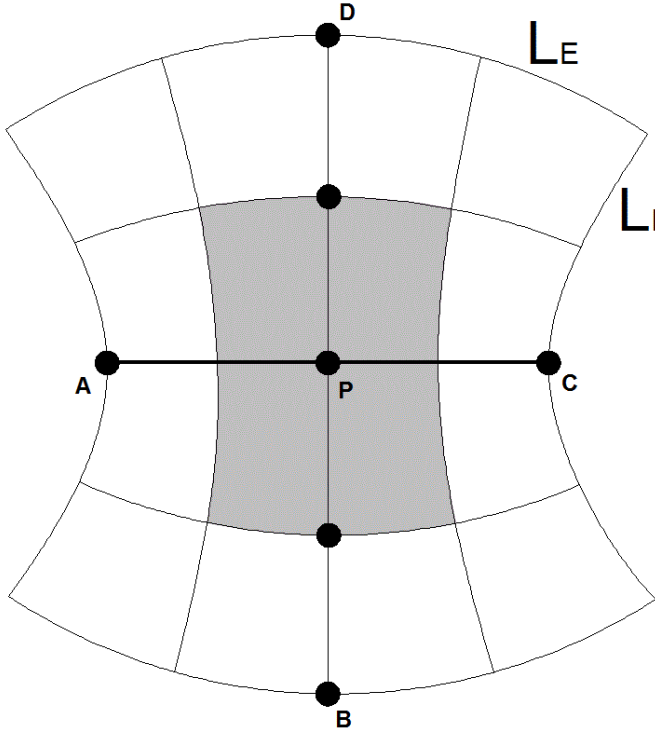
Fig. 4.2.3. point between foci

$$
4.2.3.) \quad \frac{1}{S_A} \left[\begin{array}{l} \dfrac{(\phi_C - \phi_P)}{h_v \Delta v} \cdot L_I + \dfrac{(\phi_A - \phi_P)}{h_v \Delta v} \cdot L_I + \\[3mm] + \dfrac{(\phi_B - \phi_P)}{h_u \Delta u} \cdot L_E + \dfrac{(\phi_D - \phi_P)}{h_u \Delta u} \cdot L_E \end{array} \right] = -k_t^2 \phi_p
$$

where $h = h_u(u,v) = h_v(u,v) = \dfrac{1}{a\sqrt{\sinh^2 u + \sin^2 v}}$ are scale factor of the elliptic

cylindrical coordinate system, $S_A = h_u^2 \Delta u \Delta v$ is the area of the cell and $L_I = h_v \Delta v$,

$L_E = h_u \Delta u$ are the length sides of cell. Reordering we get the final expression:

$$
4.2.4.) \quad \begin{array}{l} \dfrac{1}{h^2 \Delta v^2} \cdot \phi_A + \dfrac{1}{h^2 \Delta u^2} \cdot \phi_D + \dfrac{1}{h^2 \Delta v^2} \cdot \phi_C + \dfrac{1}{h^2 \Delta u^2} \cdot \phi_B + \\[3mm] - \left(\dfrac{2}{(h\Delta u)^2} + \dfrac{2}{(h\Delta v)^2} \right) \cdot \phi_P = -k_t^2 \phi_p \end{array}
$$

For the foci, we use (4.1.5) on the cell shown in Fig.4.2.4. This cell is bounded by the ellipse at $u = \Delta u / 2$, and by the branch of the hyperbola at $v = \Delta v / 2$ (intersecting in B and D). If S_F is the area of the cell, we get:

4.2.5.) $\qquad \dfrac{1}{S_F} \left[(\phi_C - \phi_P) \cdot 2L_e + (\phi_A - \phi_P) \cdot 2L_i \right] = -k_i^2 \phi_p$
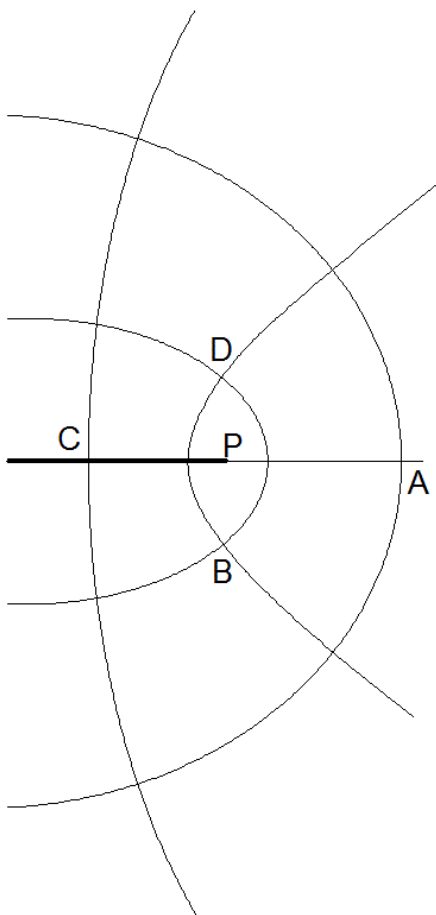
Fig. 4.2.4. Focus (P) of the ellipse

L_e and L_i are half the length of the arc of the ellipse and of the arc of the hyperbola respectively. These can be computed from the scale factor of the elliptic cylindrical coordinate system:

$$4.2.6.) \qquad h_u(u,v) = h_v(u,v) = \frac{1}{a\sqrt{\sinh^2 u + \sin^2 v}}$$

As

$$4.2.7.) \qquad L_e = \int_0^{\frac{\Delta v}{2}} h_u\left(\frac{\Delta u}{2}, v\right) dv \cong \frac{\Delta v}{4}\left(h_u\left(\frac{\Delta u}{2}, 0\right) + h_u\left(\frac{\Delta u}{2}, \frac{\Delta v}{2}\right)\right)$$

and

$$4.2.8.) \qquad L_i = \int_0^{\frac{\Delta u}{2}} h_v\left(u, \frac{\Delta v}{2}\right) du \cong \frac{\Delta u}{4}\left(h_v\left(\frac{\Delta v}{2}, 0\right) + h_v\left(\frac{\Delta u}{2}, \frac{\Delta v}{2}\right)\right)$$

TE   TM
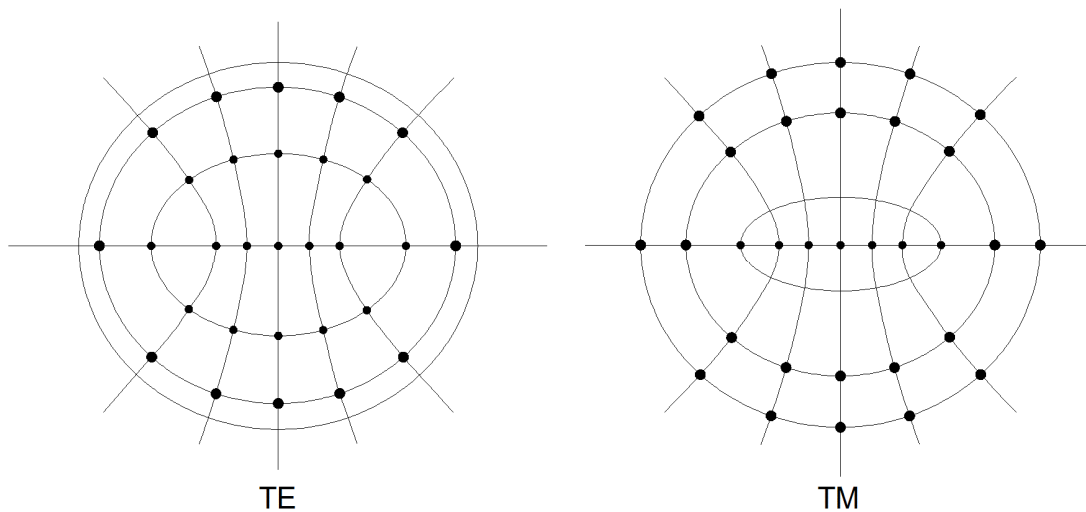
Fig. 4.2.5. Standard TE and TM grid, as suggested from BC

Finally, for a boundary point, the approach is close to the one used for a circular waveguide. For an external point in the TE grid, P in Fig.4.2.6, the BC is equivalent to $\phi_P = \phi_D$. For the TM grid, the potential in the external point D is $\phi_D = 0$.
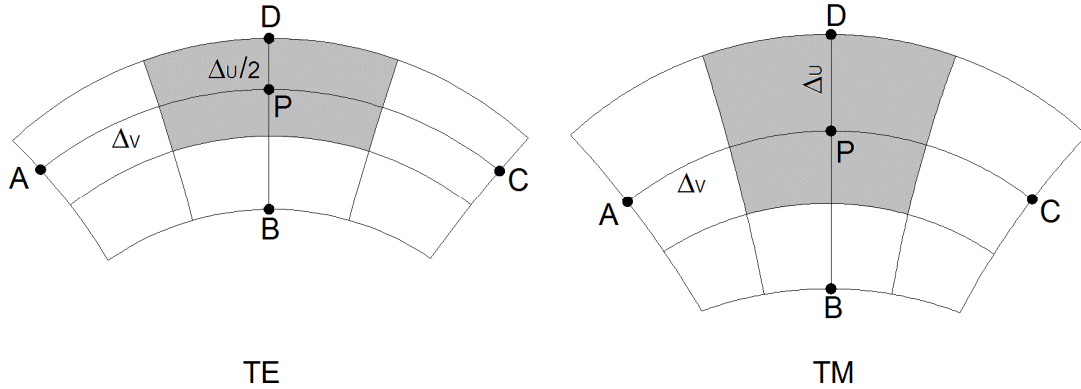
Fig. 4.2.6. Boundary point for TE case and TM case

The two discretized expression for $\nabla^2 \phi$ in P are, in TE case:

$$\frac{1}{a^2 \left(\sinh^2 p\Delta u + \sin^2 q\Delta v \right)} \cdot \left[\frac{\partial^2 \phi}{\partial u^2} + \frac{\partial^2 \phi}{\partial v^2} \right] =$$

4.2.9.)

$$= \frac{1}{\Delta v^2} \cdot \phi_A + \frac{1}{\Delta v^2} \cdot \phi_C + \frac{1}{\Delta u^2} \cdot \phi_B - \left(\frac{1}{(\Delta u)^2} + \frac{2}{(\Delta v)^2} \right) \cdot \phi_P$$

and in TM case

$$\frac{1}{a^2 \left(\sinh^2 p\Delta u + \sin^2 q\Delta v \right)} \cdot \left[\frac{\partial^2 \phi}{\partial u^2} + \frac{\partial^2 \phi}{\partial v^2} \right] =$$

4.2.10.)

$$= \frac{1}{\Delta v^2} \cdot \phi_A + \frac{1}{\Delta v^2} \cdot \phi_C + \frac{1}{\Delta u^2} \cdot \phi_B - \left(\frac{2}{(\Delta u)^2} + \frac{2}{(\Delta v)^2} \right) \cdot \phi_P$$

In order to use a single grid we must force the BC $\phi = 0$ on the TE grid. We can express the potential D through a Taylor approximation:

56

4.2.11.)
$$\phi_D = \phi_P + \left.\frac{\partial \phi}{\partial u}\right|_P \cdot \frac{\Delta u}{2} + \frac{1}{2}\left.\frac{\partial^2 \phi}{\partial u^2}\right|_P \cdot \left(\frac{\Delta u}{2}\right)^2$$

and insert the BC for TM $\phi_D = 0$. Since

4.2.12.)
$$\phi_B = \phi_P + \left.\frac{\partial \phi}{\partial u}\right|_P \cdot (-\Delta u) + \frac{1}{2}\left.\frac{\partial^2 \phi}{\partial u^2}\right|_P \cdot (-\Delta u)^2$$

We can compute $\phi_B + 2 \cdot \phi_D = \phi_B$ and therefore:

4.2.13.)
$$\left.\frac{\partial^2 \phi}{\partial u^2}\right|_P = \frac{4}{3\Delta u^2} \cdot (\phi_B - 3\phi_P)$$

The final expression is therefore:

4.2.14.)
$$\frac{1}{a^2 \left(\sinh^2 p\Delta u + \sin^2 q\Delta v\right)} \cdot \left[\frac{\partial^2 \phi}{\partial u^2} + \frac{\partial^2 \phi}{\partial v^2}\right] =$$
$$\frac{1}{\Delta v^2} \cdot \phi_A + \frac{1}{\Delta v^2} \cdot \phi_C + \frac{4}{3 \cdot \Delta u^2} \cdot \phi_B - \left(\frac{4}{\Delta u^2} + \frac{2}{\Delta v^2}\right) \cdot \phi_P$$

4.3) VECTOR POLAR FINITE DIFFERENCE

We consider the TE eigenvalue problem [24] which as shown in ct 3.4 can be written as:

$$4.3.1.) \qquad \nabla_t^2 \vec{M} + k_t^2 \vec{M} = 0$$

with additional conditions:

$$4.3.2.) \qquad \begin{cases} \nabla_t \times \vec{M} = 0 \\ \left. \vec{M} \cdot \vec{i_n} \right|_C = 0 \end{cases}$$

Of course $\vec{M}$ is evaluated only on the points of a polar grid (see Fig.4.1.1 a) with spacing $\Delta r, \Delta \vartheta$, and the equations are replaced by difference equations. For each internal grid point (see Fig.4.1.2), a second order Taylor approximation allows to evaluate the surface magnetic current in terms of the current samples at the neighboring points. Taking into account the expansion of the vector Laplace operator in polar coordinates:

$$4.3.3.) \qquad \begin{aligned} \nabla_t^2 \vec{M} &= \\ &\left[\frac{\partial^2 M_r}{\partial r^2} + \frac{1}{r} \cdot \frac{\partial M_r}{\partial r} - \frac{M_r}{r^2} + \frac{1}{r^2} \cdot \frac{\partial^2 M_r}{\partial \vartheta^2} - \frac{2}{r^2} \cdot \frac{\partial M_\vartheta}{\partial \vartheta} \right] \vec{u_r} + \\ &\left[\frac{\partial^2 M_\vartheta}{\partial r^2} + \frac{1}{r} \cdot \frac{\partial M_\vartheta}{\partial r} - \frac{M_\vartheta}{r^2} + \frac{1}{r^2} \cdot \frac{\partial^2 M_\vartheta}{\partial \vartheta^2} + \frac{2}{r^2} \cdot \frac{\partial M_r}{\partial \vartheta} \right] \vec{u_\vartheta} \end{aligned}$$

the terms in the brackets are obtained as:

$$\frac{\partial^2 M_\vartheta}{\partial \vartheta^2} = \frac{M_{A,\vartheta} + M_{C,\vartheta} - 2M_{P,\vartheta}}{\Delta \vartheta^2}$$

$$\frac{\partial M_\vartheta}{\partial \vartheta} = \frac{M_{C,\vartheta} - M_{A,\vartheta}}{2\Delta \vartheta}$$

$$\frac{\partial^2 M_\vartheta}{\partial r^2} = \frac{M_{B,\vartheta} + M_{D,\vartheta} - 2M_{P,\vartheta}}{\Delta r^2}$$

$$\frac{\partial M_\vartheta}{\partial r} = \frac{M_{D,\vartheta} - M_{B,\vartheta}}{2\Delta r}$$

$$\frac{\partial^2 M_r}{\partial r^2} = \frac{M_{B,r} + M_{D,r} - 2M_{P,r}}{\Delta r^2}$$

$$\frac{\partial M_r}{\partial r} = \frac{M_{D,r} - M_{B,r}}{2\Delta r}$$

$$\frac{\partial^2 M_r}{\partial \vartheta^2} = \frac{M_{A,r} + M_{C,r} - 2M_{P,r}}{\Delta \vartheta^2}$$

$$\frac{\partial M_r}{\partial \vartheta} = \frac{M_{C,r} - M_{A,r}}{2\Delta \vartheta}$$

the expression for an internal point P as in Fig.4.1.2 is :

4.3.4.)
$$\begin{aligned}
\nabla_t^2 \overrightarrow{M}_P = & \left[M_{B,r}K_1 + M_{D,r}K_2 + M_{A,r}K_3 + M_{C,r}K_3 - M_{P,r}K_4 M_{A,\alpha}K_5 - M_{C,\alpha}K_5 \right] \cdot \overrightarrow{u_r} + \\
& + \left[M_{B,\alpha}K_1 + M_{D,\alpha}K_2 + M_{A,\alpha}K_3 + M_{C,\alpha}K_3 - M_{P,\alpha}K_4 - M_{A,r}K_5 + M_{C,r}K_5 \right] \cdot \overrightarrow{u_\vartheta}
\end{aligned}$$

where

$$K_1 = \frac{1}{\Delta r^2} - \frac{1}{2r_p \Delta r} \qquad K_2 = \frac{1}{\Delta r^2} + \frac{1}{2r_p \Delta r}$$

$$K_3 = \frac{1}{r_p^2 \Delta \vartheta^2} \qquad\qquad K_4 = K_1 + K_2 + 2K_3 + \frac{1}{r_p^2}$$

$$K_5 = \frac{1}{2r_p^2 \Delta \vartheta}$$

To discretize the first of the (4.32) we can use a first-order Taylor expression. Since (4.32) is:

4.3.5.)
$$\nabla \times \overrightarrow{M} = \frac{1}{r} \cdot \frac{\partial (r \cdot M_\vartheta)}{\partial r} - \frac{1}{r} \cdot \frac{\partial M_r}{\partial \vartheta} = \frac{1}{r} \cdot M_\vartheta + \frac{\partial M_\vartheta}{\partial r} - \frac{1}{r} \cdot \frac{\partial M_r}{\partial \vartheta} = 0$$

then

4.3.6.)
$$\left(\frac{1}{r_p} \cdot M_{P,\vartheta} + \frac{M_{D,\vartheta} - M_{B,\vartheta}}{2\Delta r} - \frac{1}{r_p} \cdot \frac{M_{C,r} - M_{A,r}}{2\Delta\vartheta} \right) = 0$$

For a boundary point, such as P in Fig.4.3.1, using the same method apply rectangular waveguide. The BC is $M_{D',r} = 0$ and this condition can be incorporated into the FD matrix.
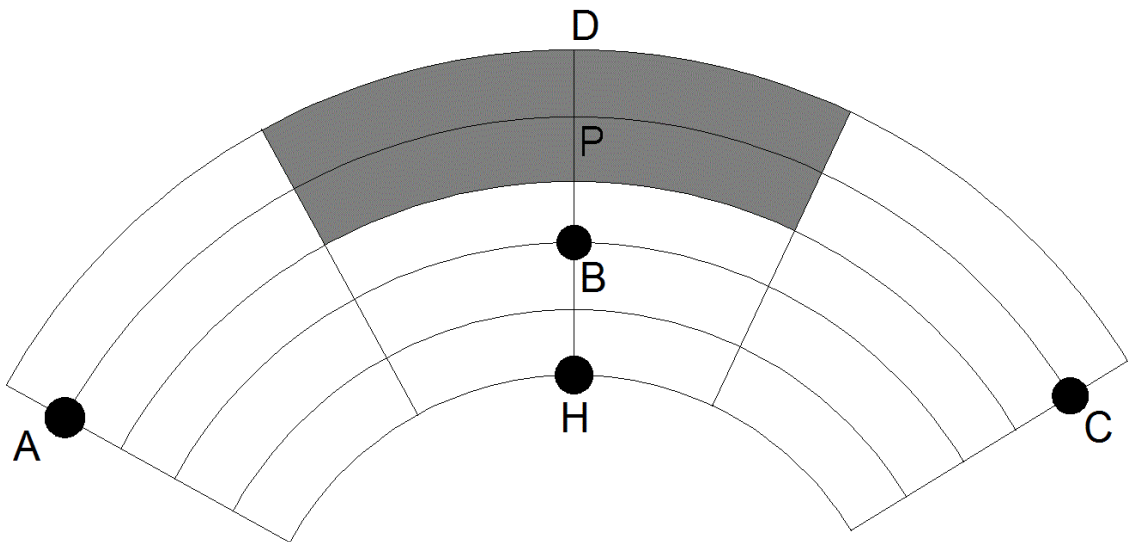
Fig.4.3.1 - Boundary point of polar framework

Also the $\vec{u}_\vartheta$ component of (4.3.6) relevant to P needs to be modified, for the same reason. To do this we need another point H. Equation (4.3.6) is then replaced by:

4.3.7.)
$$\nabla_t^2 \vec{M}_P = \left[M_{B,r} H_1 + M_{A,r} K_3 + M_{C,r} K_3 - M_{P,r} H_4 + M_{A,\vartheta} K_5 - M_{C,\vartheta} K_5 \right] \cdot \vec{u}_r +$$
$$+ \left[M_{H,\vartheta} K_1 - M_{B,\vartheta} H_2 + M_{A,\vartheta} K_3 + M_{C,\vartheta} K_3 - M_{P,\vartheta} H_5 - M_{A,r} K_5 + M_{C,r} K_5 \right] \cdot \vec{u}_\vartheta$$

where $\quad H_1 = \dfrac{4}{3\Delta r^2} - \dfrac{1}{3r_p\Delta r}, H_2 = \dfrac{2}{\Delta r^2} + \dfrac{4}{2r_p\Delta r}, H_3 = \dfrac{1}{r_p\Delta r} + \dfrac{2}{r_p\Delta\vartheta^2} \quad$ and

$H_4 = 3H_1 + H_3 + 2K_3$, $H_5 = \dfrac{1}{r_p\Delta r} + \dfrac{3}{2r_p\Delta r} - \dfrac{1}{r_p^2} - 2K_3$.

At the same time, the condition (4.3.6) becomes analogously:

4.3.8.)
$$\left(\left(\dfrac{1}{r_p} + \dfrac{3}{2\Delta r} \right) M_{P,\vartheta} + \dfrac{M_{H,\vartheta}}{2\Delta r} - \dfrac{4M_{B,\vartheta}}{2\Delta r} - \dfrac{1}{r_p} \cdot \dfrac{M_{C,r} - M_{A,r}}{2\Delta\vartheta} \right) = 0$$

It remains to consider the center of the circle. In this point it is not possible to use a Taylor expression since it is a point of singularity for the polar framework. Therefore we integrate (4.3.2), as in the scalar case, (4.1.1) and obtain:

4.3.9.)
$$\int_S \nabla_t^2 \vec{M} \cdot dS = -k_t^2 \int \vec{M} \cdot dS$$

Because of (4.3.3) the Laplace operator becomes :

4.3.10.)
$$\nabla_t^2 \vec{M} = \nabla_t \left(\nabla_t \vec{M} \right) - \nabla_t \times \nabla_t \times \vec{M} = \nabla_t \left(\nabla_t \vec{M} \right)$$

we replace (4.3.10) in (4.3.9) becomes:

$$4.3.11.) \qquad \int_S \nabla_t \left(\nabla_t \cdot \overrightarrow{M} \right) \cdot dS = -k_t^2 \int \overrightarrow{M} \ dS$$

We apply the theorem of the gradient [33] to the l.h.s of (4.3.10)

$$4.3.12.) \qquad \int_S \nabla_t \left(\nabla_t \overrightarrow{M} \right) \cdot dS = \int_C \nabla_t \overrightarrow{M} \cdot \overrightarrow{i_n} \cdot dl = \int_C \nabla_t \overrightarrow{M} \cdot \overrightarrow{i_n} \cdot \frac{\Delta r}{2} \cdot d\vartheta$$

since $dl = \dfrac{\Delta r}{2} \cdot d\vartheta$. Using the divergence of $\overrightarrow{M}$ in polar coordinate we get for

the r.h.s of (4.3.11):

$$4.3.13.) \qquad \int_C \frac{\partial (r \cdot M_r)}{\partial r} \cdot \overrightarrow{i_n} \cdot \frac{\Delta r}{2} \cdot d\vartheta + \int_C \frac{\partial M_\vartheta}{\partial \vartheta} \cdot \overrightarrow{i_n} \cdot d\vartheta$$

Since $\overrightarrow{i_n} = \overrightarrow{i_x} \cos(\vartheta) + \overrightarrow{i_y} \sin(\vartheta)$ .We decompose (4.3.12) in an x component:

$$4.3.14.) \qquad \int_C \frac{\partial (r \cdot M_r)}{\partial r} \cdot \overrightarrow{i_x} \cos(\vartheta) \cdot \frac{\Delta r}{2} \cdot d\vartheta + \int_C \frac{\partial M_\vartheta}{\partial \vartheta} \cdot \overrightarrow{i_x} \cos(\vartheta) \cdot d\vartheta$$

and a y component:

$$4.3.15.) \qquad \int_C \frac{\partial (r \cdot M_r)}{\partial r} \cdot \overrightarrow{i_y} \sin(\vartheta) \cdot \frac{\Delta r}{2} \cdot d\vartheta + \int_C \frac{\partial M_\vartheta}{\partial \vartheta} \cdot \overrightarrow{i_y} \sin(\vartheta) \cdot d\vartheta$$

compute by parts the second integral of (4.3.14) and (4.3.15)

4.3.16.) $\quad \int_C \dfrac{\partial M_\vartheta}{\partial \vartheta} \cdot \vec{i_x} \cos(\vartheta) \cdot d\vartheta = \left| M_\vartheta \cos(\vartheta)\right|_{-\pi}^{+\pi} - \int_{-\pi}^{+\pi} -M_\vartheta \sin(\vartheta) \cdot d\vartheta = \int_{-\pi}^{+\pi} M_\vartheta \sin(\vartheta) \cdot d\vartheta$

4.3.17.) $\quad \int_C \dfrac{\partial M_\vartheta}{\partial \vartheta} \cdot \vec{i_y} \sin(\vartheta) \cdot d\vartheta = - \int_{-\pi}^{+\pi} M_\vartheta \cos(\vartheta) \cdot d\vartheta$

we insert (4.3.16) with (4.3.17), (4.3.14) and (4.3.15) into (4.3.12) to get:

4.3.18.)

$$
\begin{aligned}
& \int_C \dfrac{\partial(r \cdot M_r)}{\partial r} \cdot \vec{i_x} \cos(\vartheta) \cdot \dfrac{\Delta r}{2} \cdot d\vartheta + \int_{-\pi}^{+\pi} M_\vartheta \sin(\vartheta) \cdot d\vartheta \cdot \vec{i_x} + \\
& + \int_C \dfrac{\partial(r \cdot M_r)}{\partial r} \cdot \vec{i_y} \sin(\vartheta) \cdot \dfrac{\Delta r}{2} \cdot d\vartheta + \int_{-\pi}^{+\pi} M_\vartheta \cos(\vartheta) \cdot d\vartheta \cdot \vec{i_y} = -k_t^2 A_t
\end{aligned}
$$

where $A_T = 4 / \pi \cdot \Delta r^2$. In (4.3.16) and (4.3.17) $\vec{M_0}$ must be evaluated in Cartesian coordinates: $\vec{M_0} = M_{0x} \cdot \vec{i_x} - M_{0y} \cdot \vec{i_y}$

To evaluate (4.3.15) we need $M_\vartheta\left(\dfrac{\Delta r}{2}, \vartheta\right)$, $\left. \dfrac{\partial(r \cdot M_r)}{\partial r}\right|_{r=\frac{\Delta r}{2}}$ along C, and therefore outside of the discretization grid. In order to include (4.3.16) and (4.3.17) into the FD matrix, we must express the $M_\vartheta\left(\dfrac{\Delta r}{2}, \vartheta\right)$ in terms of $\vec{M}$ an the discretization points, as averages. Since $\vec{M_0}$ does not have polar components, such averages must be computed as (compare Fig.4.3.2)
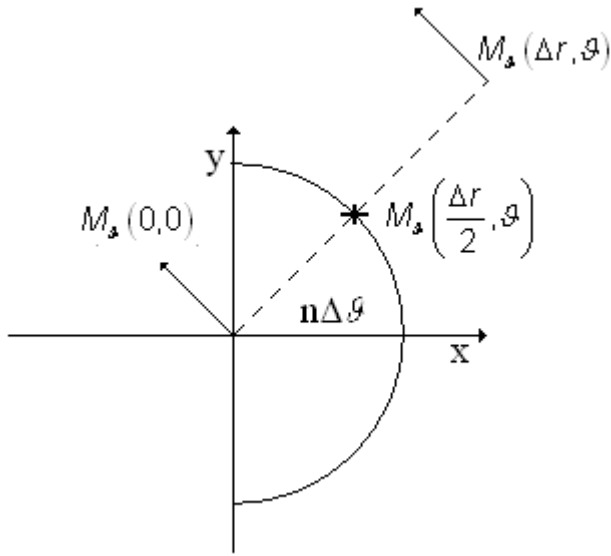
Fig.4.3.2 – component of $\vec{M}$ between center and next point.

$$M_\vartheta\left(\frac{\Delta r}{2},\vartheta\right) = \frac{1}{2}\cdot\left[M_\vartheta(\Delta r,\vartheta) + \lim_{\varepsilon\to 0} M_\vartheta(\varepsilon,\vartheta)\right] =$$

$$= \frac{1}{2}\cdot\left[M_\vartheta(\Delta r,\vartheta) + \left(M_{0,y}\cos(\vartheta) - M_{0,x}\sin(\vartheta)\right)\right]$$

4.3.19.)

$$\left.\frac{\partial(r\cdot M_r)}{\partial r}\right|_{\frac{\Delta r}{2},\vartheta} = \left[\frac{(r\cdot M_r)\big|_{\Delta r} - \lim_{\varepsilon\to 0}(r\cdot M_r)\big|_\varepsilon}{\Delta r}\right] =$$

$$= \left[\frac{\Delta r\cdot M_r(\Delta r,\vartheta) - 0}{\Delta r}\right] = M_r(\Delta r,\vartheta)$$

Now solving the first integral of (4.3.14) and (4.3.15)

4.3.20.) $\qquad \displaystyle\int_C \left.\frac{\partial(r\cdot M_r)}{\partial r}\right|_{\frac{\Delta r}{2},\vartheta}\cdot\cos(\vartheta)\cdot\frac{\Delta r}{2}\cdot d\vartheta = \sum_{q=1}^{N} M_{r,q}\cdot\cos(\vartheta_q)\cdot\Delta\vartheta$

4.3.21.) $$\int_C \left.\frac{\partial (r \cdot M_r)}{\partial r}\right|_{\frac{\Delta r}{2},\vartheta} \cdot \sin(\vartheta) \cdot \frac{\Delta r}{2} \cdot d\vartheta = \sum_{q=1}^{N} M_{r,q} \cdot \sin(\vartheta_q) \cdot \Delta \vartheta$$

where $M_{r,q} = M_r(\Delta r, q\Delta \vartheta)$; now solving (4.3.16) and (4.3.17):

4.3.22.)
$$\int_C \frac{\partial M_\vartheta}{\partial \vartheta} \cdot \cos(\vartheta) \cdot d\vartheta = \int_{-\pi}^{+\pi} M_\vartheta \sin(\vartheta) \cdot d\vartheta =$$
$$= \sum_{q=1}^{N} \left[\frac{M_{\vartheta,q} \cdot \sin(\vartheta_q) + \left(M_{0,y}^q \sin(\vartheta_q)\cos(\vartheta_q) - M_{0,x}^q \sin^2(\vartheta_q)\right)}{2} \right]$$

4.3.23.)
$$\int_C \frac{\partial M_\vartheta}{\partial \vartheta} \cdot \sin(\vartheta) \cdot d\vartheta = -\int_{-\pi}^{+\pi} M_\vartheta \cos(\vartheta) \cdot d\vartheta =$$
$$= -\sum_{q=1}^{N} \left[\frac{M_{\vartheta,q} \cdot \cos(\vartheta_q) + \left(M_{0,y}^q \cos^2(\vartheta_q) - M_{0,x}^q \sin(\vartheta_q)\cos(\vartheta_q)\right)}{2} \right] \cdot$$

where $M_{\vartheta,q} = M_\vartheta(\Delta r, q\Delta \vartheta)$; we sum (4.3.21) and (4.3.23) and we get , for the x component:

4.3.24.)
$$\int_C \left.\frac{\partial (r \cdot M_r)}{\partial r}\right|_{\frac{\Delta r}{2},\vartheta} \cdot \cos(\vartheta) \cdot \frac{\Delta r}{2} \cdot d\vartheta + \int_{-\pi}^{+\pi} M_\vartheta \sin(\vartheta) \cdot d\vartheta =$$
$$= \sum_{q=1}^{N} M_{r,q} \cdot \cos(\vartheta_q) \cdot \Delta \vartheta +$$
$$+ \sum_{q=1}^{N} \left[\frac{M_{\vartheta,q} \cdot \sin(\vartheta_q) + \left(M_{0,y}^q \sin(\vartheta_q)\cos(\vartheta_q) - M_{0,x}^q \sin^2(\vartheta_q)\right)}{2} \right] =$$
$$= \sum_{q=1}^{N} \left[\begin{array}{l} M_{r,q} \cdot \cos(\vartheta_q) \cdot \Delta \vartheta + \\ + \dfrac{M_{\vartheta,q} \cdot \sin(\vartheta_q) + \left(M_{0,y}^q \sin(\vartheta_q)\cos(\vartheta_q) - M_{0,x}^q \sin^2(\vartheta_q)\right)}{2} \end{array} \right]$$

we sum (4.3.20) and (4.3.22) and we get , for the y component:

$$\int_C \frac{\partial(r \cdot M_r)}{\partial r}\bigg|_{\frac{\Delta r}{2},\vartheta} \cdot \sin(\vartheta) \cdot \frac{\Delta r}{2} \cdot d\vartheta - \int_{-\pi}^{+\pi} M_\vartheta \cos(\vartheta) \cdot d\vartheta =$$

$$= \sum_{q=1}^{N} M_{r,q} \cdot \sin(\vartheta_q) \cdot \Delta\vartheta +$$

4.3.25.)
$$-\sum_{q=1}^{N} \left[\frac{M_{\vartheta,q} \cdot \cos(\vartheta_q) + \left(M_{0,y}^q \cos^2(\vartheta_q) - M_{0,x}^q \sin(\vartheta_q)\cos(\vartheta_q) \right)}{2} \right]$$

$$= \sum_{q=1}^{N} \left[\begin{array}{l} M_{r,q} \cdot \sin(\vartheta_q) \cdot \Delta\vartheta + \\ -\dfrac{M_{\vartheta,q} \cdot \cos(\vartheta_q) + \left(M_{0,y}^q \cos^2(\vartheta_q) - M_{0,x}^q \sin(\vartheta_q)\cos(\vartheta_q) \right)}{2} \end{array} \right]$$

4.4) VECTOR ELLYPTIC FINITE DIFFERENCE

In the same way as the circular case, in an elliptic waveguide, $\vec{M}$ is evaluated only on the points of a elliptic grid (see Fig.4.2.1) with spacing $(\Delta u, \Delta v)$. The expression of the Laplace vector operator in elliptic coordinates can be simplified if we let $\vec{A} = h\vec{M}$, where

$$4.4.1.) \quad h = \frac{1}{a_f \sqrt{\sinh^2 u + \sin^2 v}}$$

is the common value of the scale factor, $2a_f$ being the inter--focal distance. The u component of $\nabla_t^2 \vec{M}$ is

$$
4.4.2.) \quad
\begin{aligned}
&-\frac{1}{h^5} \cdot \frac{\partial h^2}{\partial u} \cdot \frac{\partial (A_u)}{\partial u} + \frac{1}{h^3} \frac{\partial^2 (A_u)}{\partial u^2} - \frac{1}{h^5} \cdot \frac{\partial h^2}{\partial u} \cdot \frac{\partial (A_v)}{\partial v} - \frac{\partial h}{\partial v} \frac{1}{h^3} \cdot \frac{\partial (A_v)}{\partial u} + \\
&\frac{\partial h}{\partial v} \cdot \frac{1}{h^3} \cdot \frac{\partial (A_u)}{\partial v} + \frac{1}{h^5} \cdot \frac{\partial h^2}{\partial v} \cdot \frac{\partial (A_v)}{\partial u} - \frac{1}{h^5} \cdot \frac{\partial h^2}{\partial v} \cdot \frac{\partial (A_u)}{\partial v} + \frac{1}{h^3} \cdot \frac{\partial^2 (A_u)}{\partial v^2}
\end{aligned}
\quad .
$$

and the v components is:

$$
4.4.3.) \quad
\begin{aligned}
&-\frac{1}{h^5} \cdot \frac{\partial h^2}{\partial v} \cdot \frac{\partial (A_u)}{\partial u} - \frac{1}{h^5} \cdot \frac{\partial h^2}{\partial v} \cdot \frac{\partial (A_v)}{\partial v} + \frac{1}{h^3} \frac{\partial^2 (A_v)}{\partial v^2} + \frac{1}{h^3} \cdot \frac{\partial^2 (A_v)}{\partial u^2} - \\
&\frac{1}{h^5} \cdot \frac{\partial h^2}{\partial u} \cdot \frac{\partial (A_v)}{\partial u} + \frac{1}{h^5} \cdot \frac{\partial h^2}{\partial u} \cdot \frac{\partial (A_u)}{\partial v}
\end{aligned}
$$

For each internal grid point, as in Fig.4.2.2, a second order Taylor approximation allows to discretize the Laplace operator (4.4.2,4.4.3) in terms of the current samples at the neighboring points. The resulting derivatives are as follows:

$$\frac{\partial(A_u)}{\partial u} = \frac{A_{D,u} - A_{B,u}}{2\Delta u}$$

$$\frac{\partial(A_u)}{\partial v} = \frac{A_{C,u} - A_{A,u}}{2\Delta v}$$

$$\frac{\partial(A_v)}{\partial v} = \frac{A_{C,v} - A_{A,v}}{2\Delta v}$$

$$\frac{\partial(A_v)}{\partial u} = \frac{A_{D,v} - A_{B,v}}{2\Delta u}$$

$$\frac{\partial^2(A_u)}{\partial u^2} = \frac{1}{(\Delta u)^2} \cdot \left(A_{D,u} + A_{B,u} - 2A_{P,u} \right)$$

$$\frac{\partial^2(A_v)}{\partial v^2} = \frac{1}{(\Delta v)^2} \cdot \left(A_{C,v} + A_{A,v} - 2A_{P,v} \right)$$

$$\frac{1}{h^3} = a_f^3 \cdot \left(\sinh^2 u + \sin^2 v \right)^{\frac{3}{2}}$$

$$\frac{1}{h^5} = a_f^5 \cdot \left(\sinh^2 u + \sin^2 v \right)^{\frac{5}{2}}$$

4.4.4.) $\dfrac{1}{h^5} \cdot \dfrac{\partial h^2}{\partial u} = -2a_f^3 \cdot \left(\sinh^2 u + \sin^2 v \right)^{\frac{3}{2}} \cdot \sinh u \cdot \cosh u$

$$\frac{1}{h^5} \cdot \frac{\partial h^2}{\partial v} = -2a_f^3 \cdot \left(\sinh^2 u + \sin^2 v \right)^{\frac{3}{2}} \cdot \sin v \cdot \cos v$$

The same simplification is obtained for the first equation 4.3.2 for elliptic case, since letting $\vec{A} = h\vec{M}$ makes this equation almost identical to the rectangular case:

4.4.5.) $\dfrac{1}{h^2} \cdot \left(\dfrac{\partial A_v}{\partial u} - \dfrac{\partial A_u}{\partial v} \right) = \dfrac{1}{h^2} \cdot \left(\dfrac{A_{C,u} - A_{A,u}}{2\Delta u} - \dfrac{A_{D,v} - A_{B,v}}{2\Delta v} \right) = 0$

The singular points of the elliptical framework, either the foci, or the points on the inter--focal segment, require a different treatment. For a focus of the ellipse, Fig.4.2.4, as in the circular case we use the integral form of the eigenvalue equation, as in (4.3.11-4.3.13). The central term of (4.3.12) becomes

$$4.4.6.) \quad \int_C \nabla_t \vec{M} \cdot \vec{i}_n \cdot dl = \int_C \frac{1}{h^2} \cdot \frac{\partial M_u}{\partial u} \cdot \vec{i}_n dl + \int_C \frac{1}{h^2} \cdot \frac{\partial M_v}{\partial v} \cdot \vec{i}_n dl$$

The integrals are divided in 4 parts. We describe here in details only the evaluation of the part over C_1. Letting $Q = \left(a, \frac{\Delta v}{2} \right)$ and $R = \left(\frac{\Delta u}{2}, 0 \right)$, we have

$$
4.4.7.) \quad
\begin{aligned}
\int_{C_1} \frac{1}{h^2} \cdot \frac{\partial M_u}{\partial u} \cdot \vec{i}_n \cdot dl &= \int_o^{\frac{\Delta u}{2}} \frac{1}{h^2} \cdot \frac{\partial M_u}{\partial u} \cdot \vec{i}_n \cdot h \cdot du = \frac{1}{h} \vec{i}_n \Big|_{x_p} \cdot \int_o^{\frac{\Delta u}{2}} \frac{\partial M_u}{\partial u} \cdot du = \\
&\frac{-\vec{i}_x}{h(Q)} \cdot \left[\frac{M_u(A) + M_u(B) + M_u(C) + M_u(D)}{4} - \frac{M_u(A) + M_u(B)}{2} \right]
\end{aligned}
$$

and

$$
4.4.8.) \quad \int_{C_1} \frac{1}{h^2} \frac{\partial M_v}{\partial v} \vec{i}_n dl = \frac{1}{h} \vec{i}_n \frac{\partial M_v}{\partial v} \Big|_Q \int_0^{\frac{\Delta u}{2}} du = \frac{1}{h(Q)} \left(-\vec{i}_x \right) \cdot \left(\frac{M_v(B) - M_v(A)}{\Delta v} \right) \frac{\Delta u}{2}
$$

The same approach can be used for points on the inter--focal segment, such as the one in Fig.4.2.3.

Chapter V

INTRODUCTION

In this chapter we extended the FD approach to waveguides (and apertures) with irregular boundaries, and therefore non-regular discretization grids. We show that a suitable FD approximation of the Laplace operator is still possible. We consider in detail a ridged-waveguide, with trapezoidal ridges, and a rounded-ended waveguide.

5.1) FINITE DIFFERENCE IN RIDGED WAVEGUIDE

In this paragraph we develop a general scheme for the FD approximation of the Laplace operator, based on a non-regular discretization [35].

In order to describe the details of the method we consider a ridge waveguide with trapezoidal ridge shape, with edge of 45 degrees (see Fig. 5.1.1).
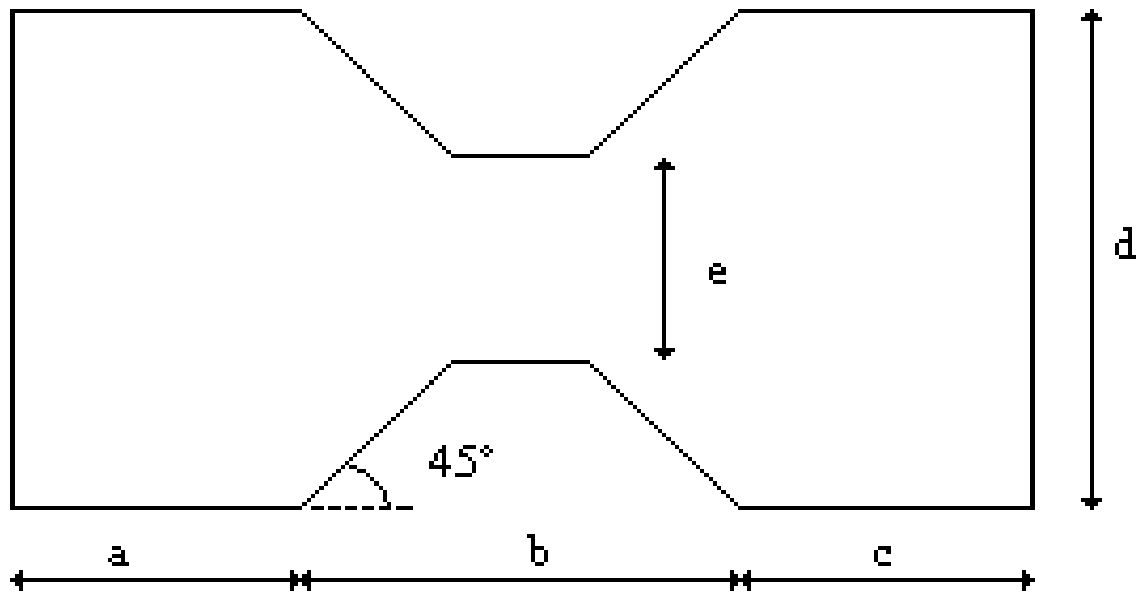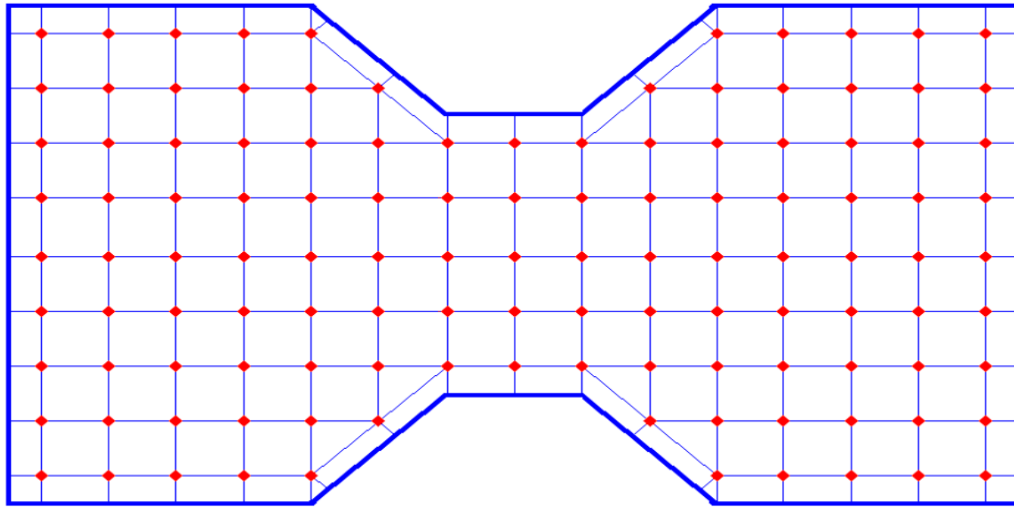
Fig. 5.1.1. Waveguides section with trapezoidal ridge, and FD corner mesh grids

We consider a " TE" grid, as in of Fig.5.1.1b. For a consider a generic point 0 of coordinates (x_0, y_0) we use the five nearby points 1, 2, 3, 4 and 5, as shown in Fig. 5.1.2 .
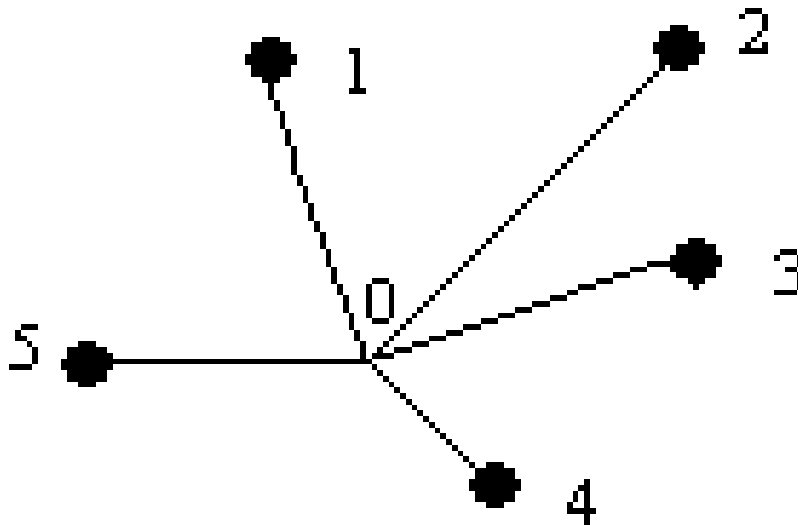
Fig. 5.1.2.   Generic internal case of five points used to develop FD scheme

Let us number with 0 the sampling point, and with i (i = 1, . . . , 5) its neighboring points. Using a second order Taylor approximation we can write for each internal grid point.

$$\phi_i - \phi_0 =$$

5.1.1.) $\left.\dfrac{\partial\phi}{\partial x}\right|_0 \cdot \Delta x_i + \left.\dfrac{\partial\phi}{\partial y}\right|_0 \cdot \Delta y_i + \dfrac{1}{2}\left.\dfrac{\partial^2\phi}{\partial x^2}\right|_0 \cdot \Delta x_i^2 +$

$$+\dfrac{1}{2}\left.\dfrac{\partial^2\phi}{\partial y^2}\right|_0 \cdot \Delta y_i^2 + \left.\dfrac{\partial^2\phi}{\partial x \partial y}\right|_0 \cdot \Delta x_i \cdot \Delta y_i$$

where all derivatives of ϕ are computed at the central sampling point, and $(\Delta x_i, \Delta y_i)$ is the position of the i–th point w.r.t point 0.

A suitable linear combination of these expansions is the sought FD approximation to the Laplace operator, up to the second order:

5.1.2.) $\qquad \nabla_t^2 \phi = \dfrac{\partial^2\phi}{\partial x^2} + \dfrac{\partial^2\phi}{\partial y^2} \cong \sum_i A_i (\phi_i - \phi_0)$

The coefficient can be easily obtained by the solution of a set of 5 linear equations. (5.1.2) can be rewritten, using (5.1.1), as

5.1.3.) $\qquad B_1\dfrac{\partial\phi}{\partial x} + B_2\dfrac{\partial\phi}{\partial y} + B_3\dfrac{\partial^2\phi}{\partial x^2} + B_4\dfrac{\partial^2\phi}{\partial y^2} + B_5\dfrac{\partial^2\phi}{\partial x \partial y}$

The B_i in (5.1.3) are linear combination of the unknown coefficient A_i.

$$B_1 = A_1\Delta x_1 + A_2\Delta x_2 + A_3\Delta x_3 + A_4\Delta x_4 + A_5\Delta x_5$$
$$B_2 = A_1\Delta y_1 + A_2\Delta y_2 + A_3\Delta y_3 + A_4\Delta y_4 + A_5\Delta y_5$$
$$5.1.4.) \qquad B_3 = A_1\Delta x_1^2 + A_2\Delta x_2^2 + A_3\Delta x_3^2 + A_4\Delta x_4^2 + A_5\Delta x_5^2$$
$$B_4 = A_1\Delta y_1^2 + A_2\Delta y_2^2 + A_3\Delta y_3^2 + A_4\Delta y_4^2 + A_5\Delta y_5^2$$
$$B_5 = A_1\Delta x_1\Delta y_1 + A_2\Delta x_2\Delta y_2 + A_3\Delta x_3\Delta y_3 + A_4\Delta x_4\Delta y_4 + A_5\Delta x_5\Delta y_5$$

Eq. (5.1.2) can approximate, to the second order, the Laplace operator if

$$5.1.5.) \qquad B_1 = B_2 = B_5 = 0 \qquad B_3 = B_4 = 1$$

which is a linear system in the A_i. Its solution gives the required coefficient of (5.1.4).

Note that use of only four points lead to an impossible system, unless the grid is rectangular, since in this case $B_5 = 0$ identically. Therefore, for each internal point of Fig.5.1.1 internal point this approach is equal to use the standard FD approssimation (3.2.9).
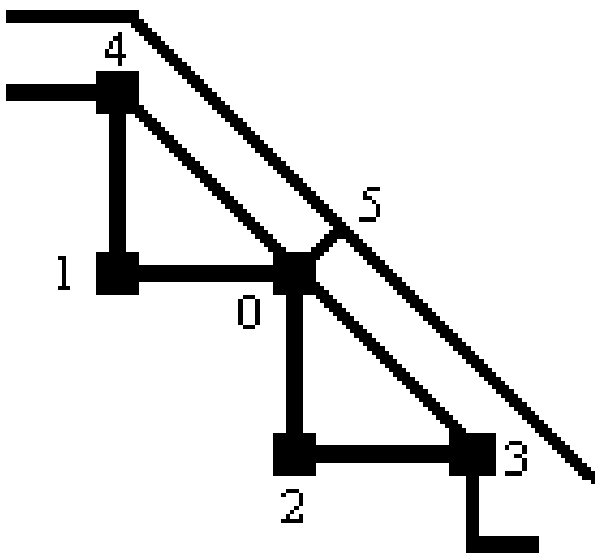
Fig. 5.1.3.   Boundary Point of trapezoidal ridge

For external sampling points (see Fig.5.1.3 and Fig.5.1.4), we require, as usual in standard FD, that the normal derivative must be equal to zero at the sampling point itself and can be expressed as:

$$5.1.6.) \qquad \left.\frac{\partial \phi}{\partial n}\right|_0 = \alpha_x \left.\frac{\partial \phi}{\partial x}\right|_0 + \alpha_y \left.\frac{\partial \phi}{\partial y}\right|_0 = 0$$

where α_x, α_y are the component of a vector normal to the boundary. Eq. (5.5) .

can be used to replace equations $B_1 = 0$, $B_2 = 0$ with a single one, to compensate for the absence of one unknown (see Fig. 5.1.4) In this way we approximate the Laplace operator, and the TE boundary condition, using 4 sapling point.
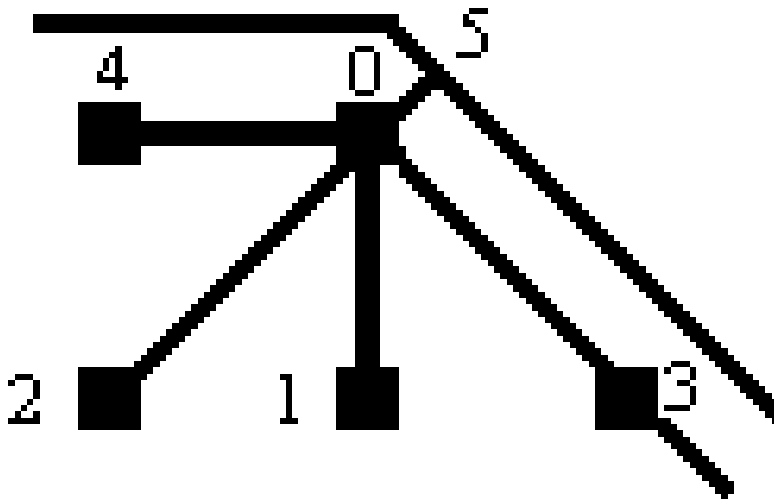
Fig. 5.1.4.   Boundary Point of trapezoidal ridge

For a boundary point as in Fig. 5.3, the coefficients are given, assuming $\Delta x_i = \Delta y_i$, by the linear system (and its solution)

5.1.7.)
$$\begin{cases} -A_1 + A_2 - 2A_3 + 2A_4 = 0 \\ A_1 + A_3 + A_4 = \dfrac{2}{\Delta x^2} \\ A_2 + A_3 + A_4 = \dfrac{2}{\Delta x^2} \\ -A_3 - A_4 = 0 \end{cases}$$

where

5.1.8.)
$$\begin{cases} A_1 = \dfrac{2}{\Delta x^2} \\ A_2 = \dfrac{2}{\Delta x^2} \\ A_3 = 0 \\ A_4 = 0 \end{cases}$$

The corresponding FD approximation of the Laplace operator is therefore

5.1.9.)
$$(\phi_1 + \phi_2)\frac{2}{\Delta x^2} - \phi_0 \frac{4}{\Delta x^2} = \frac{\partial^2 \phi}{\partial x^2} + \frac{\partial^2 \phi}{\partial y^2}$$

In the same way, for a boundary point as in Fig. 5.1.4, i.e., a point in the concave vertex of the boundary, we get:

5.1.10.)
$$(\phi_1 + \phi_4)\frac{1}{\Delta x^2} + (\phi_2 + \phi_3)\frac{1}{2\Delta x^2} - \phi_0 \frac{3}{\Delta x^2} = \frac{\partial^2 \phi}{\partial x^2} + \frac{\partial^2 \phi}{\partial y^2}$$

The proposed scheme could be used on the whole WG section, but usually it is needed only close to the boundaries, where the actual geometry cannot match the rectangular standard grid.

Eqs. (3.2.9),(3.2.10),(5.1.9),5.1.10) are used to fill the matrix equivalent of the Laplace operator, so that the continuous eigenvalue problem (3.2.1) is replaced by a matrix one.

5.2) ROUNDED-END WAVEGUIDE

In this paragraph we present a FD technique for the computation of modes and eigenvalues of a waveguide whose boundary consists of segments and arcs, taking exactly into account the curved boundary of the waveguide and therefore with no loss of accuracy. Among those waveguides, rounded-end waveguides (Fig.5.2.1) are the most interesting and therefore will be considered here.

The borden of the structure border is not coincide with the coordinate curves of any know framework, so a different approach is needed. From the edge structure, it follows that a polar grid is the better choice on the rounded part, and a Cartesian one on the horizontal parts. So we divide the whole section into three parts, as in Fig.5.2.1. In the external ones we use a polar framework, while in the central one we can use the standard Cartesian framework. The proposed approach is to use a polar grid for the curved region and a rectangular grid for the straight ones.
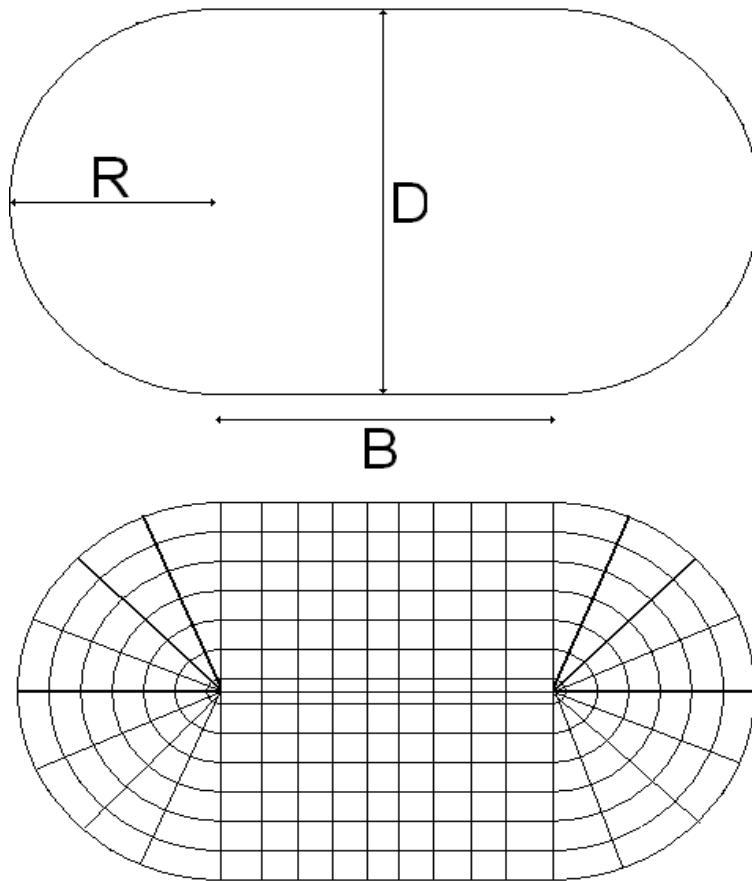
Fig. 5.2.1 A mixed mesh (cartesian-polar) of non standard waveguide and its dimension

In cartesian framework we assume a regular spacing on the coordinate lines, with steps $\Delta x, \Delta y$.

For each internal points we can use the standard expression of the Laplacian (3.2.8) and the discretized form (3.2.9). Equation (3.2.9) cannot be used for boundary points, where BC (3.2.2),(3.2.3) must be enforced. For a boundary point, using 3 nearby points, A,B,C, in Fig.3.2.4a, we can use the expression (3.2.10).

In the polar regions we use the expressions (4.1.7) and (4.1.18), so it remains to analyze the border between the polar and the cartesian regions, Fig.5.2.2. Since the grid geometry here is not a regular one, a new approximation of the laplacian

operator must be used, taylored to the geometry at hand. For this points we use the expressions (5.1.2), (5.1.3), (5.1.4), (5.1.5), (5.1.6).
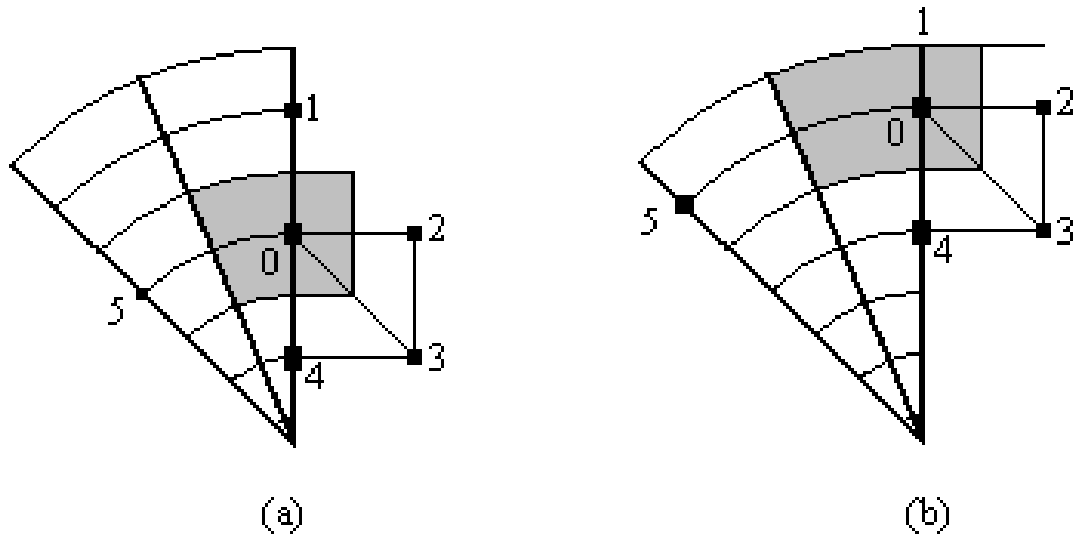
Fig. 5.2.2. (a) Point between Polar and Cartesian framework (b) Boundary point between Polar and Cartesian framework
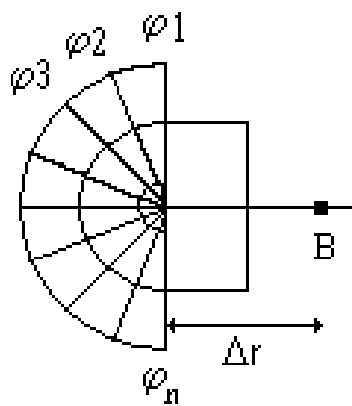
Fig. 5.2.3. Center Point between Polar and Cartesian framework

For the center of the circle, see Fig.5.2.3, we still use (4.1.5) to get:

5.1.11.) $$\left(\frac{8}{\pi\Delta r^2}\right)\cdot\sum_{q=1}^{N}\frac{\left(\phi_q-\phi_P\right)}{\Delta r}\cdot\frac{\Delta r}{2}\cdot\Delta\vartheta+\left(\frac{2}{\Delta r^2}\right)\cdot\left(\frac{\left(\phi_1+\phi_N\right)}{2}+\phi_B-\phi\varphi_P\right)=-k_t^2\phi_P$$

Chapter VI

NUMERICAL RESULTS

INTRODUCTION

In this chapter we report and discuss the numerical results about the procedures and structures, discussed in the chapter III,IV and V

6.1) FD IN SQUARE AND RECTANGULAR WAVEGUIDE

In this paragraph we will show the results of techniques presented in the paragraph 3.3. It is easy to see that k_t^2 is the eigenvalue of an highly sparse matrix, since, for each row of it, no more than 5 elements can be different from zero. Therefore, very effective routines can be used to compute the smallest eigenvalues (the only ones of interest) and the corresponding eigenvectors, i.e., the field distribution of the modes inside the waveguide. To assess the proposed technique we will analyze both square and rectangular waveguide and compare the eigenvalues of the first few TE and TM modes with their exact values.

 In the table 6.1.1 you can see the k_t of TE and TM modes calculated on the TE grids. Data of the square waveguide:

a=10, b=10 Δx=Δy=0.1

kta=kt analytical

ktp=kt of the program

ep= percentage (relative) error

Total points of the grid: 10000

In the table 6.1.2 you can see the k_t of TE and TM modes calculated on the TM grids. Data of the square waveguide:

a=10, b=10   Δx=Δy=0.1

kta=kt analytical   ktp=kt of the program

ep= percentage (relative) error ;   Total points of the grid: 9801

Table 6.1.1: comparison between our FD code and analytic results for TE and
TM modes on TE grid in a square waveguide

TE MODES	kta(TE)	ktp(TE)	ep(TE)%	TM MODES	kta(TM)	ktp(TM)	ep(TM)%
01	0,314159	0,314146	0,0041	11	0,444288	0,444271	0,0040
10	0,314159	0,314146	0,0041	12	0,702482	0,702386	0,0136
11	0,444288	0,444270	0,0041	21	0,702482	0,702386	0,0136
02	0,628319	0,628215	0,0164	22	0,888577	0,888435	0,0160
20	0,628319	0,628215	0,0164	13	0,993459	0,993134	0,0327
12	0,702482	0,702383	0,0140	31	0,993459	0,993134	0,0327
21	0,702482	0,702383	0,0140	23	1,132717	1,132380	0,0298
22	0,888577	0,888430	0,0164	32	1,132717	1,132380	0,0298
03	0,942478	0,942129	0,0370	14	1,295312	1,294531	0,0603
30	0,942478	0,942129	0,0370	41	1,295312	1,294531	0,0603
13	0,993459	0,993124	0,0337	33	1,332865	1,332386	0,0359
31	0,993459	0,993124	0,0337	24	1,404963	1,404201	0,0542
23	1,132717	1,132370	0,0307	42	1,404963	1,404201	0,0542
32	1,132717	1,132370	0,0307	34	1,570796	1,569952	0,0538
04	1,256637	1,255810	0,0658	43	1,570796	1,569952	0,0538
40	1,256637	1,255810	0,0658	15	1,601904	1,600366	0,0960
14	1,295312	1,294507	0,0622	51	1,601904	1,600366	0,0960
41	1,295312	1,294507	0,0622	25	1,691799	1,690308	0,0882
33	1,332865	1,332372	0,0370	52	1,691799	1,690308	0,0882
24	1,404963	1,404177	0,0559	44	1,777153	1,776019	0,0638
42	1,404963	1,404177	0,0559	35	1,831848	1,830331	0,0828
05	1,570796	1,569182	0,1028	53	1,831848	1,830331	0,0828
50	1,570796	1,569182	0,1028	16	1,910956	1,908285	0,1398
34	1,570796	1,569926	0,0554	61	1,910956	1,908285	0,1398
43	1,570796	1,569926	0,0554	26	1,986918	1,984319	0,1308
15	1,601904	1,600319	0,0990	62	1,986918	1,984319	0,1308
51	1,601904	1,600319	0,0990	45	2,011601	2,009877	0,0857
25	1,691799	1,690262	0,0909	54	2,011601	2,009877	0,0857
52	1,691799	1,690262	0,0909	36	2,107444	2,104873	0,1220
44	1,777153	1,775984	0,0658	63	2,107444	2,104873	0,1220

Table 6.1.2: comparison between our FD code and analytic results for TE and TM modes on TM grid in a square waveguide

TE MODES	kta(TE)	ktp(TE)	ep(TE)%	TM MODES	kta(TM)	ktp(TM)	ep(TM)%
01	0,314159	0,314145	0,0046	11	0,444288	0,444270	0,0041
10	0,314159	0,314145	0,0046	12	0,702482	0,702383	0,0140
11	0,444288	0,444268	0,0046	21	0,702482	0,702383	0,0140
02	0,628319	0,628203	0,0184	22	0,888577	0,888430	0,0164
20	0,628319	0,628203	0,0184	13	0,993459	0,993124	0,0337
12	0,702482	0,702372	0,0157	31	0,993459	0,993124	0,0337
21	0,702482	0,702372	0,0157	23	1,132717	1,132370	0,0307
22	0,888577	0,888413	0,0184	32	1,132717	1,132370	0,0307
03	0,942478	0,942088	0,0414	14	1,295312	1,294507	0,0622
30	0,942478	0,942088	0,0414	41	1,295312	1,294507	0,0622
13	0,993459	0,993084	0,0377	33	1,332865	1,332372	0,0370
31	0,993459	0,993084	0,0377	24	1,404963	1,404177	0,0559
23	1,132717	1,132328	0,0343	42	1,404963	1,404177	0,0559
32	1,132717	1,132328	0,0343	34	1,570796	1,569926	0,0554
04	1,256637	1,255713	0,0736	43	1,570796	1,569926	0,0554
40	1,256637	1,255713	0,0736	15	1,601904	1,600319	0,0990
14	1,295312	1,294412	0,0695	51	1,601904	1,600319	0,0990
41	1,295312	1,294412	0,0695	25	1,691799	1,690262	0,0909
33	1,332865	1,332313	0,0414	52	1,691799	1,690262	0,0909
24	1,404963	1,404084	0,0625	44	1,777153	1,775984	0,0658
42	1,404963	1,404084	0,0625	35	1,831848	1,830284	0,0854
05	1,570796	1,568993	0,1148	53	1,831848	1,830284	0,0854
50	1,570796	1,568993	0,1148	16	1,910956	1,908203	0,1441
34	1,570796	1,569823	0,0620	61	1,910956	1,908203	0,1441
43	1,570796	1,569823	0,0620	26	1,986918	1,984239	0,1348
15	1,601904	1,600133	0,1106	62	1,986918	1,984239	0,1348
51	1,601904	1,600133	0,1106	45	2,011601	2,009824	0,0883
25	1,691799	1,690082	0,1015	54	2,011601	2,009824	0,0883
52	1,691799	1,690082	0,1015	36	2,107444	2,104794	0,1258
44	1,777153	1,775846	0,0736	63	2,107444	2,104794	0,1258

In the table 6.1.3 you can see the kt of TE and TM modes calculated on the TE grids. Data of the rectangular waveguide:

a=10, b=5   Δx=Δy=0.1

kta=kt analytical

ktp=kt of the program

ep= percentage (relative) error

Total points of the grid: 5000

In the table 6.1.4 you can see the kt of TE and TM modes calculated on the TM grids. Data of the square waveguide:

a=10, b=5   Δx=Δy=0.1

kta=kt analytical

ktp=kt of the program

ep= percentage (relative) error

Total points of the grid: 4851

In the table 6.1.5 you can see the kt of TE and TM modes calculated on the TE grids. Data of the square waveguide:

a=2 b=10   Δx=Δy=0.1

kta=kt analytical

ktp=kt of the program

ep= percentage (relative) error

Total points of the grid: 2000

In the table 6.1.6 you can see the kt of TE and TM modes calculated on the TE grids. Data of the square waveguide:

a=2 b=10   Δx=Δy=0.1

kta=kt analytical

ktp=kt of the program

ep= percentage (relative) error   Total points of the grid: 1881

Table 6.1.3: comparison between our FD code and analytic results for TE and TM modes on TE grid in a rectangular waveguide

TE MODES	kta(TE)	ktp(TE)	ep(TE)%	TM MODES	kta(TM)	ktp(TM)	ep(TM)%
10	0,314159	0,314146	0,0041	11	0,702482	0,702389	0,0132
01	0,628319	0,628215	0,0164	21	0,888577	0,888437	0,0157
20	0,628319	0,628215	0,0164	31	1,132717	1,132382	0,0296
11	0,702482	0,702383	0,0140	12	1,295312	1,294555	0,0584
21	0,888577	0,888430	0,0164	22	1,404963	1,404202	0,0541
30	0,942478	0,942129	0,0370	41	1,404963	1,404223	0,0527
31	1,132717	1,132370	0,0307	32	1,570796	1,569972	0,0525
02	1,256637	1,255810	0,0658	51	1,691799	1,690309	0,0881
40	1,256637	1,255810	0,0658	42	1,777153	1,776037	0,0628
12	1,295312	1,294507	0,0622	13	1,910956	1,908367	0,1355
22	1,404963	1,404177	0,0559	23	1,986918	1,984320	0,1308
41	1,404963	1,404177	0,0559	61	1,986918	1,984397	0,1268
50	1,570796	1,569182	0,1028	52	2,011601	2,009892	0,0849
32	1,570796	1,569926	0,0554	33	2,107444	2,104947	0,1185
51	1,691799	1,690262	0,0909	43	2,265435	2,262752	0,1184
42	1,777153	1,775984	0,0658	62	2,265435	2,262807	0,1160
03	1,884956	1,882166	0,1480	71	2,287114	2,282956	0,1818
60	1,884956	1,882166	0,1480	53	2,453662	2,450644	0,1230
13	1,910956	1,908203	0,1441	14	2,532833	2,526661	0,2437
23	1,986918	1,984239	0,1348	72	2,532833	2,528717	0,1625
61	1,986918	1,984239	0,1348	24	2,590624	2,584378	0,2411
52	2,011601	2,009824	0,0883	81	2,590624	2,584567	0,2338
33	2,107444	2,104794	0,1258	63	2,665730	2,661961	0,1414
70	2,199115	2,194686	0,2014	34	2,684178	2,678237	0,2213
43	2,265435	2,262655	0,1227	44	2,809926	2,803842	0,2165
62	2,265435	2,262655	0,1227	82	2,809926	2,804006	0,2107
71	2,287114	2,282828	0,1874	73	2,896405	2,887471	0,3085
53	2,453662	2,450486	0,1295	91	2,896405	2,891435	0,1716
04	2,513274	2,506665	0,2630	54	2,963773	2,957670	0,2059
80	2,513274	2,506665	0,2630	92	3,094110	3,085451	0,2798

Table 6.1.4: comparison between our FD code and analytic results for TE and TM modes on TM grid in a rectangular waveguide.

TE MODES	kta(TE)	ktp(TE)	ep(TE)%	TM MODES	kta(TM)	ktp(TM)	ep(TM)%
10	0,314159	0,314145	0,0046	11	0,702482	0,702383	0,0140
01	0,628319	0,628190	0,0204	21	0,888577	0,888430	0,0164
20	0,628319	0,628203	0,0184	31	1,132717	1,132370	0,0307
11	0,702482	0,702360	0,0172	12	1,295312	1,294507	0,0622
21	0,888577	0,888404	0,0194	22	1,404963	1,404177	0,0559
30	0,942478	0,942088	0,0414	41	1,404963	1,404177	0,0559
31	1,132717	1,132322	0,0349	32	1,570796	1,569926	0,0554
02	1,256637	1,255615	0,0813	51	1,691799	1,690262	0,0909
40	1,256637	1,255713	0,0736	42	1,777153	1,775984	0,0658
12	1,295312	1,294317	0,0768	13	1,910956	1,908203	0,1441
22	1,404963	1,403997	0,0687	23	1,986918	1,984239	0,1348
41	1,404963	1,404079	0,0629	61	1,986918	1,984239	0,1348
50	1,570796	1,568993	0,1148	52	2,011601	2,009824	0,0883
32	1,570796	1,569745	0,0670	33	2,107444	2,104794	0,1258
51	1,691799	1,690077	0,1018	43	2,265435	2,262655	0,1227
42	1,777153	1,775777	0,0774	62	2,265435	2,262655	0,1227
03	1,884956	1,881520	0,1823	71	2,287114	2,282828	0,1874
60	1,884956	1,881843	0,1651	53	2,453662	2,450486	0,1295
13	1,910956	1,907565	0,1775	14	2,532833	2,526273	0,2590
23	1,986918	1,983622	0,1659	72	2,532833	2,528578	0,1680
61	1,986918	1,983924	0,1506	24	2,590624	2,584187	0,2485
52	2,011601	2,009554	0,1017	81	2,590624	2,584187	0,2485
33	2,107444	2,104197	0,1541	63	2,665730	2,661785	0,1480
70	2,199115	2,194179	0,2244	34	2,684178	2,677868	0,2351
43	2,265435	2,262064	0,1488	44	2,809926	2,803645	0,2235
62	2,265435	2,262278	0,1393	82	2,809926	2,803645	0,2235
71	2,287114	2,282334	0,2090	73	2,896405	2,887199	0,3179
53	2,453662	2,449869	0,1546	91	2,896405	2,891228	0,1788
04	2,513274	2,505176	0,3222	54	2,963773	2,957313	0,2180
80	2,513274	2,505920	0,2926	92	3,094110	3,085178	0,2887

Table 6.1.5: comparison between our FD code and analytic results for TE and TM modes on TE grid in a rectangular waveguide

TE MODES	kta(TE)	ktp(TE)	ep(TE)%	TM MODES	kta(TM)	ktp(TM)	ep(TM)%
0 1	0,314159	0,314146	0,0041	1 1	1,601904	1,600555	0,0842
0 2	0,628319	0,628215	0,0164	1 2	1,691799	1,690487	0,0776
0 3	0,942478	0,942129	0,0370	1 3	1,831848	1,830496	0,0738
0 4	1,256637	1,255810	0,0658	1 4	2,011601	2,010027	0,0782
0 5	1,570796	1,569182	0,1028	1 5	2,221442	2,219363	0,0936
1 0	1,570796	1,569182	0,1028	1 6	2,453662	2,450704	0,1206
1 1	1,601904	1,600319	0,0990	1 7	2,702500	2,698205	0,1589
1 2	1,691799	1,690262	0,0909	1 8	2,963773	2,957606	0,2081
1 3	1,831848	1,830284	0,0854	2 1	3,157262	3,146306	0,3470
0 6	1,884956	1,882166	0,1480	2 2	3,203808	3,192994	0,3375
1 4	2,011601	2,009824	0,0883	1 9	3,234468	3,225820	0,2674
0 7	2,199115	2,194686	0,2014	2 3	3,279919	3,269278	0,3244
1 5	2,221442	2,219158	0,1028	2 4	3,383599	3,373081	0,3108
1 6	2,453662	2,450486	0,1295	110	3,512407	3,500593	0,3364
0 8	2,513274	2,506665	0,2630	2 5	3,512407	3,501862	0,3002
1 7	2,702500	2,697958	0,1681	2 6	3,663695	3,652864	0,2956
0 9	2,827433	2,818025	0,3328	111	3,796001	3,780262	0,4146
1 8	2,963773	2,957313	0,2180	2 7	3,834803	3,823320	0,2994
010	3,141593	3,128689	0,4107	2 8	4,023202	4,010599	0,3133
2 0	3,141593	3,128689	0,4107	112	4,084070	4,063575	0,5018
2 1	3,157262	3,144421	0,4067	2 9	4,226581	4,212289	0,3381
2 2	3,203808	3,191136	0,3955	113	4,375732	4,349574	0,5978
1 9	3,234468	3,225460	0,2785	210	4,442883	4,426242	0,3746
2 3	3,279919	3,267461	0,3798	114	4,670313	4,637514	0,7023
2 4	3,383599	3,371314	0,3631	211	4,670313	4,650575	0,4226
011	3,455752	3,438582	0,4968	3 1	4,722849	4,685667	0,7873
110	3,512407	3,500147	0,3491	3 2	4,754092	4,717144	0,7772
2 5	3,512407	3,500147	0,3491	3 3	4,805713	4,769110	0,7616
2 6	3,663695	3,651198	0,3411	3 4	4,877063	4,840858	0,7424
012	3,769911	3,747626	0,5911	212	4,907325	4,883657	0,4823

Table 6.1.6: comparison between our FD code and analytic results for TE and TM modes on TM grid in a rectangular waveguide

TE MODES	kta(TE)	ktp(TE)	ep(TE)%	TM MODES	kta(TM)	ktp(TM)	ep(TM)%
01	0,314159	0,314145	0,0046	11	1,601904	1,600319	0,0990
02	0,628319	0,628203	0,0184	12	1,691799	1,690262	0,0909
03	0,942478	0,942088	0,0414	13	1,831848	1,830284	0,0854
04	1,256637	1,255713	0,0736	14	2,011601	2,009824	0,0883
05	1,570796	1,568238	0,1629	15	2,221442	2,219158	0,1028
10	1,570796	1,568993	0,1148	16	2,453662	2,450486	0,1295
11	1,601904	1,599392	0,1568	17	2,702500	2,697958	0,1681
12	1,691799	1,689381	0,1430	18	2,963773	2,957313	0,2180
13	1,831848	1,829453	0,1307	21	3,157262	3,144421	0,4067
06	1,884956	1,881843	0,1651	22	3,203808	3,191136	0,3955
14	2,011601	2,009025	0,1280	19	3,234468	3,225460	0,2785
07	2,199115	2,194179	0,2244	23	3,279919	3,267461	0,3798
15	2,221442	2,218357	0,1389	24	3,383599	3,371314	0,3631
16	2,453662	2,449633	0,1642	110	3,512407	3,500147	0,3491
08	2,513274	2,505920	0,2926	25	3,512407	3,500147	0,3491
17	2,702500	2,696997	0,2036	26	3,663695	3,651198	0,3411
09	2,827433	2,816982	0,3696	111	3,796001	3,779706	0,4293
18	2,963773	2,956180	0,2562	27	3,834803	3,821694	0,3418
0 10	3,141593	3,121714	0,6328	28	4,023202	4,008998	0,3530
20	3,141593	3,127287	0,4554	112	4,084070	4,062885	0,5187
21	3,157262	3,137480	0,6265	29	4,226581	4,210696	0,3758
22	3,203808	3,184295	0,6091	1 13	4,375732	4,348725	0,6172
19	3,234468	3,224090	0,3208	2 10	4,442883	4,424635	0,4107
23	3,279919	3,260771	0,5838	1 14	4,670313	4,636477	0,7245
24	3,383599	3,364805	0,5554	2 11	4,670313	4,648929	0,4579
0 11	3,455752	3,436757	0,5497	31	4,722849	4,679464	0,9186
11 0	3,512407	3,493828	0,5290	32	4,754092	4,710982	0,9068
25	3,512407	3,498470	0,3968	33	4,805713	4,763014	0,8885
26	3,663695	3,645056	0,5088	34	4,877063	4,834848	0,8656
0 12	3,769911	3,745314	0,6524	2 12	4,907325	4,881946	0,5172

In the tables 6.1.7,6.1.8 you can see the kt of TE and TM modes calculated on the TE grids where varying $\Delta x = \Delta y$. Data of the square waveguide:

a=10, b=5

kta=kt analytical

ktp=kt of the program

ep= percentage (relative) error

In the tables 6.1.9,6.1.10 you can see the kt of TE and TM modes calculated on the TM grids where varying $\Delta x = \Delta y$. Data of the square waveguide:

a=10, b=5

kta=kt analytical

ktp=kt of the program

ep= percentage (relative) error

In the tables 6.1.11,6.1.12 you can see the kt of TE and TM modes calculated on the TM grids where varying $\Delta x \neq \Delta y$. Data of the square waveguide:

a=10, b=5

kta=kt analytical

ktp=kt of the program

ep= percentage (relative) error

In the tables 6.1.13,6.1.14 you can see the kt of TE and TM modes calculated on the TM grids where varying $\Delta x \neq \Delta y$. Data of the square waveguide:

a=10, b=5

kta=kt analytical

ktp=kt of the program

ep= percentage (relative) error

Table 6.1.7: comparison between our FD code and analytic results for TE on TE grid in rectangular waveguide, when varying Δx = Δy

TE MODES	kta(TE)	Δy=Δx=0,2		Δy=Δx=0,1		Δy=Δx=0,05	
		ktp(TE)	ep(TE)%	ktp(TE)	ep(TE)%	ktp(TE)	ep(TE)%
10	0,314159	0,314108	0,0165	0,314146	0,0041	0,314156	0,0010
01	0,628319	0,627905	0,0658	0,628215	0,0164	0,628293	0,0041
20	0,628319	0,627905	0,0658	0,628215	0,0164	0,628293	0,0041
11	0,702482	0,702089	0,0559	0,702383	0,0140	0,702457	0,0035
21	0,888577	0,887992	0,0658	0,888430	0,0164	0,888540	0,0041
30	0,942478	0,941083	0,1480	0,942129	0,0370	0,942391	0,0093
31	1,132717	1,131328	0,1227	1,132370	0,0307	1,132630	0,0077
02	1,256637	1,253332	0,2630	1,255810	0,0658	1,256430	0,0165
40	1,256637	1,253332	0,2630	1,255810	0,0658	1,256430	0,0165
12	1,295312	1,292093	0,2485	1,294507	0,0622	1,295111	0,0155
22	1,404963	1,401823	0,2235	1,404177	0,0559	1,404767	0,0140
41	1,404963	1,401823	0,2235	1,404177	0,0559	1,404767	0,0140
50	1,570796	1,564345	0,4107	1,569182	0,1028	1,570393	0,0257
32	1,570796	1,567316	0,2216	1,569926	0,0554	1,570579	0,0139
51	1,691799	1,685657	0,3631	1,690262	0,0909	1,691415	0,0227
42	1,777153	1,772480	0,2630	1,775984	0,0658	1,776861	0,0164
03	1,884956	1,873813	0,5911	1,882166	0,1480	1,884258	0,0370
60	1,884956	1,873813	0,5911	1,882166	0,1480	1,884258	0,0370
13	1,910956	1,899958	0,5755	1,908203	0,1441	1,910268	0,0360
23	1,986918	1,976219	0,5385	1,984239	0,1348	1,986248	0,0337
61	1,986918	1,976219	0,5385	1,984239	0,1348	1,986248	0,0337
52	2,011601	2,004499	0,3530	2,009824	0,0883	2,011156	0,0221
33	2,107444	2,096858	0,5023	2,104794	0,1258	2,106782	0,0315
70	2,199115	2,181432	0,8041	2,194686	0,2014	2,198007	0,0504
43	2,265435	2,254333	0,4900	2,262655	0,1227	2,264740	0,0307
62	2,265435	2,254333	0,4900	2,262655	0,1227	2,264740	0,0307
71	2,287114	2,270003	0,7482	2,282828	0,1874	2,286042	0,0469
53	2,453662	2,440973	0,5172	2,450486	0,1295	2,452868	0,0324
04	2,513274	2,486899	1,0494	2,506665	0,2630	2,511621	0,0658
80	2,513274	2,486899	1,0494	2,506665	0,2630	2,511621	0,0658

Table 6.1.8: comparison between our FD code and analytic results for TM on TE grid in rectangular waveguide, when varying Δx = Δy.

TM MODES	kta(TM)	Δy=Δx=0,2		Δy=Δx=0,1		Δy=Δx=0,05	
		ktp(TM)	ep(TM)%	ktp(TM)	ep(TM)%	ktp(TM)	ep(TM)%
11	0,702482	0,702134	0,0494	0,702389	0,0132	0,702458	0,0034
21	0,888577	0,888044	0,0599	0,888437	0,0157	0,888541	0,0040
31	1,132717	1,131424	0,1142	1,132382	0,0296	1,132632	0,0075
12	1,295312	1,292474	0,2191	1,294555	0,0584	1,295117	0,0151
22	1,404963	1,402020	0,2095	1,404202	0,0541	1,404770	0,0138
41	1,404963	1,402183	0,1978	1,404223	0,0527	1,404772	0,0136
32	1,570796	1,567679	0,1985	1,569972	0,0525	1,570584	0,0135
51	1,691799	1,686027	0,3412	1,690309	0,0881	1,691421	0,0224
42	1,777153	1,772894	0,2396	1,776037	0,0628	1,776867	0,0161
13	1,910956	1,901236	0,5086	1,908367	0,1355	1,910288	0,0350
23	1,986918	1,976848	0,5068	1,984320	0,1308	1,986258	0,0332
61	1,986918	1,977455	0,4762	1,984397	0,1268	1,986268	0,0327
52	2,011601	2,005039	0,3262	2,009892	0,0849	2,011165	0,0217
33	2,107444	2,098053	0,4456	2,104947	0,1185	2,106801	0,0305
43	2,265435	2,255088	0,4567	2,262752	0,1184	2,264752	0,0301
62	2,265435	2,255519	0,4377	2,262807	0,1160	2,264759	0,0298
71	2,287114	2,270992	0,7049	2,282956	0,1818	2,286058	0,0462
53	2,453662	2,442210	0,4667	2,450644	0,1230	2,452888	0,0316
14	2,532833	2,509628	0,9162	2,526661	0,2437	2,531241	0,0629
72	2,532833	2,516923	0,6282	2,528717	0,1625	2,531786	0,0413
24	2,590624	2,566404	0,9349	2,584378	0,2411	2,589038	0,0612
81	2,590624	2,567852	0,8790	2,584567	0,2338	2,589061	0,0603
63	2,665730	2,651346	0,5396	2,661961	0,1414	2,664765	0,0362
34	2,684178	2,661834	0,8324	2,678237	0,2213	2,682646	0,0571
44	2,809926	2,786382	0,8379	2,803842	0,2165	2,808380	0,0550
82	2,809926	2,787634	0,7933	2,804006	0,2107	2,808400	0,0543
73	2,896405	2,861752	1,1964	2,887471	0,3085	2,894136	0,0783
91	2,896405	2,877345	0,6581	2,891435	0,1716	2,895137	0,0438
54	2,963773	2,940736	0,7773	2,957670	0,2059	2,962202	0,0530
92	3,094110	3,060575	1,0838	3,085451	0,2798	3,091910	0,0711

Table 6.1.9: comparison between our FD code and analytic results for TE on TM grid in rectangular waveguide, when varying Δx = Δy.

TE MODES	kta(TE)	Δy=Δx=0,2		Δy=Δx=0,1		Δy=Δx=0,05	
		ktp(TE)	ep(TE)%	ktp(TE)	ep(TE)%	ktp(TE)	ep(TE)%
10	0,314159	0,314095	0,0204	0,314145	0,0046	0,314156	0,0011
01	0,628319	0,627710	0,0969	0,628190	0,0204	0,628290	0,0046
20	0,628319	0,627808	0,0813	0,628203	0,0184	0,628291	0,0044
11	0,702482	0,701909	0,0816	0,702360	0,0172	0,702454	0,0039
21	0,888577	0,887785	0,0891	0,888404	0,0194	0,888537	0,0045
30	0,942478	0,940760	0,1823	0,942088	0,0414	0,942385	0,0098
31	1,132717	1,130951	0,1560	1,132322	0,0349	1,132624	0,0082
02	1,256637	1,251846	0,3813	1,255615	0,0813	1,256406	0,0184
40	1,256637	1,252588	0,3222	1,255713	0,0736	1,256418	0,0174
12	1,295312	1,290649	0,3600	1,294317	0,0768	1,295087	0,0174
22	1,404963	1,400450	0,3212	1,403997	0,0687	1,404744	0,0156
41	1,404963	1,401070	0,2771	1,404079	0,0629	1,404754	0,0149
50	1,570796	1,562944	0,4999	1,568993	0,1148	1,570369	0,0272
32	1,570796	1,565934	0,3096	1,569745	0,0670	1,570556	0,0153
51	1,691799	1,684285	0,4442	1,690077	0,1018	1,691392	0,0241
42	1,777153	1,770902	0,3517	1,775777	0,0774	1,776835	0,0179
03	1,884956	1,869213	0,8352	1,881520	0,1823	1,884175	0,0414
60	1,884956	1,871505	0,7136	1,881843	0,1651	1,884217	0,0392
13	1,910956	1,895419	0,8131	1,907565	0,1775	1,910186	0,0403
23	1,986918	1,971826	0,7595	1,983622	0,1659	1,986169	0,0377
61	1,986918	1,973968	0,6517	1,983924	0,1506	1,986207	0,0357
52	2,011601	2,002477	0,4536	2,009554	0,1017	2,011122	0,0238
33	2,107444	2,092603	0,7043	2,104197	0,1541	2,106705	0,0351
70	2,199115	2,177974	0,9613	2,194179	0,2244	2,197942	0,0534
43	2,265435	2,250096	0,6771	2,262064	0,1488	2,264664	0,0340
62	2,265435	2,251588	0,6112	2,262278	0,1393	2,264691	0,0328
71	2,287114	2,266625	0,8958	2,282334	0,2090	2,285978	0,0497
53	2,453662	2,436545	0,6976	2,449869	0,1546	2,452789	0,0356
04	2,513274	2,477315	1,4308	2,505176	0,3222	2,511425	0,0736
80	2,513274	2,482084	1,2410	2,505920	0,2926	2,511523	0,0697

Table 6.1.10: comparison between our FD code and analytic results for TE on TM grid in rectangular waveguide when varying Δx = Δy

TM MODES	kta(TM)	Δy=Δx=0,2		Δy=Δx=0,1		Δy=Δx=0,05	
		ktp(TM)	ep(TM)%	ktp(TM)	ep(TM)%	ktp(TM)	ep(TM)%
11	0,702482	0,702089	0,0559	0,702383	0,0140	0,702457	0,0035
21	0,888577	0,887992	0,0658	0,888430	0,0164	0,888540	0,0041
31	1,132717	1,131328	0,1227	1,132370	0,0307	1,132630	0,0077
12	1,295312	1,292093	0,2485	1,294507	0,0622	1,295111	0,0155
22	1,404963	1,401823	0,2235	1,404177	0,0559	1,404767	0,0140
41	1,404963	1,401823	0,2235	1,404177	0,0559	1,404767	0,0140
32	1,570796	1,567316	0,2216	1,569926	0,0554	1,570579	0,0139
51	1,691799	1,685657	0,3631	1,690262	0,0909	1,691415	0,0227
42	1,777153	1,772480	0,2630	1,775984	0,0658	1,776861	0,0164
13	1,910956	1,899958	0,5755	1,908203	0,1441	1,910268	0,0360
23	1,986918	1,976219	0,5385	1,984239	0,1348	1,986248	0,0337
61	1,986918	1,976219	0,5385	1,984239	0,1348	1,986248	0,0337
52	2,011601	2,004499	0,3530	2,009824	0,0883	2,011156	0,0221
33	2,107444	2,096858	0,5023	2,104794	0,1258	2,106782	0,0315
43	2,265435	2,254333	0,4900	2,262655	0,1227	2,264740	0,0307
62	2,265435	2,254333	0,4900	2,262655	0,1227	2,264740	0,0307
71	2,287114	2,270003	0,7482	2,282828	0,1874	2,286042	0,0469
53	2,453662	2,440973	0,5172	2,450486	0,1295	2,452868	0,0324
14	2,532833	2,506657	1,0335	2,526273	0,2590	2,531192	0,0648
72	2,532833	2,515848	0,6706	2,528578	0,1680	2,531769	0,0420
24	2,590624	2,564943	0,9913	2,584187	0,2485	2,589013	0,0622
81	2,590624	2,564943	0,9913	2,584187	0,2485	2,589013	0,0622
63	2,665730	2,649972	0,5911	2,661785	0,1480	2,664743	0,0370
34	2,684178	2,659004	0,9379	2,677868	0,2351	2,682599	0,0588
44	2,809926	2,784871	0,8916	2,803645	0,2235	2,808355	0,0559
82	2,809926	2,784871	0,8916	2,803645	0,2235	2,808355	0,0559
73	2,896405	2,859697	1,2674	2,887199	0,3179	2,894102	0,0795
91	2,896405	2,875730	0,7138	2,891228	0,1788	2,895110	0,0447
54	2,963773	2,937999	0,8696	2,957313	0,2180	2,962157	0,0545

.

Table 6.1.11: comparison between our FD code and analytic results for TE on TE grid in rectangular waveguide, when varying $\Delta x \neq \Delta y$.

TE MODES	kta(TE)	Δx=0.01 ; Δy=0,05		Δx=0.01 ; Δy=0,025	
		ktp(TE)	ep(TE)%	ktp(TE)	ep(TE)%
10	0,314159	0,314146	0,0041	0,314146	0,0041
01	0,628319	0,628215	0,0164	0,628215	0,0164
20	0,628319	0,628293	0,0041	0,628312	0,0010
11	0,702482	0,702453	0,0041	0,702470	0,0016
21	0,888577	0,888485	0,0103	0,888499	0,0087
30	0,942478	0,942129	0,0370	0,942129	0,0370
31	1,132717	1,132413	0,0269	1,132424	0,0259
02	1,256637	1,255810	0,0658	1,255810	0,0658
40	1,256637	1,256430	0,0165	1,256585	0,0041
12	1,295312	1,295108	0,0157	1,295259	0,0041
22	1,404963	1,404212	0,0534	1,404221	0,0528
41	1,404963	1,404732	0,0164	1,404871	0,0066
50	1,570796	1,569182	0,1028	1,569182	0,1028
32	1,570796	1,570422	0,0238	1,570546	0,0160
51	1,691799	1,690291	0,0892	1,690298	0,0887
42	1,777153	1,776423	0,0411	1,776532	0,0349
03	1,884956	1,882166	0,1480	1,882166	0,1480
60	1,884956	1,884258	0,0370	1,884781	0,0093
13	1,910956	1,910266	0,0361	1,910782	0,0091
23	1,986918	1,984263	0,1336	1,984270	0,1333
61	1,986918	1,986223	0,0350	1,986720	0,0100
52	2,011601	2,010211	0,0691	2,010308	0,0643
33	2,107444	2,106665	0,0370	2,107132	0,0148
70	2,199115	2,194686	0,2014	2,194686	0,2014
43	2,265435	2,263000	0,1075	2,263086	0,1037
62	2,265435	2,264396	0,0459	2,264831	0,0266
71	2,287114	2,282849	0,1865	2,282854	0,1862
53	2,453662	2,452093	0,0640	2,452495	0,0476
04	2,513274	2,506665	0,2630	2,506665	0,2630
80	2,513274	2,511621	0,0658	2,512861	0,0164

Table 6.1.12: comparison between our FD code and analytic results for TM on TE grid in rectangular waveguide, when varying Δx ≠Δy.

		Δx=0.01 ; Δy=0,05		Δx=0.01 ; Δy=0,025	
TM MODES	kta(TM)	ktp(TM)	ep(TM)%	ktp(TM)	ep(TM)%
11	0,702482	0,702453	0,0040	0,702470	0,0016
21	0,888577	0,888488	0,0100	0,888501	0,0085
31	1,132717	1,132422	0,0261	1,132432	0,0252
12	1,295312	1,295114	0,0152	1,295259	0,0040
22	1,404963	1,404234	0,0518	1,404243	0,0513
41	1,404963	1,404739	0,0160	1,404873	0,0064
32	1,570796	1,570433	0,0231	1,570553	0,0155
51	1,691799	1,690336	0,0865	1,690343	0,0861
42	1,777153	1,776444	0,0399	1,776550	0,0339
13	1,910956	1,910287	0,0350	1,910785	0,0090
23	1,986918	1,984342	0,1296	1,984348	0,1293
61	1,986918	1,986244	0,0339	1,986723	0,0098
52	2,011601	2,010253	0,0670	2,010346	0,0624
33	2,107444	2,106688	0,0359	2,107139	0,0145
43	2,265435	2,263072	0,1043	2,263155	0,1006
62	2,265435	2,264427	0,0445	2,264847	0,0259
71	2,287114	2,282975	0,1810	2,282981	0,1807
53	2,453662	2,452140	0,0620	2,452528	0,0462
14	2,532833	2,529003	0,1512	2,529078	0,1483
72	2,532833	2,531240	0,0629	2,532427	0,0160
24	2,590624	2,584395	0,2404	2,584400	0,2402
81	2,590624	2,589043	0,0610	2,590204	0,0162
63	2,665730	2,663338	0,0897	2,663695	0,0763
34	2,684178	2,682557	0,0604	2,683678	0,0186
44	2,809926	2,804101	0,2073	2,804168	0,2049
82	2,809926	2,808133	0,0638	2,809203	0,0257
73	2,896405	2,887486	0,3079	2,887490	0,3078
91	2,896405	2,892703	0,1278	2,893032	0,1165
54	2,963773	2,961582	0,0739	2,962597	0,0397
92	3,094110	3,085686	0,2723	3,085747	0,2703

Table 6.1.13: comparison between our FD code and analytic results for TE on TM grid in rectangular waveguide, when varying $\Delta x \neq \Delta y$.

		Δx=0.01 ; Δy=0,05		Δx=0.01 ; Δy=0,025	
TE MODES	kta(TE)	ktp(TE)	ep(TE)%	ktp(TE)	ep(TE)%
10	0,314159	0,314145	0,0046	0,314145	0,0046
01	0,628319	0,628203	0,0184	0,628203	0,0184
20	0,628319	0,628290	0,0046	0,628290	0,0046
11	0,702482	0,702449	0,0046	0,702449	0,0046
21	0,888577	0,888474	0,0115	0,888474	0,0115
30	0,942478	0,942088	0,0414	0,942088	0,0414
31	1,132717	1,132377	0,0301	1,132377	0,0301
02	1,256637	1,255713	0,0736	1,255713	0,0736
40	1,256637	1,256406	0,0184	1,256406	0,0184
12	1,295312	1,295084	0,0176	1,295084	0,0176
22	1,404963	1,404123	0,0598	1,404123	0,0598
41	1,404963	1,404704	0,0184	1,404704	0,0184
50	1,570796	1,568993	0,1148	1,568993	0,1148
32	1,570796	1,570377	0,0267	1,570377	0,0267
51	1,691799	1,690114	0,0996	1,690114	0,0996
42	1,777153	1,776336	0,0460	1,776336	0,0460
03	1,884956	1,881843	0,1651	1,881843	0,1651
60	1,884956	1,884175	0,0414	1,884175	0,0414
13	1,910956	1,910184	0,0404	1,910184	0,0404
23	1,986918	1,983956	0,1491	1,983956	0,1491
61	1,986918	1,986141	0,0391	1,986141	0,0391
52	2,011601	2,010048	0,0772	2,010048	0,0772
33	2,107444	2,106572	0,0414	2,106572	0,0414
70	2,199115	2,194179	0,2244	2,194179	0,2244
43	2,265435	2,262717	0,1200	2,262717	0,1200
62	2,265435	2,264272	0,0513	2,264272	0,0513
71	2,287114	2,282361	0,2078	2,282361	0,2078
53	2,453662	2,451908	0,0715	2,451908	0,0715
04	2,513274	2,505920	0,2926	2,505920	0,2926
80	2,513274	2,511425	0,0736	2,511425	0,0736

Table 6.1.14: comparison between our FD code and analytic results for TM on TM grid in rectangular waveguide, when varying Δx ≠Δy

		Δx=0.01 ; Δy=0,05		Δx=0.01 ; Δy=0,025	
TM MODES	kta(TM)	ktp(TM)	ep(TM)%	ktp(TM)	ep(TM)%
11	0,702482	0,702453	0,0041	0,702453	0,0041
21	0,888577	0,888485	0,0103	0,888485	0,0103
31	1,132717	1,132413	0,0269	1,132413	0,0269
12	1,295312	1,295108	0,0157	1,295108	0,0157
22	1,404963	1,404212	0,0534	1,404212	0,0534
41	1,404963	1,404732	0,0164	1,404732	0,0164
32	1,570796	1,570422	0,0238	1,570422	0,0238
51	1,691799	1,690291	0,0892	1,690291	0,0892
42	1,777153	1,776423	0,0411	1,776423	0,0411
13	1,910956	1,910266	0,0361	1,910266	0,0361
23	1,986918	1,984263	0,1336	1,984263	0,1336
61	1,986918	1,986223	0,0350	1,986223	0,0350
52	2,011601	2,010211	0,0691	2,010211	0,0691
33	2,107444	2,106665	0,0370	2,106665	0,0370
43	2,265435	2,263000	0,1075	2,263000	0,1075
62	2,265435	2,264396	0,0459	2,264396	0,0459
71	2,287114	2,282849	0,1865	2,282849	0,1865
53	2,453662	2,452093	0,0640	2,452093	0,0640
14	2,532833	2,528886	0,1558	2,528886	0,1558
72	2,532833	2,531191	0,0648	2,531191	0,0648
24	2,590624	2,584206	0,2477	2,584206	0,2477
81	2,590624	2,588995	0,0629	2,588995	0,0629
63	2,665730	2,663265	0,0925	2,663265	0,0925
34	2,684178	2,682507	0,0622	2,682507	0,0622
44	2,809926	2,803923	0,2136	2,803923	0,2136
82	2,809926	2,808077	0,0658	2,808077	0,0658
73	2,896405	2,887216	0,3173	2,887216	0,3173
91	2,896405	2,892590	0,1317	2,892590	0,1317
54	2,963773	2,961515	0,0762	2,961515	0,0762
92	3,094110	3,085430	0,2805	3,085430	0,2805

We have made several tests by varying the steps (Δx,Δy). The results of the tables 6.1.1 to 6.1.14 shows that our technique has a very low error, as long as the steps are small

6.2) FD IN CIRCULAR AND ELLIPTYCAL WAVEGUIDE

In this paragraph we will show the results of techniques presented in the paragraph 4.1 and 4.2 To assess the proposed technique, we will analyze both circular and elliptical waveguide.

In the table 6.2.1 you can see the kt of TE and TM modes calculated on the TE grids.

Data of the circular waveguide:

r=4, $\Delta\theta$=1° Δr=0.079208

kta=kt analytical

ktp=kt of the program

ep= percentage (relative) error

Total points of the grid: 18001

In the table 6.2.2 , 6.2.3 you can see the kt of TE and TM modes calculated on the TE grids where varying Δr

Data of the circular waveguide:

r=4, $\Delta\theta$=1°

kta=kt analytical

ktp=kt of the program

ep= percentage (relative) error

In the table 6.2.4 , 6.2.5 you can see the kt of TE and TM modes calculated on the TE grids where varying $\Delta\theta$

Data of the circular waveguide:

r=4, Δr= 0.079208

kta=kt analytical

ktp=kt of the program

ep= percentage (relative) error

Table 6.2.1: comparison between our FD code and analytic results for TE and
TM modes on TE grid in circular waveguide

TE MODES	Kta	Ktp	ep%	TM MODES	Kta	Ktp	ep%
11	0,460296	0,460292	0,0008	01	0,601200	0,601141	0,0098
11	0,460296	0,460292	0,0008	11	0,957925	0,957796	0,0135
21	0,7635592	0,763531	0,0037	11	0,957925	0,957796	0,0135
21	0,7635592	0,763531	0,0037	21	1,283900	1,283680	0,0171
01	0,9579265	0,957697	0,0240	21	1,283900	1,283680	0,0171
31	1,0502972	1,050204	0,0088	02	1,380025	1,379330	0,0504
31	1,0502972	1,050204	0,0088	31	1,595050	1,594670	0,0238
41	1,3293883	1,329170	0,0164	31	1,595050	1,594670	0,0238
41	1,3293883	1,329170	0,0164	12	1,753900	1,752912	0,0563
12	1,3328607	1,332475	0,0290	12	1,753900	1,752912	0,0563
12	1,3328607	1,332475	0,0290	41	1,897075	1,896501	0,0302
51	1,6039041	1,603482	0,0263	41	1,897075	1,896501	0,0302
51	1,6039041	1,603482	0,0263	22	2,104300	2,102992	0,0622
22	1,6765333	1,675952	0,0347	22	2,104300	2,102992	0,0622
22	1,6765333	1,675952	0,0347	03	2,163425	2,160829	0,1200
02	1,7538967	1,752487	0,0804	51	2,192875	2,191983	0,0407
61	1,8753165	1,874590	0,0387	51	2,192875	2,191983	0,0407
61	1,8753165	1,874590	0,0387	32	2,440250	2,438539	0,0701
32	2,0038092	2,002971	0,0418	32	2,440250	2,438539	0,0701
32	2,0038092	2,002971	0,0418	61	2,484025	2,482728	0,0522
13	2,1340791	2,132172	0,0894	61	2,484025	2,482728	0,0522
13	2,1340791	2,132172	0,0894	13	2,543375	2,540060	0,1303
71	2,1444591	2,143311	0,0536	13	2,543375	2,540060	0,1303
71	2,1444591	2,143311	0,0536	42	2,766175	2,763979	0,0794
42	2,3205991	2,319424	0,0506	42	2,766175	2,763979	0,0794
42	2,3205991	2,319424	0,0506	71	2,771593	2,769754	0,0663
81	2,4118554	2,410147	0,0708	71	2,771593	2,769754	0,0663
81	2,4118554	2,410147	0,0708	23	2,904950	2,900901	0,1394
23	2,492367	2,489910	0,0986	23	2,904950	2,900901	0,1394

Table 6.2.2: comparison between our FD code and analytic results for TE modes on TE grid in circular waveguide , when varying Δr

| TE MODES | Kta | $\Delta r=0.156863$ | | $\Delta r=0.079208$ | | $\Delta r=0.039409$ | |
		Ktp	ep%	Ktp	ep%	Ktp	ep%
11	0,460296	0,460294	0,0005	0,460292	0,0008	0,460292	0,0009
11	0,460296	0,460294	0,0005	0,460292	0,0008	0,460292	0,0009
21	0,763559	0,763537	0,0030	0,763531	0,0037	0,763530	0,0038
21	0,763559	0,763537	0,0030	0,763531	0,0037	0,763530	0,0038
01	0,957927	0,957026	0,0940	0,957697	0,0240	0,957870	0,0059
31	1,050297	1,050216	0,0077	1,050204	0,0088	1,050202	0,0091
31	1,050297	1,050216	0,0077	1,050204	0,0088	1,050202	0,0091
41	1,329388	1,329191	0,0149	1,329170	0,0164	1,329165	0,0168
41	1,329388	1,329191	0,0149	1,329170	0,0164	1,329165	0,0168
12	1,332861	1,331358	0,1128	1,332475	0,0290	1,332762	0,0074
12	1,332861	1,331358	0,1128	1,332475	0,0290	1,332762	0,0074
51	1,603904	1,603513	0,0244	1,603482	0,0263	1,603474	0,0268
51	1,603904	1,603513	0,0244	1,603482	0,0263	1,603474	0,0268
22	1,676533	1,674350	0,1302	1,675952	0,0347	1,676364	0,0101
22	1,676533	1,674350	0,1302	1,675952	0,0347	1,676364	0,0101
02	1,753897	1,748379	0,3146	1,752487	0,0804	1,753548	0,0199
61	1,875317	1,874634	0,0364	1,874590	0,0387	1,874579	0,0393
61	1,875317	1,874634	0,0364	1,874590	0,0387	1,874579	0,0393
32	2,003809	2,000842	0,1481	2,002971	0,0418	2,003519	0,0145
32	2,003809	2,000842	0,1481	2,002971	0,0418	2,003519	0,0145
13	2,134079	2,126606	0,3502	2,132172	0,0894	2,133604	0,0223
13	2,134079	2,126606	0,3502	2,132172	0,0894	2,133604	0,0223
71	2,144459	2,143369	0,0508	2,143311	0,0536	2,143296	0,0542
71	2,144459	2,143369	0,0508	2,143311	0,0536	2,143296	0,0542
42	2,320599	2,316728	0,1668	2,319424	0,0506	2,320117	0,0208
42	2,320599	2,316728	0,1668	2,319424	0,0506	2,320117	0,0208
81	2,411855	2,410222	0,0677	2,410147	0,0708	2,410129	0,0716
81	2,411855	2,410222	0,0677	2,410147	0,0708	2,410129	0,0716
23	2,492367	2,482826	0,3828	2,489910	0,0986	2,491732	0,0255

Table 6.2.3: comparison between our FD code and analytic results for TM modes on TE grid in circular waveguide , when varying Δr

		Δr=0.156863		Δr=0.079208		Δr=0.039409	
TM MODES	Kta	Ktp	ep%	Ktp	ep%	Ktp	ep%
01	0,601200	0,600954	0,0409	0,601141	0,0098	0,601190	0,0017
11	0,957925	0,957447	0,0499	0,957796	0,0135	0,957890	0,0036
11	0,957925	0,957447	0,0499	0,957796	0,0135	0,957890	0,0036
21	1,283900	1,283164	0,0573	1,283680	0,0171	1,283824	0,0059
21	1,283900	1,283164	0,0573	1,283680	0,0171	1,283824	0,0059
02	1,380025	1,377392	0,1908	1,379330	0,0504	1,379846	0,0130
31	1,595050	1,593983	0,0669	1,594670	0,0238	1,594867	0,0115
31	1,595050	1,593983	0,0669	1,594670	0,0238	1,594867	0,0115
12	1,753900	1,750200	0,2110	1,752912	0,0563	1,753645	0,0146
12	1,753900	1,750200	0,2110	1,752912	0,0563	1,753645	0,0146
41	1,897075	1,895640	0,0756	1,896501	0,0302	1,896754	0,0169
41	1,897075	1,895640	0,0756	1,896501	0,0302	1,896754	0,0169
22	2,104300	2,099493	0,2285	2,102992	0,0622	2,103950	0,0166
22	2,104300	2,099493	0,2285	2,102992	0,0622	2,103950	0,0166
03	2,163425	2,153543	0,4568	2,160829	0,1200	2,162778	0,0299
51	2,192875	2,190948	0,0879	2,191983	0,0407	2,192295	0,0265
51	2,192875	2,190948	0,0879	2,191983	0,0407	2,192295	0,0265
32	2,440250	2,434227	0,2468	2,438539	0,0701	2,439733	0,0212
32	2,440250	2,434227	0,2468	2,438539	0,0701	2,439733	0,0212
61	2,484025	2,481520	0,1009	2,482728	0,0522	2,483100	0,0372
61	2,484025	2,481520	0,1009	2,482728	0,0522	2,483100	0,0372
13	2,543375	2,530872	0,4916	2,540060	0,1303	2,542530	0,0332
13	2,543375	2,530872	0,4916	2,540060	0,1303	2,542530	0,0332
42	2,766175	2,758834	0,2654	2,763979	0,0794	2,765419	0,0273
42	2,766175	2,758834	0,2654	2,763979	0,0794	2,765419	0,0273
71	2,771593	2,768374	0,1161	2,769754	0,0663	2,770189	0,0506
71	2,771593	2,768374	0,1161	2,769754	0,0663	2,770189	0,0506
23	2,904950	2,889818	0,5209	2,900901	0,1394	2,903906	0,0359
23	2,904950	2,889818	0,5209	2,900901	0,1394	2,903906	0,0359

Table 6.2.4: comparison between our FD code and analytic results for TE modes on TE grid in circular waveguide , when varying Δθ

TE MODES	Kta	Δθ=2°		Δθ=1°		Δθ=0.5°	
		Ktp	ep%	Ktp	ep%	Ktp	ep%
11	0,460296	0,460280	0,0034	0,460292	0,0008	0,460295	0,0001
11	0,460296	0,460280	0,0034	0,460292	0,0008	0,460295	0,0001
21	0,763559	0,763442	0,0153	0,763531	0,0037	0,763554	0,0007
21	0,763559	0,763442	0,0153	0,763531	0,0037	0,763554	0,0007
01	0,957927	0,957697	0,0240	0,957697	0,0240	0,957697	0,0240
31	1,050297	1,049914	0,0364	1,050204	0,0088	1,050277	0,0019
31	1,050297	1,049914	0,0364	1,050204	0,0088	1,050277	0,0019
41	1,329388	1,328497	0,0671	1,329170	0,0164	1,329339	0,0037
41	1,329388	1,328497	0,0671	1,329170	0,0164	1,329339	0,0037
12	1,332861	1,332461	0,0300	1,332475	0,0290	1,332478	0,0287
12	1,332861	1,332461	0,0300	1,332475	0,0290	1,332478	0,0287
51	1,603904	1,602184	0,1073	1,603482	0,0263	1,603806	0,0061
51	1,603904	1,602184	0,1073	1,603482	0,0263	1,603806	0,0061
22	1,676533	1,675850	0,0408	1,675952	0,0347	1,675977	0,0332
22	1,676533	1,675850	0,0408	1,675952	0,0347	1,675977	0,0332
02	1,753897	1,752487	0,0804	1,752487	0,0804	1,752487	0,0804
61	1,875317	1,872370	0,1571	1,874590	0,0387	1,875146	0,0091
61	1,875317	1,872370	0,1571	1,874590	0,0387	1,875146	0,0091
32	2,003809	2,002641	0,0583	2,002971	0,0418	2,003054	0,0377
32	2,003809	2,002641	0,0583	2,002971	0,0418	2,003054	0,0377
13	2,134079	2,132158	0,0900	2,132172	0,0894	2,132176	0,0892
13	2,134079	2,132158	0,0900	2,132172	0,0894	2,132176	0,0892
71	2,144459	2,139811	0,2168	2,143311	0,0536	2,144186	0,0127
71	2,144459	2,139811	0,2168	2,143311	0,0536	2,144186	0,0127
42	2,320599	2,318663	0,0834	2,319424	0,0506	2,319615	0,0424
42	2,320599	2,318663	0,0834	2,319424	0,0506	2,319615	0,0424
81	2,411855	2,404954	0,2861	2,410147	0,0708	2,411446	0,0170
81	2,411855	2,404954	0,2861	2,410147	0,0708	2,411446	0,0170
23	2,492367	2,489804	0,1028	2,489910	0,0986	2,489937	0,0975

Table 6.2.5: comparison between our FD code and analytic results for TM modes on TE grid in circular waveguide , when varying $\Delta\theta$

		$\Delta\theta=2°$		$\Delta\theta=1°$		$\Delta\theta=0.5°$	
TM MODES	Kta	Ktp	ep%	Ktp	ep%	Ktp	ep%
01	0,601200	0,601141	0,0098	0,601141	0,0098	0,601141	0,0098
11	0,957925	0,957783	0,0148	0,957796	0,0135	0,957799	0,0132
11	0,957925	0,957783	0,0148	0,957796	0,0135	0,957799	0,0132
21	1,283900	1,283583	0,0247	1,283680	0,0171	1,283704	0,0153
21	1,283900	1,283583	0,0247	1,283680	0,0171	1,283704	0,0153
02	1,380025	1,379330	0,0504	1,379330	0,0504	1,379330	0,0504
31	1,595050	1,594356	0,0435	1,594670	0,0238	1,594749	0,0189
31	1,595050	1,594356	0,0435	1,594670	0,0238	1,594749	0,0189
12	1,753900	1,752899	0,0571	1,752912	0,0563	1,752916	0,0561
12	1,753900	1,752899	0,0571	1,752912	0,0563	1,752916	0,0561
41	1,897075	1,895774	0,0686	1,896501	0,0302	1,896683	0,0207
41	1,897075	1,895774	0,0686	1,896501	0,0302	1,896683	0,0207
22	2,104300	2,102888	0,0671	2,102992	0,0622	2,103018	0,0609
22	2,104300	2,102888	0,0671	2,102992	0,0622	2,103018	0,0609
03	2,163425	2,160829	0,1200	2,160829	0,1200	2,160829	0,1200
51	2,192875	2,190588	0,1043	2,191983	0,0407	2,192332	0,0248
51	2,192875	2,190588	0,1043	2,191983	0,0407	2,192332	0,0248
32	2,440250	2,438199	0,0840	2,438539	0,0701	2,438624	0,0667
32	2,440250	2,438199	0,0840	2,438539	0,0701	2,438624	0,0667
61	2,484025	2,480352	0,1479	2,482728	0,0522	2,483323	0,0283
61	2,484025	2,480352	0,1479	2,482728	0,0522	2,483323	0,0283
13	2,543375	2,540046	0,1309	2,540060	0,1303	2,540064	0,1302
13	2,543375	2,540046	0,1309	2,540060	0,1303	2,540064	0,1302
42	2,766175	2,763195	0,1077	2,763979	0,0794	2,764174	0,0723
42	2,766175	2,763195	0,1077	2,763979	0,0794	2,764174	0,0723
71	2,771593	2,766023	0,2010	2,769754	0,0663	2,770687	0,0327
71	2,771593	2,766023	0,2010	2,769754	0,0663	2,770687	0,0327
23	2,904950	2,900794	0,1431	2,900901	0,1394	2,900928	0,1384
23	2,904950	2,900794	0,1431	2,900901	0,1394	2,900928	0,1384

In the table 6.2.6 , 6.2.7 you can see the kt of TE and TM modes calculated on the TM grids when varying Δr

Data of the circular waveguide:

r=4, $\Delta\theta$=1°

kta=kt analytical

ktp=kt of the program

ep= percentage (relative) error

In the table 6.2.8 , 6.2.9 you can see the kt of TE and TM modes calculated on the TM grids when varying $\Delta\theta$

Data of the circular waveguide:

r=4, Δr= 0.079208

kta=kt analytical

ktp=kt of the program

ep= percentage (relative) error

In the Figures 6.2.1, 6.2.2. comparison between our FD code and analytic results and FIT(CST) results for TE modes in circular waveguide calculated on the TE grids.

Data of the circular waveguide figure 6.2.1:

r=4, $\Delta\theta$=1° Δr=0.079208

Data of the circular waveguide figure 6.2.2:

r=4, $\Delta\theta$=0.5° Δr=0.079208

Table 6.2.6: comparison between our FD code and analytic results for TM modes on TM grid in circular waveguide , when varying Δr

		Δr=0.153846		Δr=0.078431		Δr=0.039604	
TM MODES	Kta	Ktp	ep%	Ktp	ep%	Ktp	ep%
01	0,601200	0,600970	0,0382	0,601143	0,0094	0,601190	0,0017
11	0,957925	0,957439	0,0507	0,957796	0,0135	0,957890	0,0037
11	0,957925	0,957439	0,0507	0,957796	0,0135	0,957890	0,0037
21	1,283900	1,283103	0,0621	1,283674	0,0176	1,283822	0,0060
21	1,283900	1,283103	0,0621	1,283674	0,0176	1,283822	0,0060
02	1,380025	1,377342	0,1944	1,379326	0,0506	1,379843	0,0132
31	1,595050	1,593839	0,0759	1,594655	0,0247	1,594864	0,0117
31	1,595050	1,593839	0,0759	1,594655	0,0247	1,594864	0,0117
12	1,753900	1,750000	0,2224	1,752893	0,0574	1,753638	0,0150
12	1,753900	1,750000	0,2224	1,752893	0,0574	1,753638	0,0150
41	1,897075	1,895385	0,0891	1,896474	0,0317	1,896749	0,0172
41	1,897075	1,895385	0,0891	1,896474	0,0317	1,896749	0,0172
22	2,104300	2,099080	0,2480	2,102949	0,0642	2,103939	0,0172
22	2,104300	2,099080	0,2480	2,102949	0,0642	2,103939	0,0172
03	2,163425	2,153229	0,4713	2,160800	0,1213	2,162762	0,0307
51	2,192875	2,190552	0,1059	2,191940	0,0426	2,192287	0,0268
51	2,192875	2,190552	0,1059	2,191940	0,0426	2,192287	0,0268
32	2,440250	2,433541	0,2749	2,438465	0,0731	2,439717	0,0218
32	2,440250	2,433541	0,2749	2,438465	0,0731	2,439717	0,0218
61	2,484025	2,480953	0,1237	2,482665	0,0548	2,483090	0,0376
61	2,484025	2,480953	0,1237	2,482665	0,0548	2,483090	0,0376
13	2,543375	2,530209	0,5177	2,539993	0,1330	2,542506	0,0342
13	2,543375	2,530209	0,5177	2,539993	0,1330	2,542506	0,0342
42	2,766175	2,757814	0,3023	2,763867	0,0834	2,765397	0,0281
42	2,766175	2,757814	0,3023	2,763867	0,0834	2,765397	0,0281
71	2,771593	2,767606	0,1438	2,769667	0,0695	2,770176	0,0511
71	2,771593	2,767606	0,1438	2,769667	0,0695	2,770176	0,0511
23	2,904950	2,888710	0,5590	2,900784	0,1434	2,903873	0,0371
23	2,904950	2,888710	0,5590	2,900784	0,1434	2,903873	0,0371

Table 6.2.7: comparison between our FD code and analytic results for TE modes on TM grid in circular waveguide , when varying Δr

TE MODES	Kta	Δr=0.153846		Δr=0.078431		Δr=0.039604	
		Ktp	ep%	Ktp	ep%	Ktp	ep%
11	0,460296	0,460271	0,0054	0,460289	0,0015	0,460291	0,0010
11	0,460296	0,460271	0,0054	0,460289	0,0015	0,460291	0,0010
21	0,763559	0,763432	0,0166	0,763522	0,0049	0,763530	0,0039
21	0,763559	0,763432	0,0166	0,763522	0,0049	0,763530	0,0039
01	0,957927	0,956850	0,1124	0,957669	0,0269	0,957863	0,0066
31	1,050297	1,049995	0,0288	1,050185	0,0106	1,050201	0,0091
31	1,050297	1,049995	0,0288	1,050185	0,0106	1,050201	0,0091
41	1,329388	1,328828	0,0421	1,329139	0,0187	1,329166	0,0167
41	1,329388	1,328828	0,0421	1,329139	0,0187	1,329166	0,0167
12	1,332861	1,330816	0,1534	1,332400	0,0345	1,332748	0,0084
12	1,332861	1,330816	0,1534	1,332400	0,0345	1,332748	0,0084
51	1,603904	1,602992	0,0569	1,603436	0,0292	1,603475	0,0268
51	1,603904	1,602992	0,0569	1,603436	0,0292	1,603475	0,0268
22	1,676533	1,673297	0,1930	1,675813	0,0430	1,676341	0,0114
22	1,676533	1,673297	0,1930	1,675813	0,0430	1,676341	0,0114
02	1,753897	1,747142	0,3851	1,752325	0,0896	1,753517	0,0216
61	1,875317	1,873948	0,0730	1,874528	0,0421	1,874581	0,0392
61	1,875317	1,873948	0,0730	1,874528	0,0421	1,874581	0,0392
32	2,003809	1,999156	0,2322	2,002750	0,0529	2,003485	0,0162
32	2,003809	1,999156	0,2322	2,002750	0,0529	2,003485	0,0162
13	2,134079	2,124348	0,4560	2,131877	0,1032	2,133554	0,0246
13	2,134079	2,124348	0,4560	2,131877	0,1032	2,133554	0,0246
71	2,144459	2,142518	0,0905	2,143230	0,0573	2,143298	0,0541
71	2,144459	2,142518	0,0905	2,143230	0,0573	2,143298	0,0541
42	2,320599	2,314304	0,2713	2,319103	0,0645	2,320070	0,0228
42	2,320599	2,314304	0,2713	2,319103	0,0645	2,320070	0,0228
81	2,411855	2,409212	0,1096	2,410047	0,0750	2,410131	0,0715
81	2,411855	2,409212	0,1096	2,410047	0,0750	2,410131	0,0715
23	2,492367	2,479353	0,5221	2,489451	0,1170	2,491659	0,0284

Table 6.2.8: comparison between our FD code and analytic results for TM modes on TM grid in circular waveguide , when varying $\Delta\theta$

		$\Delta\theta=2°$		$\Delta\theta=1°$		$\Delta\theta=0.5°$	
TM MODES	Kta	Ktp	ep%	Ktp	ep%	Ktp	ep%
01	0,601200	0,601143	0,0094	0,601143	0,0094	0,601143	0,0094
11	0,957925	0,957783	0,0149	0,957796	0,0135	0,957799	0,0132
11	0,957925	0,957783	0,0149	0,957796	0,0135	0,957799	0,0132
21	1,283900	1,283578	0,0251	1,283674	0,0176	1,283698	0,0157
21	1,283900	1,283578	0,0251	1,283674	0,0176	1,283698	0,0157
02	1,380025	1,379326	0,0506	1,379326	0,0506	1,379326	0,0506
31	1,595050	1,594341	0,0445	1,594655	0,0247	1,594734	0,0198
31	1,595050	1,594341	0,0445	1,594655	0,0247	1,594734	0,0198
12	1,753900	1,752879	0,0582	1,752893	0,0574	1,752896	0,0572
12	1,753900	1,752879	0,0582	1,752893	0,0574	1,752896	0,0572
41	1,897075	1,895747	0,0700	1,896474	0,0317	1,896656	0,0221
41	1,897075	1,895747	0,0700	1,896474	0,0317	1,896656	0,0221
22	2,104300	2,102845	0,0691	2,102949	0,0642	2,102975	0,0629
22	2,104300	2,102845	0,0691	2,102949	0,0642	2,102975	0,0629
03	2,163425	2,160800	0,1213	2,160800	0,1213	2,160800	0,1213
51	2,192875	2,190545	0,1063	2,191940	0,0426	2,192289	0,0267
51	2,192875	2,190545	0,1063	2,191940	0,0426	2,192289	0,0267
32	2,440250	2,438126	0,0870	2,438465	0,0731	2,438550	0,0697
32	2,440250	2,438126	0,0870	2,438465	0,0731	2,438550	0,0697
61	2,484025	2,480288	0,1504	2,482665	0,0548	2,483259	0,0308
61	2,484025	2,480288	0,1504	2,482665	0,0548	2,483259	0,0308
13	2,543375	2,539979	0,1335	2,539993	0,1330	2,539996	0,1328
13	2,543375	2,539979	0,1335	2,539993	0,1330	2,539996	0,1328
42	2,766175	2,763084	0,1118	2,763867	0,0834	2,764063	0,0764
42	2,766175	2,763084	0,1118	2,763867	0,0834	2,764063	0,0764
71	2,771593	2,765936	0,2041	2,769667	0,0695	2,770601	0,0358
71	2,771593	2,765936	0,2041	2,769667	0,0695	2,770601	0,0358
23	2,904950	2,900676	0,1471	2,900784	0,1434	2,900810	0,1425
23	2,904950	2,900676	0,1471	2,900784	0,1434	2,900810	0,1425

Table 6.2.9: comparison between our FD code and analytic results for TE modes on TM grid in circular waveguide , when varying Δθ

		Δθ=2°		Δθ=1°		Δθ=0.5°	
TE MODES	Kta	Ktp	ep%	Ktp	ep%	Ktp	ep%
11	0,460296	0,460277	0,0042	0,460289	0,0015	0,460292	0,0009
11	0,460296	0,460277	0,0042	0,460289	0,0015	0,460292	0,0009
21	0,763559	0,763433	0,0166	0,763522	0,0049	0,763544	0,0020
21	0,763559	0,763433	0,0166	0,763522	0,0049	0,763544	0,0020
01	0,957927	0,957669	0,0269	0,957669	0,0269	0,957669	0,0269
31	1,050297	1,049895	0,0383	1,050185	0,0106	1,050258	0,0037
31	1,050297	1,049895	0,0383	1,050185	0,0106	1,050258	0,0037
41	1,329388	1,328466	0,0694	1,329139	0,0187	1,329308	0,0061
41	1,329388	1,328466	0,0694	1,329139	0,0187	1,329308	0,0061
12	1,332861	1,332387	0,0356	1,332400	0,0345	1,332404	0,0343
12	1,332861	1,332387	0,0356	1,332400	0,0345	1,332404	0,0343
51	1,603904	1,602138	0,1101	1,603436	0,0292	1,603760	0,0090
51	1,603904	1,602138	0,1101	1,603436	0,0292	1,603760	0,0090
22	1,676533	1,675711	0,0490	1,675813	0,0430	1,675838	0,0415
22	1,676533	1,675711	0,0490	1,675813	0,0430	1,675838	0,0415
02	1,753897	1,752325	0,0896	1,752325	0,0896	1,752325	0,0896
61	1,875317	1,872307	0,1605	1,874528	0,0421	1,875083	0,0124
61	1,875317	1,872307	0,1605	1,874528	0,0421	1,875083	0,0124
32	2,003809	2,002420	0,0693	2,002750	0,0529	2,002833	0,0487
32	2,003809	2,002420	0,0693	2,002750	0,0529	2,002833	0,0487
13	2,134079	2,131863	0,1038	2,131877	0,1032	2,131881	0,1030
13	2,134079	2,131863	0,1038	2,131877	0,1032	2,131881	0,1030
71	2,144459	2,139730	0,2205	2,143230	0,0573	2,144105	0,0165
71	2,144459	2,139730	0,2205	2,143230	0,0573	2,144105	0,0165
42	2,320599	2,318342	0,0973	2,319103	0,0645	2,319293	0,0563
42	2,320599	2,318342	0,0973	2,319103	0,0645	2,319293	0,0563
81	2,411855	2,404854	0,2903	2,410047	0,0750	2,411346	0,0211
81	2,411855	2,404854	0,2903	2,410047	0,0750	2,411346	0,0211
23	2,492367	2,489344	0,1213	2,489451	0,1170	2,489477	0,1159

Fig. 6.2.1. Comparison between our FD code and analitic results and FIT(CST) results for TE modes in circular wave guide with r=4 mm Δr =0.0792 mm and θ =1°;
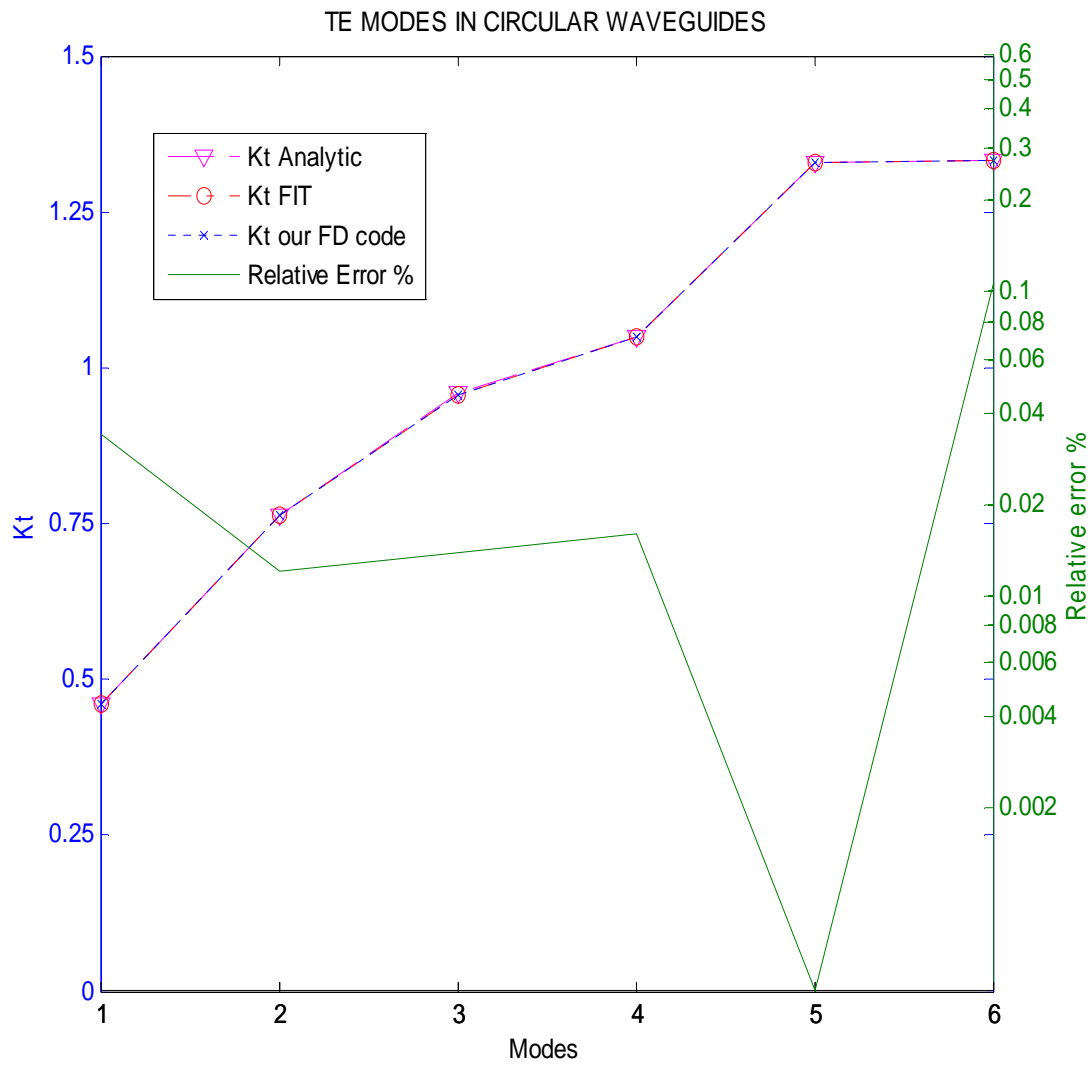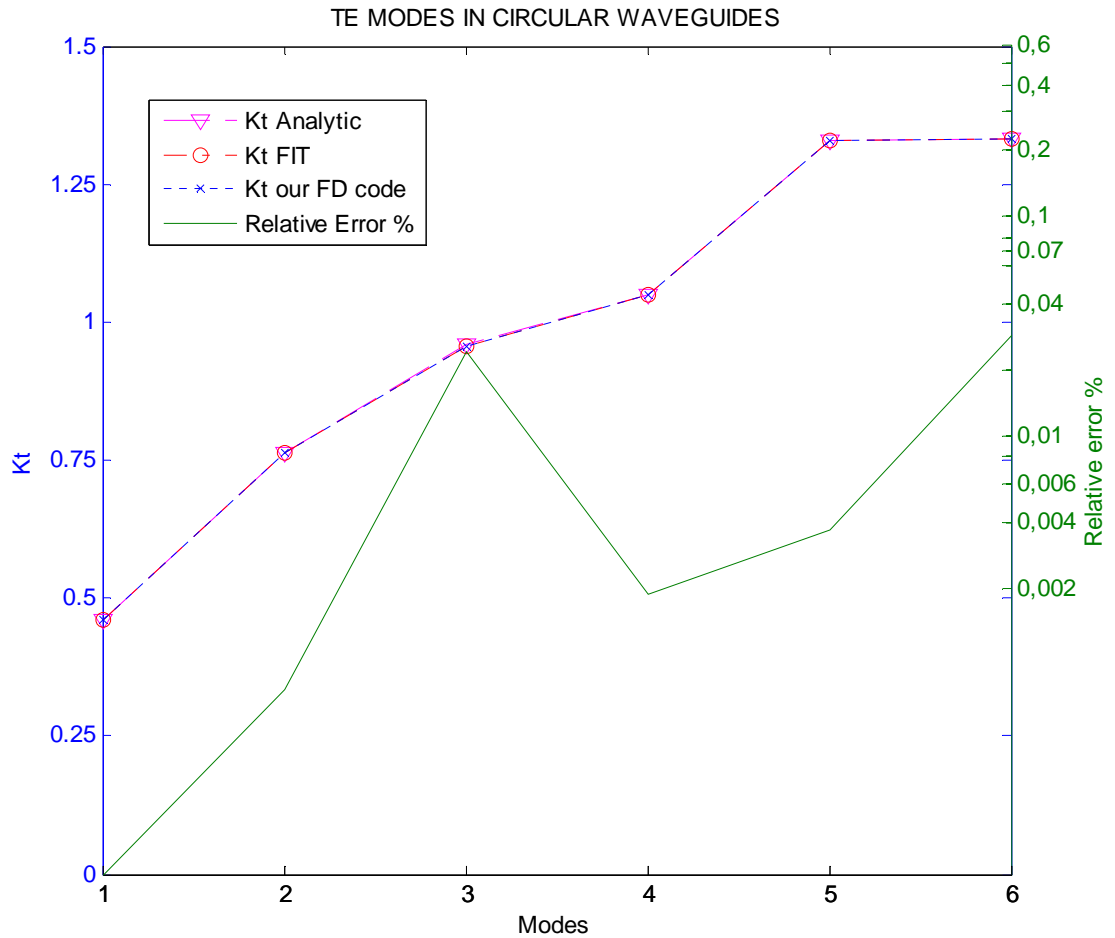
Fig. 6.2. Comparison between our FD code and analitic results and FIT(CST) results for TE modes in circular wave guide with r=4 mm Δr =0.0792 mm and $\Delta\theta$ =0,5°;

We have made several tests by varying the steps ($\Delta r, \Delta\theta$). The results of the tables and Figures (6.2.1,6.2.2) shows that our technique has a very low error, as long as the steps are small. When compared to CST our results are better, and can be obtained in a fraction of the computational time required by the former. However, the comparison of FIT and analytical results show that CST is

quite accurate, too, and can be used to test our approach for waveguide. S without known analytical solutions.

In the table 6.2.10 you can see the kt of TE and TM modes calculated on the TE grids, where varying Δu.

Data of the elliptic waveguide:

major axis=8.6558

minor axis=4

eccentricity=0.8868

Δv=1°

ktcst=kt of CST

ktp=kt of the program

ep= percentage (relative) error

In the table 6.2.11 you can see the kt of TE and TM modes calculated on the TE grids, where varying Δv.

Data of the elliptic waveguide:

major axis=8.6558

minor axis=4

eccentricity=0.8868

Δu= 0,002488

ktcst=kt of CST

ktp=kt of the program

ep= percentage (relative) error

Table 6.2.10: comparison between our FD code and FIT (CST) results for TE and TM modes on TE grid in elliptic waveguide , with different Δu

		Du=0,009804		Du=0,00495		Du=0,002488	
TE MODES	Ktcst	Ktp	ep%	Ktp	ep%	Ktp	ep%
I	0,216761	0,216519	0,1118	0,216590	0,0793	0,216635	0,0582
II	0,396308	0,395816	0,1241	0,395990	0,0801	0,396100	0,0524
III	0,439542	0,439368	0,0396	0,439382	0,0364	0,439391	0,0345
IV	0,566608	0,566490	0,0208	0,566483	0,0222	0,566489	0,0211
V	0,572023	0,571366	0,1149	0,571657	0,0640	0,571839	0,0322
VI	0,703570	0,703502	0,0097	0,703468	0,0144	0,703472	0,0139
VII	0,745401	0,744851	0,0738	0,745251	0,0200	0,745499	0,0133
VIII	0,840046	0,840037	0,0011	0,840362	0,0376	0,840452	0,0483
IX	0,847613	0,847548	0,0076	0,847488	0,0147	0,847488	0,0147
X	0,917454	0,916716	0,0804	0,917201	0,0275	0,917499	0,0049

		Du=0,009804		Du=0,00495		Du=0,002488	
TM MODES	Ktcst	Ktp	ep%	Ktp	ep%	Ktp	ep%
I	0,464520	0,464404	0,0251	0,464440	0,0172	0,464453	0,0145
II	0,604530	0,604413	0,0194	0,604491	0,0066	0,604510	0,0034
III	0,754913	0,754794	0,0159	0,754979	0,0086	0,755022	0,0144
IV	0,849685	0,849803	0,0139	0,850105	0,0494	0,850197	0,0602
V	0,911798	0,911963	0,0181	0,912364	0,0621	0,912465	0,0732
VI	0,979441	0,978743	0,0712	0,979020	0,0429	0,979111	0,0337
VII	1,075333	1,073525	0,1682	1,074296	0,0964	1,074508	0,0768
VIII	1,115153	1,114329	0,0739	1,114573	0,0521	1,114662	0,0441
IX	1,241573	1,237907	0,2953	1,239242	0,1877	1,239628	0,1566
X	1,241775	1,239674	0,1692	1,240780	0,0801	1,241088	0,0553

Table 6.2.11: comparison between our FD code and FIT (CST) results for TE and TM modes on TE grid in elliptic waveguide , when varying $\Delta\theta$

		Dv=2°		Dv=1°		Dv=0,5°	
TE MODES	Ktcst	Ktp	ep%	Ktp	ep%	Ktp	ep%
I	0,216761	0,216608	0,0708	0,216635	0,0582	0,216645	0,0539
II	0,396308	0,395976	0,0839	0,396100	0,0524	0,396138	0,0430
III	0,439542	0,439381	0,0366	0,439391	0,0345	0,439393	0,0340
IV	0,566608	0,566423	0,0327	0,566489	0,0211	0,566505	0,0182
V	0,572023	0,571502	0,0911	0,571839	0,0322	0,571933	0,0158
VI	0,703570	0,703247	0,0458	0,703472	0,0139	0,703527	0,0060
VII	0,745401	0,744793	0,0815	0,745500	0,0133	0,745689	0,0387
VIII	0,840046	0,840431	0,0458	0,840452	0,0483	0,840457	0,0489
IX	0,847613	0,846957	0,0774	0,847488	0,0147	0,847620	0,0009
X	0,917454	0,916227	0,1337	0,917499	0,0049	0,917833	0,0413

		Dv=2°		Dv=1°		Dv=0,5°	
TM MODES	Ktcst	Ktp	ep%	Ktp	ep%	Ktp	ep%
I	0,464520	0,464441	0,0170	0,464453	0,0145	0,464456	0,0139
II	0,604530	0,604430	0,0166	0,604510	0,0034	0,604530	0,0000
III	0,754913	0,754756	0,0209	0,755022	0,0144	0,755089	0,0233
IV	0,849685	0,850176	0,0577	0,850197	0,0602	0,850202	0,0608
V	0,911798	0,911843	0,0049	0,912465	0,0732	0,912624	0,0906
VI	0,979441	0,978984	0,0466	0,979111	0,0337	0,979143	0,0304
VII	1,075333	1,073307	0,1885	1,074508	0,0768	1,074815	0,0482
VIII	1,115153	1,114278	0,0785	1,114662	0,0441	1,114757	0,0355
IX	1,241573	1,237575	0,3220	1,239628	0,1566	1,240155	0,1142
X	1,241775	1,241056	0,0579	1,241088	0,0553	1,241096	0,0547

For elliptic waveguide we have considered different axial ratios and we compared our FD results only with FIT simulations. We present her only this case of an axial ratio of 2, giving a relative error of less that 0.2% but other aspect ratios gives comparable accuracy.

6.3) FD IN ROUNDED-END WAVEGUIDE

In this paragraph we will show the results of techniques presented in the paragraph 5.2. To assess our FD code in this case, we have evaluated a few TE modes, for different structures.
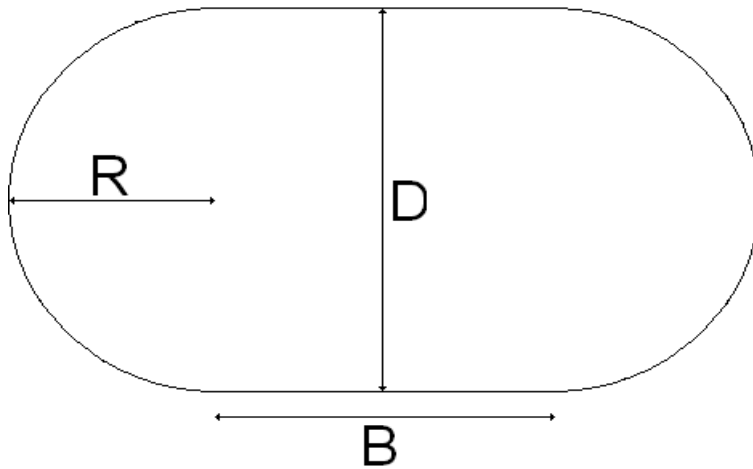

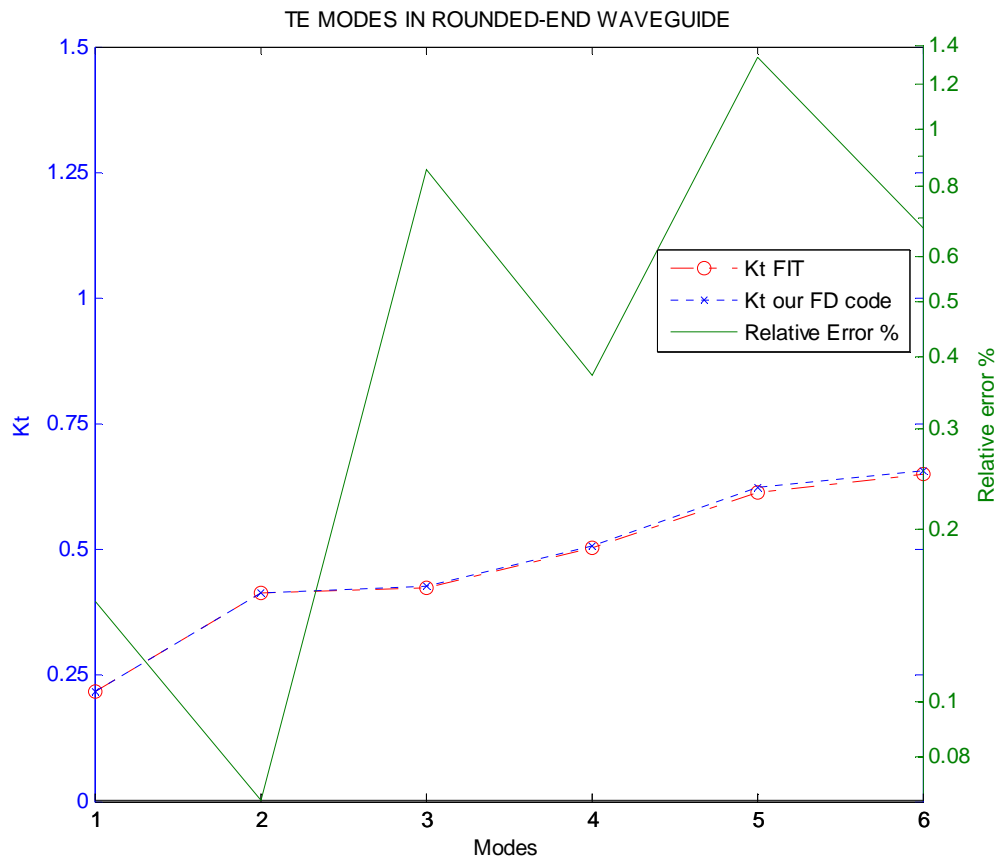Fig.6.3.1 – 6.3.6 shows the comparison between our results and CST ones.

Fig. 6.3.1. Comparison between our FD code and and FIT (CST) results for TE modes in Rounded-end wave guide with $\Delta x = \Delta y = \Delta r = 0{,}1569$ mm D=B=8 mm and $\theta = 1°$;

Fig. 6.3.2. Comparison between our FD code and FIT (CST) results for TE modes in Rounded-end wave guide with $\Delta x = \Delta y = \Delta r = 0,0792$ mm D=B=8 mm and $\Delta\theta = 1°$;

Fig. 6.3.3. Comparison between our FD code and and FIT (CST) results for TE modes in Rounded-end wave guide with $\Delta x = \Delta y = \Delta r = 0,03980$ mm D=B=8 mm and $\theta = 1°$;
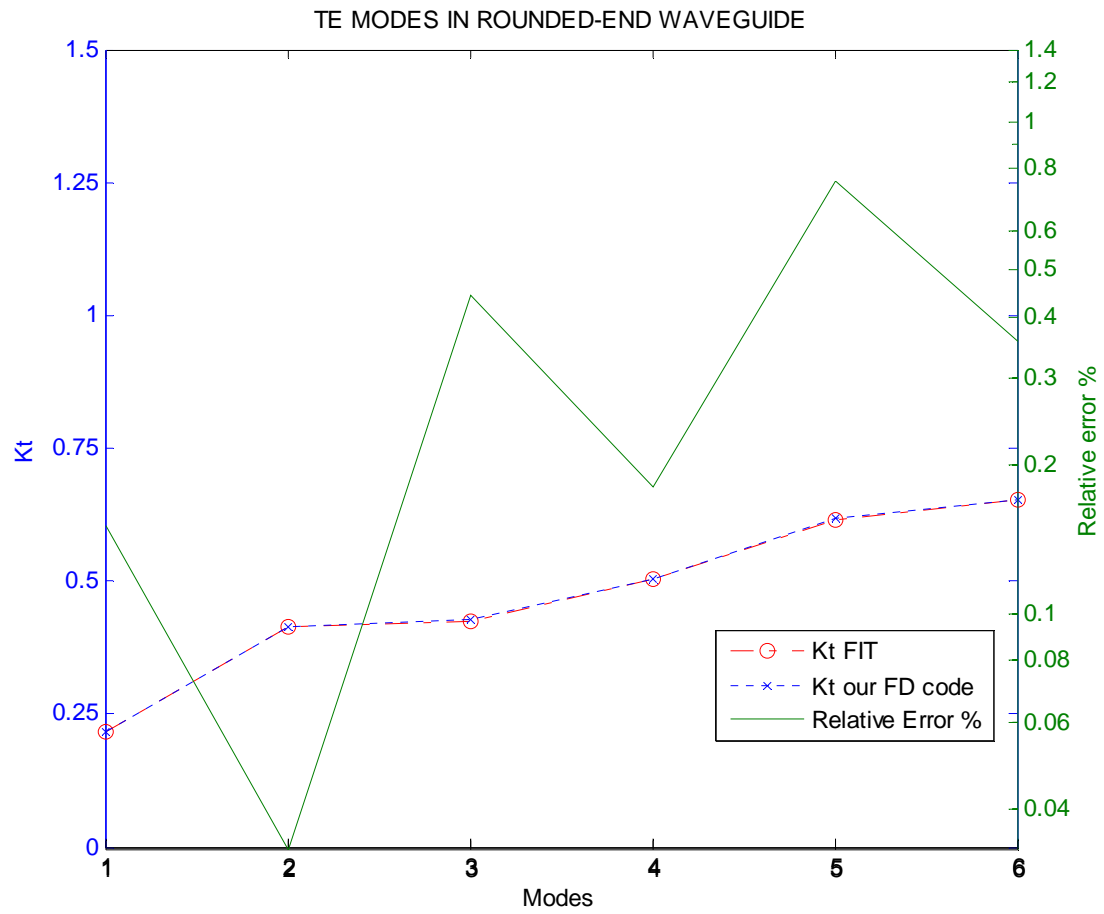
Fig. 6.3.4. Comparison between our FD code and and FIT (CST) results for TE modes in Rounded-end wave guide with $\Delta x = \Delta y = \Delta r = 0,01995$ mm D=B=8 mm and θ=1°;

Fig. 6.3.5. Comparison between our FD code and and FIT (CST) results for TE modes in Rounded-end wave guide with $\Delta x = \Delta y = \Delta r = 0{,}0792$ mm D=8 mm B=16 mm and θ=1°;
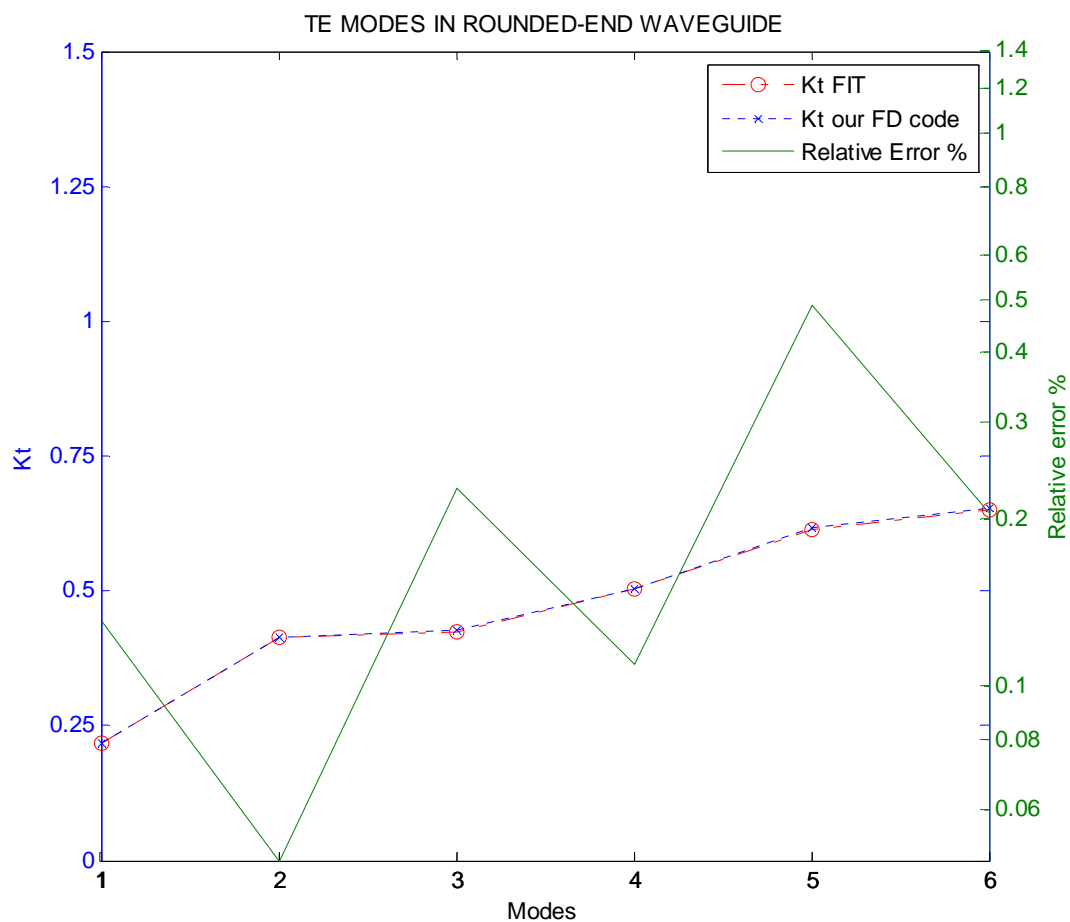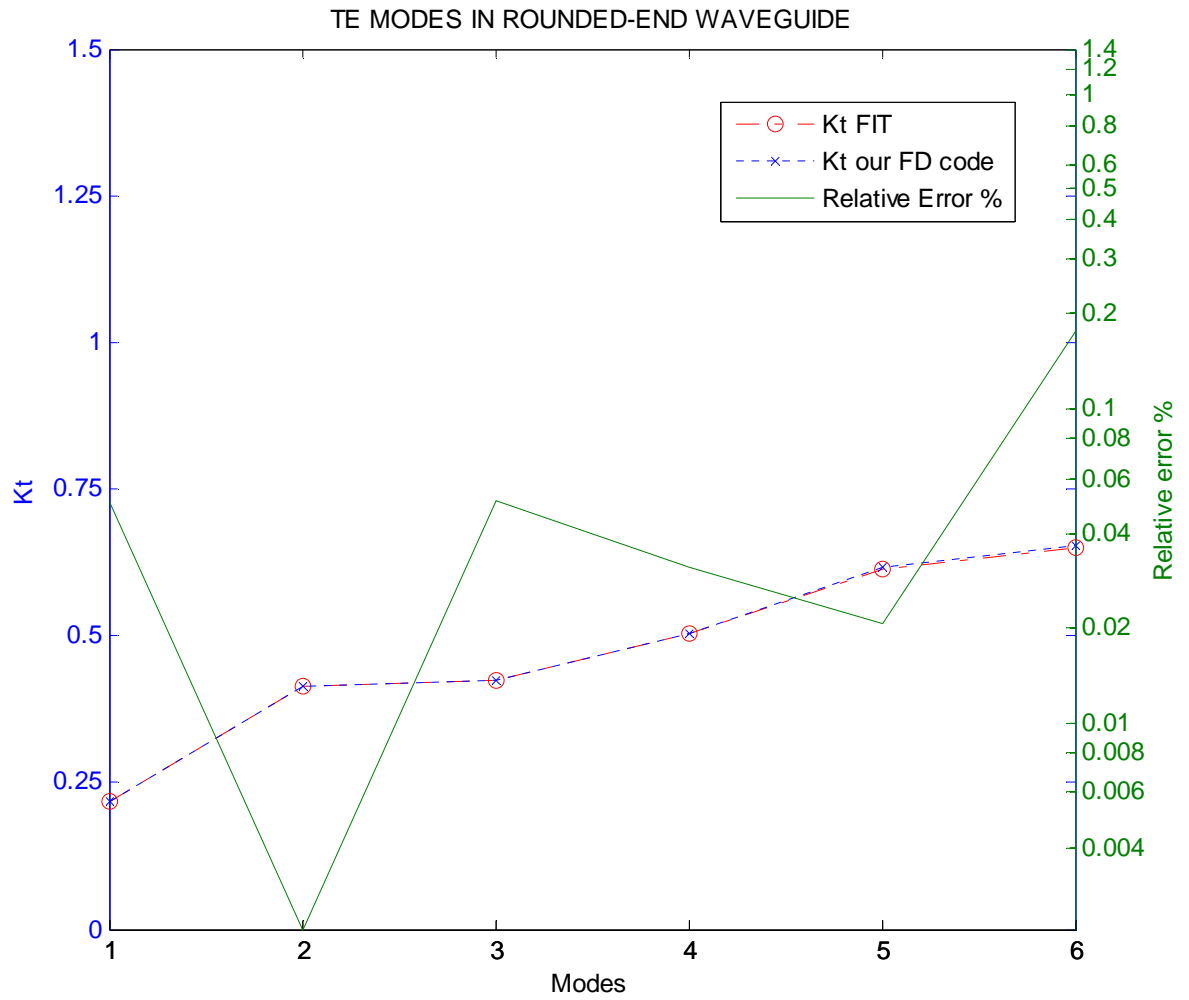
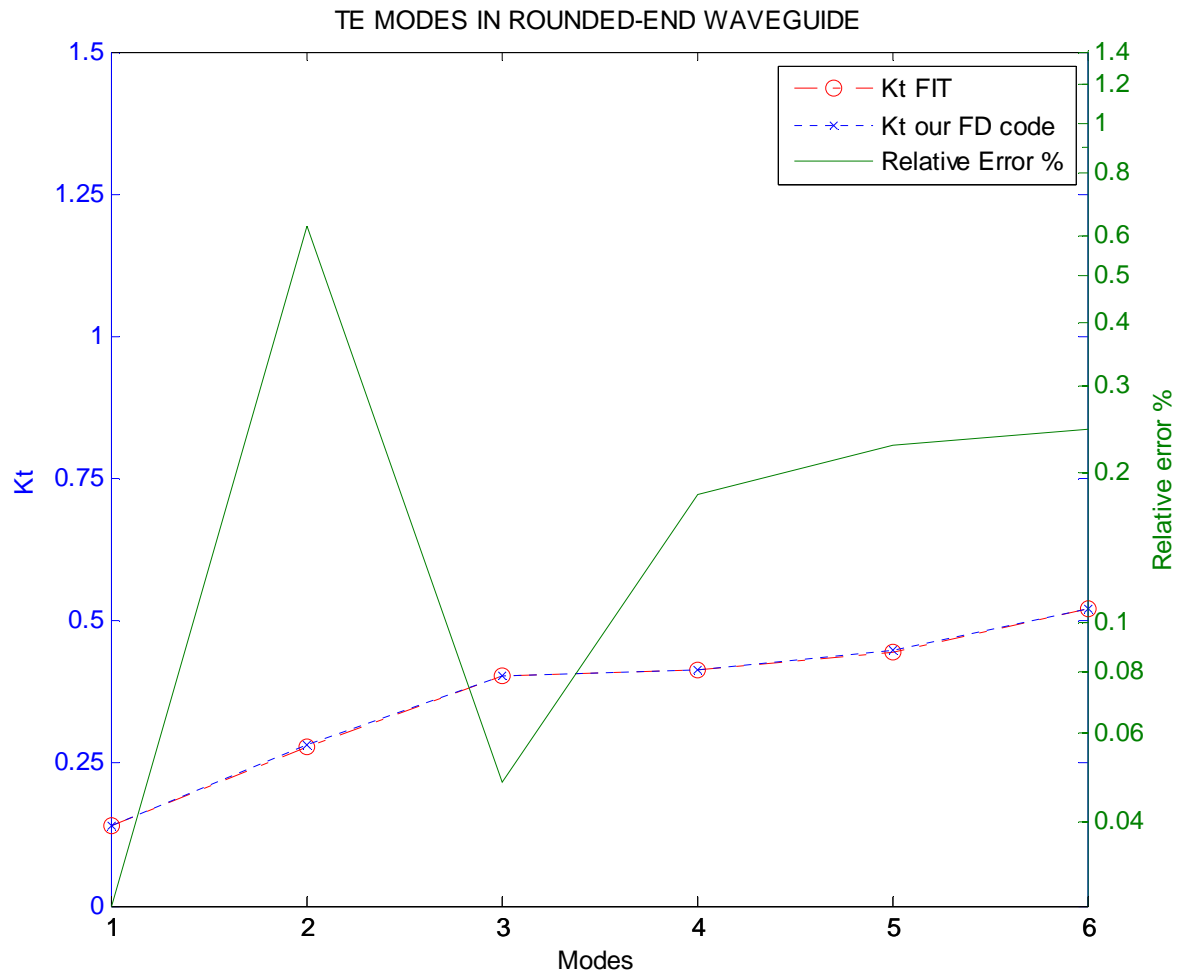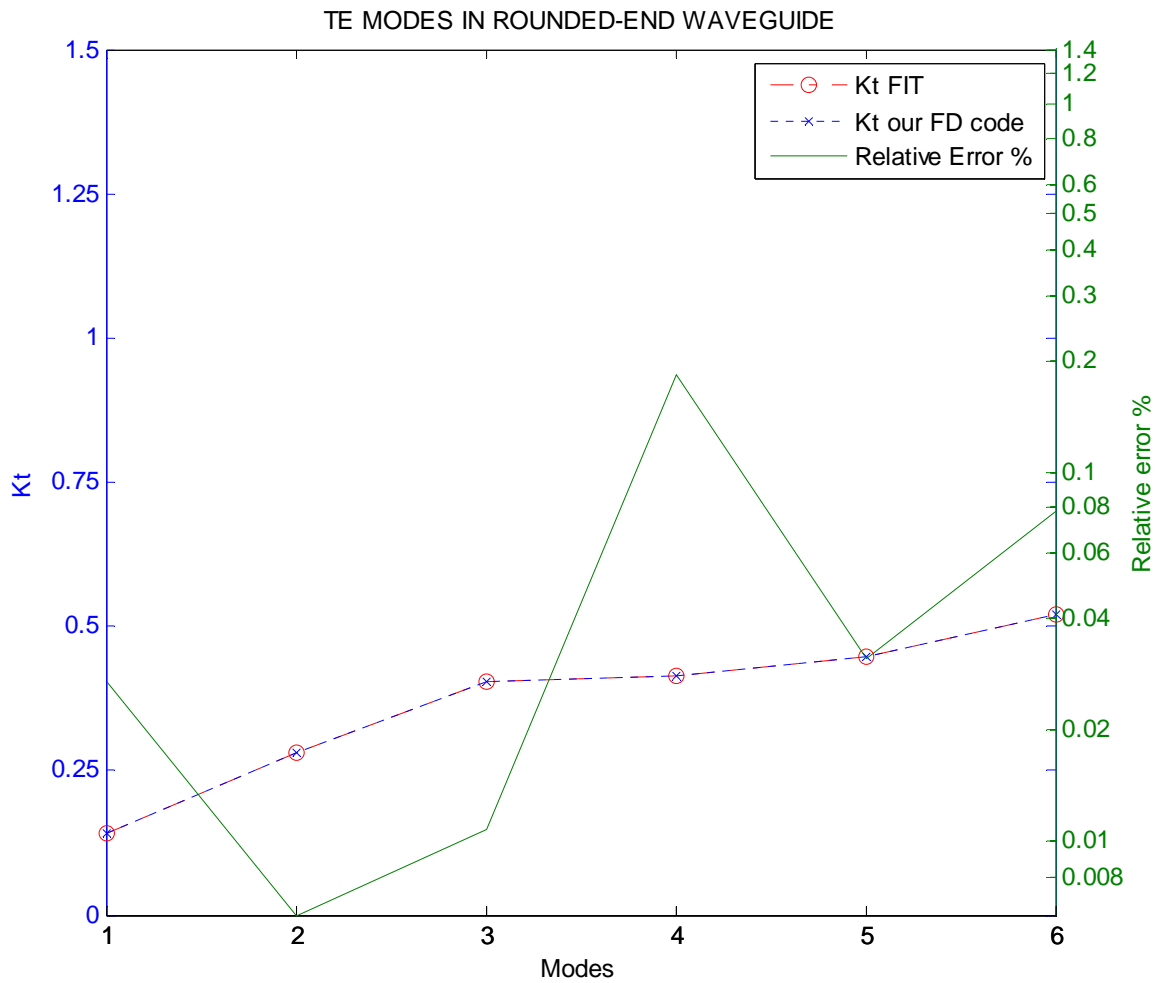Fig. 6.3.6. Comparison between our FD code and and FIT (CST) results for TE modes in Rounded-end wave guide with $\Delta x = \Delta y = \Delta r = 0{,}03980$ mm D=8 mm B=16 mm and $\theta = 1°$;

The results shows that our FD approach allows an high accuracy, when the discretization step is suitably chosen. But even a quite large steps, as in the case of Figure 6.3.3, allows a quite accurate mode evaluation.

6.4) VECTOR FD IN RECTANGULAR WAVEGUIDE

In this paragraph we will show the results of techniques presented in the paragraph 3.4. To assess the proposed technique we have analyzed a Rectangular waveguide and compared the eigenvalues and eigenvectors of the first few TE modes with their exact values. In the table 6.4.1 you can see the kt and Max eigenvectors error percentage of TE modes calculated on the TE grids.

Data of the rectangular waveguide:

a=3.35, b=1.65 $\Delta x = \Delta y = 0.05$

kta=kt analytical

ktps=kt of the program use scalar FD

ktpv=kt of the program use vector FD

epv= percentage (relative) error between kta and Ktpv

Max eigenvectors error%= Max eigenvectors error percentage of TE modes calculated.

Table 6.4.1: comparison between our vector FD code and analytic results for TE modes on TE grid in rectangular waveguide

TE MODES	Kta	Ktps	Ktpv	epv%	Max eigenvectors error %
10	0,937789	0,937703	0,937707	0,008211	0,000634
20	1,875578	1,874890	1,874921	0,065649	0,005065
01	1,903996	1,903277	1,903342	0,065364	0,005218
11	2,122415	2,121732	2,121742	0,067299	0,054902
21	2,672637	2,671643	2,671576	0,106113	0,017336
30	2,813367	2,811048	2,811151	0,221568	0,017055
31	3,397092	3,394768	3,394683	0,240807	0,124122
40	3,751155	3,745660	3,745904	0,525173	0,040353
02	3,807991	3,802242	3,802760	0,523096	0,041615
12	3,921765	3,916163	3,916553	0,521283	0,153269
41	4,206705	4,201479	4,201458	0,524732	0,233309
22	4,244831	4,239370	4,239449	0,538210	0,244167
50	4,688944	4,678213	4,678687	1,025698	0,078287
32	4,734536	4,728534	4,728267	0,626906	0,240676
51	5,060770	5,050558	5,050698	1,007252	0,322581
42	5,345275	5,337322	5,336782	0,849241	0,142042

Data of the rectangular waveguide:

a=3.35, b=1.65 $\Delta x=\Delta y=0.025$

kta=kt analytical

ktps=kt of the program use scalar FD

ktpv=kt of the program use vector FD

epv= percentage (relative) error between kta and Ktpv

Max eigenvectors error%= Max eigenvectors error percentage of TE modes calculated.

Table 6.4.2: comparison between our vector FD code and analytic results for TE modes on TE grid in rectangular waveguide

TE MODES	Kta	Ktps	Ktpv	epv%	Max eigenvectors relative error%
10	0,937789	0,937767	0,937768	0,0021	0,0001
20	1,875578	1,875406	1,875410	0,0168	0,0006
01	1,903996	1,903816	1,903824	0,0172	0,0007
11	2,122415	2,122245	2,122246	0,0170	0,0139
21	2,672637	2,672389	2,672380	0,0257	0,0021
30	2,813367	2,812787	2,812800	0,0567	0,0022
31	3,397092	3,396511	3,396500	0,0592	0,0313
40	3,751155	3,749781	3,749812	0,1344	0,0051
02	3,807991	3,806553	3,806618	0,1373	0,0053
12	3,921765	3,920364	3,920413	0,1352	0,0361
41	4,206705	4,205398	4,205395	0,1310	0,0557
22	4,244831	4,243465	4,243474	0,1356	0,0583
50	4,688944	4,686260	4,686320	0,2624	0,0100
32	4,734536	4,733035	4,733001	0,1535	0,0544
51	5,060770	5,058216	5,058233	0,2537	0,0806
42	5,345275	5,343286	5,343218	0,2056	0,0174

The results of Tables 6.4.1, 6.4.2 shows that our technique has a very low error, as long as the discretization steps are small.

6.5) VECTOR FD IN CIRCULAR WAVEGUIDE

In this paragraph we will show the results of techniques presented in the paragraph 4.3. To assess the proposed technique we have analyzed a Circular waveguide and compared the eigenvalues and eigenvectors of the first few TE modes with their exact values. In the table 6.5.1 you can see the kt and RMS error on eigenvectors of TE modes calculated on the TE grids.

Table 6.5.1: comparison between our vector FD code and analytic results for TE modes on TE grid in circular waveguide

n,p	Kta	Ktpv	ep%	RMS_error *1.0e-006
11	0,460296	0,460292	0,000793	0.0001
21	0,763559	0,763531	0,003656	0.0007
01	0,957927	0,957697	0,023982	0.0008
31	1,050297	1,050204	0,008831	0.0011
41	1,329388	1,329170	0,016382	0.0013
12	1,332861	1,332475	0,028974	0.0173
51	1,603904	1,603482	0,026341	0.0015
22	1,676533	1,675952	0,034689	0.0682
02	1,753897	1,752487	0,080364	0.0012
61	1,875317	1,874590	0,038724	0.0015
32	2,003809	2,002971	0,041806	0.1195
13	2,134079	2,132172	0,089353	0.1302
71	2,144459	2,143311	0,053550	0.0016
42	2,320599	2,319424	0,050620	0.1734
81	2,411855	2,410147	0,070825	0.0017

The same comparison has been made in Table 6.5.1 for a circular waveguide, with a radius equal to 4 (in normalized units), and using discretization steps of $\Delta r = 0.0396$, $\Delta \vartheta = 1^o$. In both tables k_{ta} and k_{tpv} are the eigenvalues computed analytically [6] and using our approach, $ep\%$ is the percentage error between them, and the last column shows the RMS difference between analytical mode vectors, and those compured using (I.9).

From these data, it appears that our technique is able to give all mode data with a very small error, both on eigenvalues and on eigenvectors. The error on the formes is significantly smaller for the circular case. The RMS error on normalized modes is even smaller, being less than $5 \cdot 10^{-8}$ in circular case.

6.6) VECTOR FD IN ELLYPTIC WAVEGUIDE

In this paragraph we will show the results of techniques presented in the paragraph 4.4. To assess the proposed technique we have analyzed a Ellyptical waveguide and compared the eigenvalues and eigenvectors of the first few TE modes with their exact values. Tables 6.6.1,6.6.2,6.6.3 shows the validation test for an elliptic waveguide, with a length of the minor axis (in normalized units) equal to 4, and different eccentricities ex, discretized with $\Delta v = 1^o$, and a different number Nu of discretization ellipses. Though an analytical solution is available for elliptic waveguides [11], it effectiveness is very poor, and many numerical techniques has been proposed in the literature. As in many of those papers, we use, for our comparison, the eigenvalues k_{ta} obtained from the cut-off wavelength data reported in [36]. From the data in Tables 6.6.1,6.6.2,6.6.3, it is clear that, for all cases shown, the eigenvalues k_{tpv} computed from our techniques are very accurate.

Table 6.6.1: comparison between our vector FD code and analytic results for TE modes on TE grid in ellyptic waveguide with ex=0,1 , $\Delta v = 1^o$ and Δu variable.

ex=0,1	kta	Nu=100	e%	Nu=200	e%	Nu=400	e%
TEc1-1	0,4581763	0,4582208	0,0097	0,4581167	0,0130	0,4580902	0,0188
TEs1-1	0,4602013	0,4603401	0,0302	0,4602356	0,0074	0,4602092	0,0017
TEc2-1	0,7616249	0,7618597	0,0308	0,7616784	0,0070	0,7616328	0,0010
TEs2-1	0,7616464	0,7618813	0,0308	0,7616999	0,0070	0,7616542	0,0010
TEc0-1	0,9555448	0,9551314	0,0433	0,9554371	0,0113	0,9555118	0,0035
TEc3-1	1,0476538	1,0479783	0,0310	1,0477170	0,0060	1,0476516	0,0002
TEs3-1	1,0476539	1,0479785	0,0310	1,0477172	0,0060	1,0476517	0,0002
TEc4-1	1,3260436	1,3264481	0,0305	1,3261025	0,0044	1,3260164	0,0021
TEs4-1	1,3260436	1,3264481	0,0305	1,3261025	0,0044	1,3260164	0,0021
TEc1-2	1,3277392	1,3265297	0,0911	1,3274329	0,0231	1,3276602	0,0059
TEs1-2	1,3313232	1,3300634	0,0946	1,3310037	0,0240	1,3312421	0,0061
TEc5-1	1,5998694	1,6003400	0,0294	1,5999051	0,0022	1,5997974	0,0045
TEs5-1	1,5998694	1,6003400	0,0294	1,5999051	0,0022	1,5997974	0,0045
TEc2-2	1,6722143	1,6699783	0,1337	1,6716427	0,0342	1,6720643	0,0090
TEs2-2	1,6723449	1,6701076	0,1338	1,6717729	0,0342	1,6721948	0,0090
TEc0-2	1,7496312	1,7459051	0,2130	1,7486822	0,0542	1,7493761	0,0146
TEc2-3	2,4857717	2,4763404	0,3794	2,4836944	0,0836	2,4855461	0,0091
TEs6-2	2,9263444	2,9185745	0,2655	2,9242314	0,0722	2,9256595	0,0234
TEc11-1	3,1985589	3,2154367	0,5277	3,1977907	0,0240	3,1975337	0,0321

Table 6.6.2: comparison between our vector FD code and analytic results for TE modes on TE grid in ellyptic waveguide with ex=0,5 , $\Delta v = 1^o$ and Δu variable.

ex=0,5	kta	Nu=100	e%	Nu=200	e%	Nu=400	e%
TEc1-1	0,4007537	0,4007794	0,0064	0,4007558	0,0005	0,4007477	0,0015
TEs1-1	0,4573402	0,4573597	0,0043	0,4573447	0,0010	0,4573409	0,0001
TEc2-1	0,6977267	0,6977632	0,0052	0,6977281	0,0002	0,6977169	0,0014
TEs2-1	0,7129897	0,7130268	0,0052	0,7129942	0,0006	0,7129861	0,0005
TEc0-1	0,9072690	0,9071392	0,0143	0,9072289	0,0044	0,9072557	0,0015
TEc3-1	0,9697687	0,9698069	0,0039	0,9697602	0,0009	0,9697479	0,0021
TEs3-1	0,9731326	0,9731735	0,0042	0,9731259	0,0007	0,9731138	0,0019
TEc1-2	1,2056011	1,2053633	0,0197	1,2054972	0,0086	1,2055450	0,0047
TEc4-1	1,2301100	1,2301380	0,0023	1,2300769	0,0027	1,2300614	0,0040
TEs4-1	1,2307620	1,2307916	0,0024	1,2307297	0,0026	1,2307142	0,0039
TEs1-2	1,2982175	1,2977695	0,0345	1,2981032	0,0088	1,2981879	0,0023
TEc5-1	1,4849816	1,4849813	0,0000	1,4849048	0,0052	1,4848852	0,0065
TEs5-1	1,4850990	1,4850993	0,0000	1,4850225	0,0052	1,4850033	0,0064
TEc2-2	1,5162727	1,5158575	0,0274	1,5160720	0,0132	1,5161445	0,0085
TEs2-2	1,5741075	1,5735833	0,0333	1,5739680	0,0089	1,5740659	0,0026
TEc0-2	1,6945503	1,6934183	0,0668	1,6942624	0,0170	1,6944732	0,0046
TEc1-4	2,0884337	2,0861798	0,1079	2,0878626	0,0273	2,0882878	0,0070
TEs6-2	2,7535930	2,7493575	0,1538	2,7525100	0,0393	2,7533090	0,0103
TEc0-4	3,2687699	3,2595013	0,2835	3,2663930	0,0727	3,2681693	0,0184

Table 6.6.3: comparison between our vector FD code and analytic results for TE modes on TE grid in ellyptic waveguide with ex=0,9 , $\Delta v = 1^o$ and Δu variable.

ex=0,9	kta	Nu=100	e%	Nu=200	e%	Nu=400	e%
TEc1-1	0,2044955	0,2044593	0,0177	0,2044777	0,0087	0,2044887	0,0033
TEc2-1	0,3744120	0,3743190	0,0248	0,3743640	0,0128	0,3743908	0,0057
TEs1-1	0,4375153	0,4375027	0,0029	0,4375116	0,0009	0,4375138	0,0004
TEc3-1	0,5410773	0,5409102	0,0309	0,5409863	0,0168	0,5410313	0,0085
TEs2-1	0,5570149	0,5570002	0,0027	0,5570071	0,0014	0,5570088	0,0011
TEs3-1	0,6856484	0,6856239	0,0036	0,6856284	0,0029	0,6856296	0,0028
TEc4-1	0,7060436	0,7057903	0,0359	0,7058971	0,0208	0,7059600	0,0118
TEs4-1	0,8209958	0,8209498	0,0056	0,8209517	0,0054	0,8209522	0,0053
TEc0-1	0,8373801	0,8372581	0,0146	0,8373480	0,0038	0,8373707	0,0011
TEc5-1	0,8697291	0,8693819	0,0399	0,8695147	0,0247	0,8695927	0,0157
TEc1-2	0,9562268	0,9560986	0,0134	0,9561867	0,0042	0,9562090	0,0019
TEs5-1	0,9612009	0,9611177	0,0087	0,9611169	0,0087	0,9611166	0,0088
TEc6-1	1,0322693	1,0318234	0,0432	1,0319741	0,0286	1,0320626	0,0200
TEc2-2	1,0813326	1,0811866	0,0135	1,0812725	0,0056	1,0812943	0,0035
TEs6-1	1,1048916	1,1047514	0,0127	1,1047479	0,0130	1,1047470	0,0131
TEc7-1	1,1937006	1,1931511	0,0460	1,1933100	0,0327	1,1934033	0,0249
TEs7-1	1,2510720	1,2508515	0,0176	1,2508455	0,0181	1,2508440	0,0182
TEc5-2	1,4870521	1,4867331	0,0215	1,4868168	0,0158	1,4868391	0,0143
TEc12-1	1,9845625	1,9832412	0,0666	1,9833291	0,0621	1,9835141	0,0528
TEc4-3	2,1094353	2,1082575	0,0558	2,1089925	0,0210	2,1091784	0,0122

6.7) EXTENSION TO 3D PROBLEM

In this paragraph we will show the results of techniques presented in the paragraph 3.7. In the table 6.6.4 you can see the k_t of modes calculated on the Newmann grid. Data of the rectangular cavite waveguide:

a=10, b=2, c=2 $\Delta x=\Delta y=\Delta z=0.1$

kta=kt analytical

ktp=kt of the program

ep= percentage (relative) error

Total points of the grid: 40000

Table 6.6.4: comparison between our 3D FD code and analytic results for modes on Newmann grid in a rectangular cavity.

n	p	z	kta(Newmann)	ktp(Newmann)	ep(Newmann)%
1	0	0	0,3141593	0,3141463	0,0013
2	0	0	0,6283185	0,6282152	0,0103
3	0	0	0,9424778	0,9421290	0,0349
4	0	0	1,2566371	1,2558104	0,0827
0	0	1	1,5707963	1,5691819	0,1614
0	1	0	1,5707963	1,5691819	0,1614
5	0	0	1,5707963	1,5691819	0,1614
1	0	1	1,6019042	1,6003187	0,1586
1	1	0	1,6019042	1,6003187	0,1586
2	0	1	1,6917994	1,6902622	0,1537
2	1	0	1,6917994	1,6902622	0,1537
3	0	1	1,8318476	1,8302838	0,1564
3	1	0	1,8318476	1,8302838	0,1564
6	0	0	1,8849556	1,8821663	0,2789
4	0	1	2,0116008	2,0098238	0,1777
4	1	0	2,0116008	2,0098238	0,1777
7	0	0	2,1991149	2,1946862	0,4429
0	1	1	2,2214415	2,2191583	0,2283
5	0	1	2,2214415	2,2191583	0,2283
5	1	0	2,2214415	2,2191583	0,2283
1	1	1	2,2435459	2,2412835	0,2262
2	1	1	2,3085897	2,3063647	0,2225
3	1	1	2,4131031	2,4108652	0,2238
6	0	1	2,4536623	2,4504860	0,3176
6	1	0	2,4536623	2,4504860	0,3176
8	0	0	2,5132741	2,5066647	0,6609
4	1	1	2,5522419	2,5498477	0,2394
7	0	1	2,7025002	2,6979584	0,4542
7	1	0	2,7025002	2,6979584	0,4542

6.8) ELABORATION TIME

The elaboration time in the scalar case is shown in table 6.5.1 for TE eigenvalue of a rectangular structure. This time is sum of the filling matrix time(program in Fortran code) and the time needed to extract eigenvalue and eigenvectors of the matrix (Matlab code). The characteristics of the PC where we performed the simulations are: Intel(R) Core(TM) 2 CPU 6600 @ 2.40 Ghz and 4,00 GB RAM with Win Xp 64 bit and Matlab version r2009b.

Np= number of points for rectangularstructure

Tfm= Time (s) of filling matrix

Time extract TE= time (s) needed to extract eigenvalue and eigenvectors TE of the matrix

Time extract TM= time (s) needed to extract eigenvalue and eigenvectors TMof the matrix

Np	Tfm	Time extract TE	Time extract TM
2000	0,28	0,38	0,24
5000	0,83	0,49	0,35
10000	1,83	0,77	0,62
20000	3,71	1,26	1,15
40000	7,24	2,75	2,47

The latter is very small since we deal with highly sparse matrix. It is worth noting that the filling time scales with the number of grid point. The eigenvectors computation time, on the other hand, increases very slowly with it. The same behavior is obtained for all other structures.

For the vector FD, instead, the computation time of eigenvectors is two order of magnitude large than the scalar case, since the matrix is full. However, the total time is shell smaller than that require by CST

Chapter VII

CONCLUSION

In this thesis the use of a finite differences approach for the computation of the modes of electromagnetic structures with arbitrary geometry has been discussed. We have considered essentially the computation of waveguide modes, but the extension to 3D structure has been partly considered.

The main point is how to overcome the main drawbacks of FD, to get an effective strategy.

The standard discretization through a cartesian grid is derived from the expression of the Laplace operator in Cartesian coordinates. In this work, a different grid polar and elliptic deriving from the Laplace operator written in a form suitable to different structures under test, has been proposed.

The first test involved a circular guide, using the Laplace operator and a discretization grid in polar coordinates. Good results have been obtained with a low computational load, compared to FEM technique; and an high precision, comparable, with analytic results. In particular, as shown in chapter IV, this approach can be extended to elliptic waveguides.

Another problem, described in chapter 3, has been the redefinition of the Laplace operator based on boundary conditions in order to use a single grid for both TE and TM modes.

In chapter V it has been presented a FD technique for the computation of modes and eigenvalues of a waveguide whose boundary are irregular, such as polygonal, or consisting of segments and circular arcs, taking exactly into account the boundary of the waveguide and therefore with no loss of accuracy.

As an extension of scalar FD described in the paragraphs (3.4),(3.5),(3.7),(4.3), the Vector finite differences method has been proposed. In this case the computation of the TE and TM modes has been obtained by solving the vector

Helmholtz equation. The problem is reduced to a constrained eigenvalues problem. The vector finite difference approximation of the vector Helmholtz eigenvalues equation both on a Cartesian and on a curvilinear grid have been considered.

The results obtained analysing different cases of scalar and vector FD are very accurate. From these data, it appears that the proposed techniques are able to evaluate modes with a very small error, both on eigenvalues and on eigenvectors. The error on the eigenvalue is no larger than 0.3% . The RMS error on normalized modes is even small, being less than $5 \cdot 10^{-8}$ in all cases, as shown in the tests reported in chapter VI. Future developments of this thesis are the extension of FD:

- to 3D cases for the study of close structures, in particular to evaluate modes of the resonant cavities

- to optical fibers and dielectric guides..

Appendix

I) CONSTRAINED EIGENVALUE PROBLEMS

The constrained eigenvalue problems is:

I.1.
$$\begin{cases} Ax = \lambda x \\ C^T x = 0 \end{cases}$$

where A is a (2n,2n) matrix, and C is (2n,m) with n>m and $\lambda = -k_i^2$.

We can solve (I.1) using the QR factorization $C = Q \cdot R$ where Q is an orthogonal (2n,2n) matrix $\left(Q^{-1} = Q^T \right)$ and R is a upper triangular matrix (2n,m) that form is ; then substitute in second equation of (I.1):

I.2.
$$C^T \cdot x = (Q \cdot R)^T \cdot x = R^T \cdot Q^T \cdot x = R^T \cdot \left(Q^T \cdot x \right) = 0$$

which suggest to change the unknown as:

I.3.
$$y = Q^T \cdot x \Rightarrow x = Q \cdot y$$

(I.2) becomes:

I.4.
$$C^T \cdot x = R^T \cdot y = 0$$

Replacing $x = Q \cdot y$ in the first of (I.1) and multiplying all member to Q^T we obtaine:

I.5.
$$A \cdot Q \cdot y = \lambda \cdot Q \cdot y \Rightarrow Q^T \cdot A \cdot Q \cdot y = Q^T \cdot \lambda \cdot Q \cdot y \Rightarrow By = \lambda y$$

where $B = Q^T \cdot A \cdot Q$ is a (2n,2n) matrix. The unknown can be partitioned in two vector $y = \begin{vmatrix} u \\ v \end{vmatrix}$, where u and v are (n,1) vector. Then equations (I.4), (I.5) on rewritten in portioned form as::

I.6.
$$\begin{cases} B \cdot y = \lambda \cdot y & \Rightarrow \begin{vmatrix} B_{11} & B_{12} \\ B_{21} & B_{22} \end{vmatrix} \cdot \begin{vmatrix} u \\ v \end{vmatrix} = \lambda \cdot \begin{vmatrix} u \\ v \end{vmatrix} \\ R^T \cdot y = 0 & \Rightarrow \begin{vmatrix} T_1 & 0 \end{vmatrix} \cdot \begin{vmatrix} u \\ v \end{vmatrix} = 0 \end{cases}$$

where B_{ij} is a (n,n) matrix. T_1, are (invertible) triangular matrix . The second equation of (I.6) becomes:

I.7. $T_1 \cdot u = 0 \qquad \rightarrow u = 0$

Therefore the first of I.7 becomes:

I.8. $B_{22} \cdot v = \lambda v$

and we need to extract the eigenvalues of B_{22}.

This discretized eigenvalues problem must be solved by numerical routine and, the full matrix routines of Matlab have been used. The waveguide modes can then be obtained as

I.9. $x = Q \cdot \begin{vmatrix} 0 \\ v \end{vmatrix}$

134

List of papers by the author

Journal Paper:

[1] A.FANTI, G.MAZZARELLA. "A Finite Difference Polar-Cartesian Grid Approach For Mode Computation in Rounded-End Waveguides", Aces Journal , Vol.26, no. 9, September 2011.

Submitted Journal Paper:

[2] A. FANTI, G. MAZZARELLA,, " Computation of TE and TM Modes of Circular and Elliptic Waveguides with Curvilinear Finite Difference", (submitted to IEEE Trans. Microwave Theory and Techniques)

[3] A. FANTI, G. MAZZARELLA, G. MONTISCI, "Curvilinear Vector Finite Difference Approach to the Computation of Waveguide Modes", (submitted to ADVANCED ELECTROMAGNETICS)

[4] A. GIFUNI, A. SORRENTINO, A. FANTI, G. FERRARA, M. MIGLIACCIO, G. MAZZARELLA, F. CORONA, "On the Evaluation of the Shielding Effectiveness of Electrically Large Enclosure", (submitted to ADVANCED ELECTROMAGNETICS)

Journal Paper (In Preparation):

[5] A.FANTI, G.MAZZARELLA. "Finite difference single grid evaluation of TE and TM modes in waveguides.

International Conference Papers:

1. A.FANTI, G.MAZZARELLA. "Finite difference variable grid evaluation of TE modes in metallic ridge waveguides", Proc. Int. Conf. Mathematical Methods in Electromagnetic Theory (MMET*10), Kiev, 06–08 September 2010,WGC-5.

2. A.FANTI, G.MAZZARELLA. "Curvilinear Finite Difference Approach to the Computation of Modes of Circular and Elliptic Waveguides"Proc. Int. Conf. on Applied Electromagnetics and Communications (ICECom 2010), Dubrovnik, Croazia, 20-23 September 2010.

3. A.FANTI, G.MAZZARELLA. "Finite difference single grid evaluation of TE and TM modes in metallic waveguides ", Proc. Int. Conf. Loughborough Antennas and Propagation Conference (LAPC2010), UK, pp. 517-520, 08-09 Nov. 2010.

4. A.FANTI, G.MAZZARELLA. "A finite difference polar-cartesian grid approach for mode computation in rounded-end waveguides", Proc. Int. Conf. Eighth International Conference on Computation in Electromagnetics (CEM2011),Wroclaw, Poland 11-14 April 2011

5. A.FANTI, G.MAZZARELLA. " Computation of TE modes with Vector finite difference in to rectangular waveguides",Proc. 13th International Symposium on Microwave and Optical Technology ISMOT 2011 Prague, Czech Republic, EU, June 20-23, 2011

6. A.FANTI, G.MAZZARELLA. " Finite difference computation of TE and TM modes using a single grid", Proc. 13th International Symposium on Microwave and Optical Technology ISMOT 2011 Prague, Czech Republic, EU, June 20-23, 2011

7. A.FANTI, G.MAZZARELLA. " Vector Finite Difference Approach to the Computation of Circular Waveguide Modes", Proc.10th International Conference on Applied Electromagnetics - PES 2011, Nis, Serbia 25-29 September 2011

8. A.FANTI, G.MAZZARELLA. "Vector Finite Difference Approach to the Computation of TM Waveguide Modes.", Proc.Int. Conf. Loughborough Antennas and Propagation Conference (LAPC2011), UK, 14-15 Nov. 2011

9. A.CASULA, PAOLO.MAXIA, A.FANTI. "A cylindrical resonant cavity for biological experiments and chemical catalysis," Proc.Int. Conf. Loughborough Antennas and Propagation Conference (LAPC2011), UK, 14-15 Nov. 2011

10. A.GIFUNI, A.SORRENTINO, G.FERRARA, M.MIGLIACCIO, A.FANTI, G.MAZZARELLA. "Measurements on the Reflectivity of Materials in a Reverberating Chamber" , Proc.Int. Conf. Loughborough Antennas and Propagation Conference (LAPC2011), UK, 14-15 Nov. 2011

11. A. GIFUNI, A. SORRENTINO, A. FANTI, G. FERRARA, M. MIGLIACCIO, G. MAZZARELLA, F. CORONA, "On the Evaluation of the Shielding Effectiveness of Electrically Large Enclosure", Proc.Int. Conf. Advanced Electromagnetic Symposium (AES2012) 16-19 April 2012, Paris. (Accepted)

12. A. FANTI, G. MAZZARELLA, G. MONTISCI, "Curvilinear Vector Finite Difference Approach to the Computation of Waveguide Modes", Proc.Int. Conf. Advanced Electromagnetic Symposium (AES2012) 16-19 April 2012, Paris. (Accepted)

13. A. FANTI, M. FRANCESCHELLI, P.MAXIA, D. SALPIETRO,"ELU-1:Emotions Language Unified is a BCI for communication support", Proc.Int. Conf. Advanced Electromagnetic Symposium (AES2012) 16-19 April 2012, Paris. (Accepted)

National Conference Papers:

14. A.FANTI, G.MAZZARELLA. "Una tecnica di calcolo dei modi per guide d'onda e aperture non standard ". RiNEm XVII Riunione Nazionale di Elettromagnetismo. Lecce, 15-18 settembre 2008, p. #134

Bibliography

[1] A. Wexler, "Solution of waveguide discontinuities by modal analysis," IEEE Trans. Microwave Theory and Techniques, vol. MTT-15, pp. 508-517, September 1967.

[2] A. Pellegrini, S. Bertini, A. Monorchio, G. Manara, "A Mode Matching - Finite Element - Spectral Decomposition Approach for the Analysis of Large Finite Arrays of Horn Antennas," ACES Journal, vol.24 no.2 pp.233–240, April 2009.

[3] K.L.Chan and S.R.Judah, "Mode-matching analysis of a waveguide junction formed by a circular and a larger elliptic waveguide," IEEE Trans. Microwaves, Antennas and Propagation, IEE Proceedings - Vol.145, pp.123 - 127, February 1998.

[4] Lin, S. L., L. W. Li, T. S. Yeo, and M. S. Leong, " Novel unified mode matching analysis of concentric waveguide junctions," IEEE Trans. on Antennas and Propagation, Vol. 148, No. 6, pp.369–374, December 2001.

[5] R.Sorrentino, F.Alessandri, M.Mongiardo, G.Avitabile, L.Roselli, "Full-wave modeling of via hole grounds in microstrip by three-dimensional mode matching technique," IEEE Trans. Microwave Theory and Techniques, vol. MTT-40, no.12, pp. 2228-2234, December 1992.

[6] Collin.R.E.," Field theory of guided waves", 2nd ed, IEEE Press,N.Y., 1991

[7] G. Mazzarella, G. Montisci: A Rigorous Analysis of Dielectric-Covered Narrow Longitudinal Shunt Slots with Finite Wall Thickness;" Electromagnetics", Vol. 19, pp. 407-418, October 1999.

[8] G. Montisci, M. Musa, G. Mazzarella: Waveguide slot antennas for circularly polarized radiated field; IEEE Trans. on Antennas and Propagation, vol 52, pp. 619-623, Feb 2004.

[9] G. Mazzarella, G. Montisci: "Accurate Characterization of the Interaction between Coupling Slots and Waveguide Bends in Waveguide slot Arrays," IEEE Trans. Microwave Theory and Techniques, vol.48, issue(7), pp. 1154-1157, July 2000.

[10] Roger F. Harrington," Time-Harmonic Electromagnetic", IEEE Press Wiley-Interscience John Wiley & Sons, INC.

[11] L. J. Chu, "Electromagnetic waves in elliptic hollow pipes of metal," J.Appl. Phys., l. 9, pp. 583-591, Sept.1938.

[12] N.Marcuvitz, Waveguide Handbook. London: Peter Peregrinius, 1986, pp. 80-84

[13] J. G. Kretzschmar, "Wave propagation in hollow conducting elliptical waveguides," IEEE Trans. Microwave Theory Tech., vol. MTT-18, pp.547-554, Sept. 1970.

[14] D. A. Goldberg, L. J. Laslett, and R. A. Rimmer, "Modes of elliptical waveguides: A correction," IEEE Trans . Microwave Theory Tech., vol.MTT-38, no. 11, pp. 1603-1608, Nov. 1990.

[15] T.Rozzi,L.Pierantoni, M.Ronzitti. "Analysis of the Suspended Strip in Elliptical Cross Section by Separation of Variables" IEEE Trans . Microwave Theory Tech., vol.MTT-45, no. 11, pp. 1778-1784, Nov. 1997.

[16] B.K.Wang, K.Y.Lam, M S. Leong, and P.S.Kooi, "Elliptical waveguide analysis using improved polynomial approximation ," Proc.Inst.Elect.Eng., vol.141, pp.483-488, 1994.

[17] C. Shu. "Analysis of Elliptical Waveguides by Differential Quadrature method" IEEE Trans Microwave Theory Tech., vol.48, no. 02, pp. 319-322, Feb. 2000

[18] Bernard Dacorogna, "Direct methods in the calculus of variations", 2nd ed, Springer, 2007

[19] Norrie, Douglas H. and Gerard De Vries, "The Finite Element Method: Fundamentals and Applications", Press, New York, 1973

[20] K.W. Morton and D.F. Mayers, Numerical Solution of Partial Differential Equations, An Introduction. Cambridge University Press, 2005

[21] M. J. Beaubien and A. Wexler, An Accurate Finite-Difference Method for Higher Order Waveguide Modes," IEEE Trans. Microwave Theory and Techniques, Vol. MTT-16, no. 12, pp. 1007-1017, December 1968

[22] A.Fanti, G.Mazzarella. "A Finite Difference Polar-Cartesian Grid Approach For Mode Computation in Rounded-End Waveguides", Aces Journal , Vol.26, no. 9, September 2011.

[23] A.Fanti, G.Mazzarella. "Curvilinear Finite Difference Approach to the Computation of Modes of Circular and Elliptic Waveguides"Proc. Int. Conf. on Applied Electromagnetics and Communications (ICECom 2010), Dubrovnik, Croazia, 20-23 September 2010.

[24] A.Fanti, G.Mazzarella. " Vector Finite Difference Approach to the Computation of Circular Waveguide Modes", Proc.10th International Conference on Applied Electromagnetics - PES 2011, Nis, Serbia 25-29 September 2011

[25] A.Fanti, G.Mazzarella, G. Montisci, "Curvilinear Vector Finite Difference Approach to the Computation of Waveguide Modes", Proc. Int. Conf. Advanced Electromagnetic Symposium (AES2012) 16-19 April 2012, Paris. (Accepted)

[26] A.Fanti, G.Mazzarella. "Finite difference single grid evaluation of TE and TM modes in metallic waveguides ", Proc. Int. Conf. Loughborough Antennas and Propagation Conference (LAPC2010), UK, pp. 517-520, 08-09 Nov. 2010.

[27] A.Fanti, G.Mazzarella. " Finite difference computation of TE and TM modes using a single grid", Proc. 13th International Symposium on Microwave and Optical Technology ISMOT 2011 Prague, Czech Republic, EU, June 20-23, 2011.

[28] A.Fanti, G.Mazzarella. " Computation of TE modes with Vector finite difference in to rectangular waveguides",Proc. 13th International Symposium on Microwave and Optical Technology ISMOT 2011 Prague, Czech Republic, EU, June 20-23, 2011

[29] A.Fanti, G.Mazzarella. "Vector Finite Difference Approach to the Computation of TM Waveguide Modes.", Proc.Int. Conf. Loughborough Antennas and Propagation Conference (LAPC2011), UK, 14-15 Nov. 2011

[30] A.Fanti, G.Mazzarella. "A finite difference polar-cartesian grid approach for mode computation in rounded-end waveguides", Proc. Int. Conf. Eighth International Conference on Computation in Electromagnetics (CEM2011),Wroclaw, Poland 11-14 April 2011

[31] G. Franceschetti, Campi elettromagnetici, Boringhieri, Torino, 1983.

[32] G H.Golub, C F.Van Loan," Matrix Computation" , Johns Hopkins Univ. Press, 1989.

[33] J.Van Bladel," Electromagnetic Fields", A SUMMA Book, pp.503, hpc,1985

[34] A.Fanti, G.Mazzarella. "Una tecnica di calcolo dei modi per guide d'onda e aperture non standard ". RiNEm XVII Riunione Nazionale di Elettromagnetismo. Lecce, 15-18 settembre 2008, p. #134

[35] A.Fanti, G.Mazzarella. "Finite difference variable grid evaluation of TE modes in metallic ridge waveguides", Proc. Int. Conf. Mathematical Methods in Electromagnetic Theory (MMET*10), Kiev, 06–08 September 2010,WGC-5.

[36] Sh. Zhang, Y. Chen, Eigenmodes Sequence for an Elliptical Waveguides with Arbitrary Ellipticity, IEEE Trans. Microwave Theory and Techniques, vol.43, issue(1), pp. 227-230, Jan. 1995.

Acknowledgements

I thank all my friends for their invaluable friendship during this years. Finally, I thank my parents Augusto and Bonaria, my brother Stefano, my sisters Sara and Veronica my fiancèe Alessia, for their help during all the hardest moments of my studies.